Bangor University

DOCTOR OF PHILOSOPHY

The cognitive and neural mechanisms of human hand selection

Fitzpatrick, Aoife

Award date:
2019

Awarding institution:
Bangor University

Link to publication

The cognitive and neural mechanisms of human hand selection

Aoife M. Fitzpatrick

Thesis submitted to the School of Psychology, Bangor University, in partial fulfilment
of the requirements for the degree of Doctor of Philosophy

Bangor, United Kingdom I October 2019

DECLARATION

Yr wyf drwy hyn yn datgan mai canlyniad fy ymchwil fy hun yw'r thesis hwn, ac eithrio lle nodir yn wahanol. Caiff ffynonellau eraill eu cydnabod gan droednodiadau yn rhoi cyfeiriadau eglur. Nid yw sylwedd y gwaith hwn wedi cael ei dderbyn o'r blaen ar gyfer unrhyw radd, ac nid yw'n cael ei gyflwyno ar yr un pryd mewn ymgeisiaeth am unrhyw radd oni bai ei fod, fel y cytunwyd gan y Brifysgol, am gymwysterau deuol cymeradwy.

I hereby declare that this thesis is the results of my own investigations, except where otherwise stated. All other sources are acknowledged by bibliographic references. This work has not previously been accepted in substance for any degree and is not being concurrently submitted in candidature for any degree unless, as agreed by the University, for approved dual awards.

SUMMARY

Humans are dependent on the integral functions performed by the hands. Hand *selection* is a prerequisite for the execution of any manual action. Ultimately, how hand selection unfolds, and the neural mechanisms underpinning how these actions are formulated, is not yet understood. This thesis employs a multi-method approach to investigate the cognitive and neural mechanisms of human hand selection.

At the outset of the empirical chapters, a new model of human hand selection is proposed: The Posterior Parietal Interhemispheric Competition (PPIC) model. The PPIC model posits that cell populations in bilateral posterior intraparietal and superior parietal cortex (pIP-SPC) encode multiple action plans in hand-specific terms which compete for selection. There is a dominant representation of the contralateral hand within each hemisphere. A hand is selected, and an action is executed, once a competing action plan reaches suprathreshold levels. Using a multi-method approach, the hypotheses of the PPIC model are tested throughout this thesis.

In *Chapter 2*, functional MRI was used to identify brain areas involved in hand selection. Participants performed a reaching task in free-choice and instructed hand use conditions. Consistent with the PPIC model, bilateral pIP-SPC was preferentially modulated in the free-choice condition, with specificity for the contralateral hand. Further, the pattern of fMRI responses within parietal areas and behavioural data are consistent with the notion that hand selection unfolds via a neural competition.

These areas were targeted using continuous theta-burst stimulation (cTBS) in *Chapter 3*. Participants performed a reaching task in three sessions, following cTBS to Left-pIP-SPC, Right-pIP-SPC, and Sham stimulation. Continuous TBS to pIP-SPC was expected to supress cortical excitability, and bias action competition in favour of ipsilateral hand choice. Contrary to these predictions, hand choice was comparable across sessions and largely insensitive to cTBS.

In a follow up experiment, outlined in *Chapter 4*, the efficacy of cTBS in inducing cortical inhibition is examined. The change in excitability of left primary motor cortex was compared after the application of active or sham cTBS. Results

demonstrate high inter-participant variability, though a group-level facilitative effect on cortical excitability following active cTBS.

Overall, our results partly support the PPIC model of hand selection. The act of choosing a hand for action is shown to modulate bilateral pIP-SPC. The data are consistent with a competitive process underlying hand choice. Continuous TBS applied to pIP-SPC does not significantly alter hand choice behaviour, though the efficacy of induced cortical inhibition is uncertain. The implications of these results are discussed with reference to both the theoretical and clinical fields.

LIST OF TABLES

1. Introduction

The hand and the brain have evolved in parallel over millions of years, shaped by the interactive demands of the environment. Developed from our earliest ancestors Lucy (Johanson, Edey, & Edey, 1990) and Ardi (White et al., 2009) the capabilities of human hand today are unique throughout the animal kingdom; able to produce the vast array of movements and prehensile actions that subserve the most elemental behaviours of survival, as well as mediating object manipulation and tool use, social interaction and communication. These behaviours, though diverse, share a common feature – *hand selection*. A hand must be selected before any manual action can be performed. While the study of the hand has captured the attention of scientists spanning across disciplines for over a century (Lundborg, 2013; Iverson & Thelen, 1999; Wilson, 1998; Napier, 1956; Schwarz & Taylor, 1955), a fundamental feature of all hand use remains an enigma – how do you choose a hand for action?

Hand actions underpin countless activities within daily human motor behaviour. Though we produce these actions seamlessly, often even without explicit attention, performing an action with the hand is the culmination of intricate and extensive neural computation. Take, for example, the act of reaching for a glass of water. From the array of complicated visual information in the environment, attention must be diverted toward the position of the glass to locate it. The coordinates of the glass with respect to the position of the hand in space need to be understood, requiring the use of proprioceptive signals and an internal representation of the body in different positional frames of reference. The visual features of the object need to be extracted, such as size, shape, and contents, in order to correctly preshape the hand for interaction with the glass. A sense of any imposing environmental and biomechanical constraints also needs to be integrated into the movement plan. The intention or will of the agent performing the action also influences the movement to be executed. This constellation of information is synthesised and transformed into the motor parameters that will produce the kinematic features required to successfully reach and grasp the glass. In a matter of milliseconds.

The cooperation of cell populations spanning multiple cerebral regions is required to *select, plan,* and *control* an appropriate action for execution (Kalaska, 1996). In an environment presenting various executable actions in any one instance, the processes of *action selection* determine the hand- and movement-specific information related to the preferred action choice (Cisek & Kalaska, 2010). While *action planning* refers to the specification of the motor parameters critical for movement prior to action onset, *online control* pertains to the integration of sensory feedback with internal feedforward models during the execution of an action (Desmurget & Grafton, 2000).

To date, the neural underpinnings of hand selection remain a topic of considerable debate (Freedman & Assad, 2011; Gallivan, Chapman, Wolpert, & Flanagan, 2018), centred on whether hand choice occurs in regions separable from the sensorimotor systems of action planning (Padoa-Schioppa, 2011; Tversky & Kahneman, 1981), or in tandem (Cisek, 2007; Cisek & Kalaska, 2010). To address this issue, this thesis will investigate both the cognitive and neural mechanisms of human hand selection. At the outset, an overview of the neural representation of visuomotor behaviour is presented. Integrating the insights from clinical observations with brain damaged patients and cognitive theory, a history of the role of the posterior parietal cortex in motor behaviour is introduced. Neurophysiological investigations with non-human primates and human neuroimaging studies will then be outlined to frame how reaching actions are mediated in the brain. Finally, the cognitive and neural mechanisms of action selection will be discussed. Introducing this literature will outline the rationale for the empirical chapters of the thesis.

1.1 The cortical representation of visuomotor behaviour

The posterior parietal cortex (PPC) and interconnected premotor regions formulate the sensorimotor network imperative for both the planning and online control of visually guided reaching behaviour. In the following paragraphs, a brief history of the role of PPC in sensorimotor behaviour is outlined. In particular, how the scientific consensus with respect to the functions of PPC developed over time, originally from a primary somatosensory integration region to a role in visuomotor behaviour. Here, reference to clinical neuropsychology as well as the *Two Visual*

Streams hypothesis (Goodale & Milner, 1992), in particular, are used to introduce the cortical representation of visuomotor behaviour.

1.1.1 The posterior parietal cortex: A brief history

The PPC is a subdivision of the parietal lobe, comprised of the interposing tissue between primary somatosensory area (S1) and the boundaries of the parietal lobe, identified by cytoarchitectonic criteria as Brodmann's areas 5, 7, 39, and 40. The PPC is transected by the intraparietal sulcus, forming the inferior and superior parietal lobules. The PPC was initially described as *association cortex*, involved in the higher order processing of visual information, important to encode the position and form of the body in space (Andersen, 1995; Colby, Duhamel, & Goldberg, 1995; Mountcastle, Lynch, Georgopoulos, Sakata, & Acuna, 1975; Robinson, Goldberg, & Stanton, 1978). The first evidence in support of a role of the PPC in *visuomotor* function was established by clinical observation. In a seminal report by Bálint (1909), now recognised as the first documented instance of *Bálint's syndrome,* a patient is described presenting a trifecta of symptoms; 1) Paralysis of gaze – an inability to attend to more than one object at a time; 2) Spatial inattention – an unintentional neglect of left-hemispace; and 3) Optic ataxia – impairments in visually guided reaching (Bálint, 1909; see also Rafal, 2003). It was noted that the observed deficits could not be attributed to either the sensory or motor modality in isolation, as visual acuity and gross motor abilities were preserved in the patient. An autopsy later revealed extensive lesion mostly restricted to bilateral PPC (Bálint, 1909).

While amounting patient neuropsychological (Bálint, 1909; Hecaen & De Ajuriaguerra, 1954; Rondot & Dumas, 1977), animal lesion (Grünbaum & Sherrington, 1902; Peele, 1944), and single-cell electrophysiology (Mountcastle et al., 1975) evidence implicated a role of the PPC in visuomotor behaviour, whether these observations were evidence for a purely sensory, rather than motoric, deficit is a debate that persisted for many years (Hyvärinen, 1982; Robinson et al., 1978). In a seminal model put forward by Mishkin and Ungerleider (1982), it was proposed that the visual system was modular, with inputs to the striate cortex being processed by distinct neural streams dedicated to spatial versus object vision. Goodale and Milner (1992) revised this framework, to shift the emphasis toward the *output requirements*

of the visual and sensorimotor systems. They proposed the *Two Visual Streams hypothesis,* which outlines that distinct neural steams are dedicated to vision-for-perception, the *"ventral stream"*, and vision-for-action, the *"dorsal stream"* (Goodale & Milner, 1992; Milner & Goodale, 2008; Mishkin & Ungerleider, 1982; Ungerleider, Mishkin, Ingle, Goodale, & Mansfield, 1982).

1.1.2 Two visual pathways

Goodale and Milner (1992) proposed that the information extracted by the visual system is transmitted to distinct, but interconnected, regions of cortex in order to be processed (see Figure 1.1). Where and how the information is encoded, is dependent on its *purposes*. The ventral – or "What" – stream, mediates visual perception by extracting and processing intrinsic features of an object – such as size or shape – to permit identification and recognition. Alternatively, the dorsal – "Where" or "How" – stream extracts similar (e.g. size, shape) visual information, though performs different operations on this input to allow for the visuomotor control of actions. The ventral stream is subtended by striate projections to inferotemporal cortex, while the dorsal stream processes information along an occipitoparietal projection system.
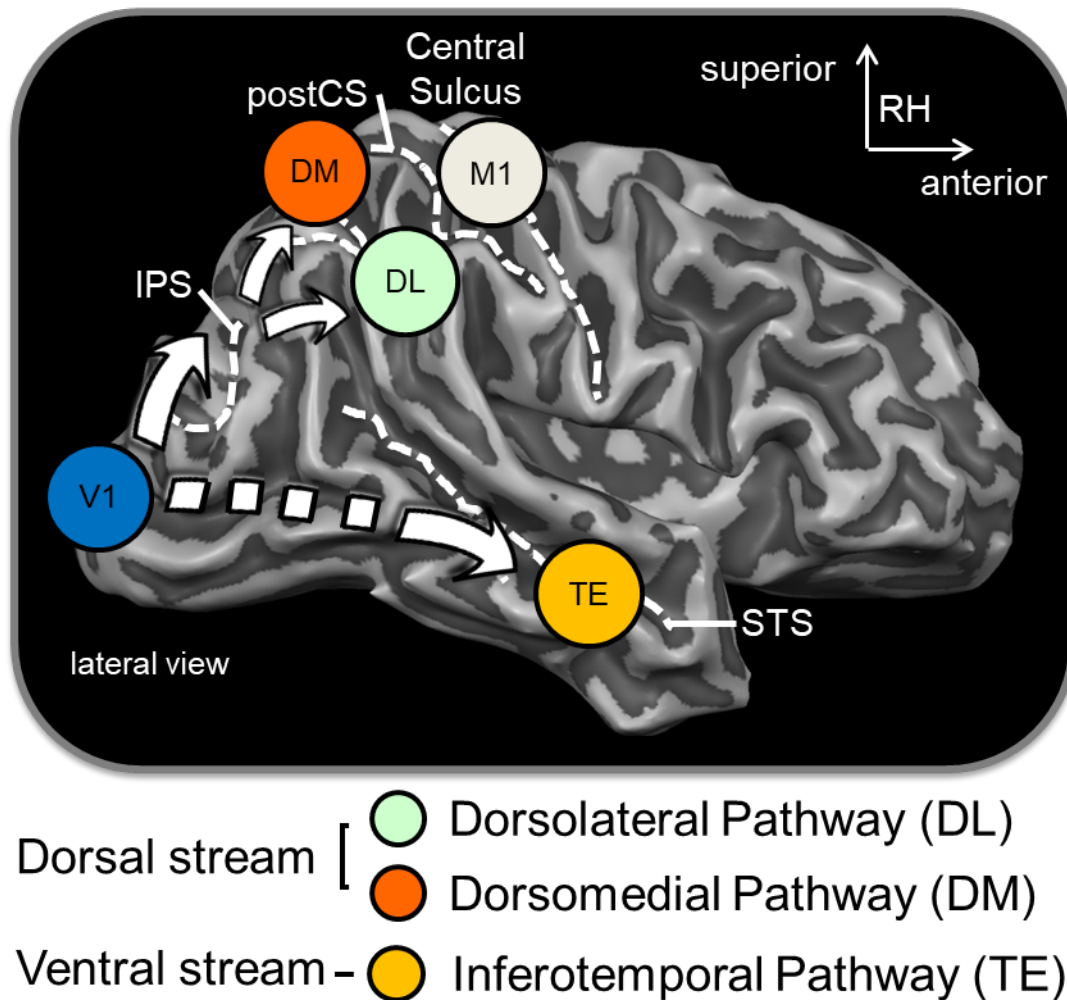
Figure 1.1. Visual streams. Schematic representation of the two visual streams outlined by Goodale and Milner (1992), with additional dorsolateral and dorsomedial pathways of the dorsal stream (Rizzolatti and Matelli 2003, Binkofski and Buxbaum 2013), shown on the 3D cortical surface of the right hemisphere of a human brain. The cortical surface was defined at the grey-white matter boundary and partially inflated. Sulci are indicated as dashed lines: postCS, post-central sulcus; IPS, intraparietal sulcus; STS, superior temporal sulcus. Areas: V1, early visual cortex; upward white arrow depicts the initiation of the dorsal stream; rightward arrow initiates the ventral stream; TE, inferotemporal cortex; DM, dorsomedial projection pathway – implicated in reaching behaviour; DL, dorsolateral projection pathway – associated with grasping; M1, primary motor cortex.

A series of studies conducted with D.F, a patient with a damaged ventral stream presenting with visual agnosia, provided the foundational empirical evidence in support of the *two visual streams hypothesis* (Goodale & Milner, 1992; Goodale, Milner, Jakobson, & Carey, 1991; Milner & Goodale, 1995). Visual form agnosia describes a specific deficit in visual discrimination, characterised by "seeing without recognition" (Benson & Greenberg, 1969). For instance, patient D.F could not perceptually differentiate between objects of varied size or shape, or provide a verbal or manual description of the orientation of a letterbox-like slot, deficits that could not be attributed to a simple sensory impairment (Goodale et al., 1991). However, an

important behavioural dissociation was observed. D.F could reliably preshape the hand to correctly grasp different objects (Carey, Harvey, & Milner, 1996; Goodale et al., 1991), as well as accurately orient the hand to "post" through the slot at differing angles (Goodale et al., 1991). The opposite pattern was later observed in patient with optic ataxia after bilateral damage to the occipitoparietal regions encompassing the dorsal stream (Goodale et al., 1994). The authors proposed that this pattern of behaviour is accounted for under a model which dissociates visual processing into distinct functional-anatomical pathways (Goodale & Milner, 1992).

The notion of disparate cortical representation for vision-for-recognition and vision-for-action is supported by further patient (Jakobson, Archibald, Carey, & Goodale, 1991; Kimura, 1963; Perenin & Vighetto, 1988; Ratcliff & Davies-Jones, 1972; Warrington, 1982; Warrington & James, 1967), animal lesion (Hwang, Hauschild, Wilke, & Andersen, 2012; Pohl, 1973), and neural recording (Gross, Rocha-Miranda, & Bender, 1972; Hyvärinen & Poranen, 1974; Robinson et al., 1978; Taira, Mine, Georgopoulos, Murata, & Sakata, 1990) studies. Over time, the *two visual streams hypothesis* put forward by Goodale and Milner (1992) was elaborated, as the strict perception versus action dichotomy could not account for a range of anatomical and behavioural observations (see Binkofski & Buxbaum, 2013 and Rizzolatti & Matelli, 2003; Galletti & Fattori, 2018; Milner & Goodale, 2008). Perhaps most noteworthy, the dorsal stream is now understood to consist of at least two separable sub-streams: the *dorsolateral pathway*, responsible for, among other functions, grasping behaviour, and the *dorsomedial pathway*, implicated in reaching (see Figure 1.1). Nonetheless, the impact of the model has been substantial.

This thesis focuses on the neural mechanisms underpinning visuomotor behaviour, for which the occipitoparietal areas of the dorsal visual stream are known to play an essential role. The data related to the occipitotemporal ventral stream are not discussed. Further, the frontoparietal networks serving hand and arm actions, or *reaching* – i.e. the dorsomedial pathway – rather than grasping, tool use, or eye-movement behaviour are specifically assessed in order to frame the literature relevant for subsequent portions of the thesis.

1.2 The reaching network in non-human primates

In the following paragraphs, neurophysiological data detailing the reaching network in non-human primates is discussed, before introducing the putative human counterparts. The evidence which implicate the functional role of each critical node of the network is outlined. First, however, a note on the comparison of the neurobiological architecture across non-human primate and human species. It is important to note that the non-human primate and human lineages diverged in evolution a considerable time ago (Kay, Williams, Ross, Takai, & Shigehara, 2004). Despite this, studies with non-human primates offer invaluable insights that can be used to guide human investigation. Neurophysiological studies reveal a general correspondence between the non-human primate and human brain areas recruited in a number of cognitive functions. For the PPC in particular, plausible homologies are supported in the literature (Astafiev et al., 2003; Connolly, Andersen, & Goodale, 2003; Culham & Kanwisher, 2001; Grefkes & Fink, 2005). It has also been recently suggested that human behaviour may be best conceptualised under the constraints of "*phylogenetic refinement*" (Cisek, 2019). That is, human behaviours and the neural mechanisms through which they are mediated should be assessed within the context of how they evolved. To this end, a comparison with our closest phylogenetic relation, the non-human primate, is certainly informative.

1.2.1 Connectivity

Interposed directly between primary visual and motor regions, the PPC is ideally situated to mediate the neural processes of visuomotor behaviour. The earliest anatomical studies of parietal lobe revealed that the PPC shares a number of reciprocal connections with the adjacent regions, including commissural fibres with the symmetrical parietal areas, as well as subcortical – including the thalamus and basal ganglia – and cerebellar structures (Hyvärinen, 1982; Peele, 1942, 1944). Substantial corticocortical reciprocal connections with premotor and primary motor regions in the frontal lobe are also evidenced (Cavada & Goldman-Rakic, 1989; Chavis & Pandya, 1976; Ghosh, Brinkman, & Porter, 1987; Johnson, Ferraina, Bianchi, & Caminiti, 1996; Johnson, Ferraina, & Caminiti, 1993; Kurata, 1991; Petrides & Pandya, 1984; Strick & Kim, 1978). The motor areas receive signals from

multiple regions in the PPC, though a series of distinct frontoparietal circuits can be distinguished (Rizzolatti, Luppino, & Matelli, 1998). In particular, those mediating reach behaviour include areas of the superior parietal lobule (area 5, area 6) and medial intraparietal area projecting to dorsal premotor (dPMC) cortex (area 1, area 2, and area 7). This circuit is largely separable from the connections underpinning, for example, grasping actions, which are subtended by anterior intraparietal area projections to ventral premotor cortex (Figure 1.2) (Rizzolatti et al., 1998; see also Caminiti et al., 2017; Gamberini, Passarelli, Fattori, & Galletti, 2019).
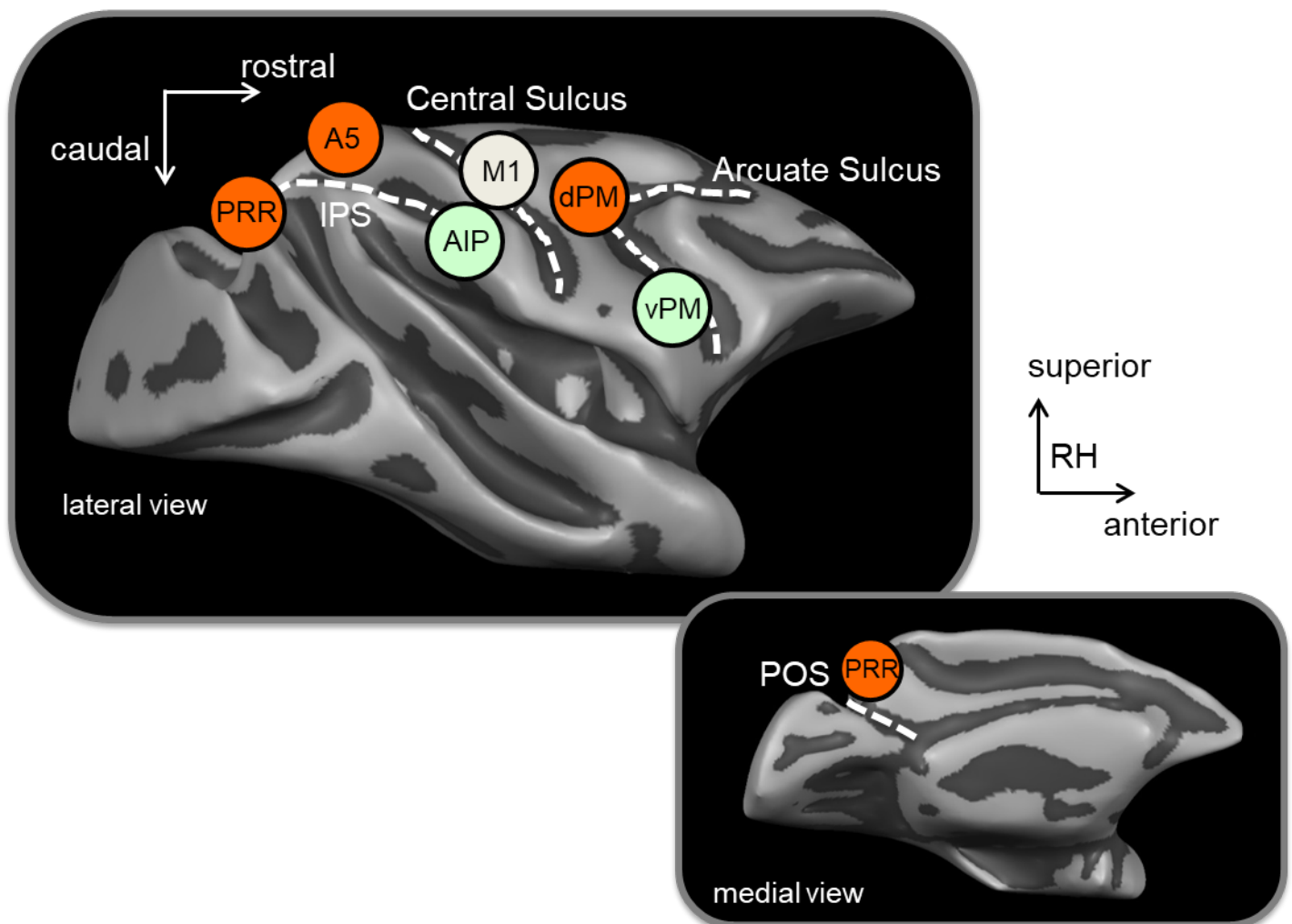
Figure 1.2. The reaching network in the non-human primate. Schematic representation of the areas which perform the sensorimotor transformations necessary for visually guided reaching (dorsomedial pathway - orange) shown on the cortical surface (right hemisphere) of the macaque monkey. Areas implicated in grasp behaviour are illustrated for reference (dorsolateral pathway – light green). The cortical surface was defined at the grey-white matter boundary and partially inflated, shown in lateral (above) and medial (inset) views. Dashed lines indicate the sulci: IPS, intraparietal sulcus, POS, parieto-occipital sulcus. Reaching areas: PRR, parietal reach region; A5, area 5 of the superior parietal lobule, also referred to as area PE, dPM, dorsal premotor cortex. Grasping areas: AIP, anterior intraparietal area; vPM, ventral premotor cortex. M1, primary motor cortex. The macaque MRI data used to create the cortical reconstruction was generously provided by Prof. Stefan Everling.

1.2.2 The superior parietal lobule

To perform a reach, the hand must be transported in space to the location of an object or goal. The PPC is now understood to perform the multimodal integration of visuospatial information critical for the generation such actions. Information is encoded in multiple *reference frames,* or, sets of axes that describe the location of an object or goal of movement (Cohen & Andersen, 2002). Cells in area 5, also referred to as PE, in the rostral area of the superior parietal lobule (SPL) are shown to encode the position, posture, and joint configuration of the arm when stationary and during movement in a body-centred frame of reference (Lacquaniti, Guigon, Bianchi, Ferraina, & Caminiti, 1995). Area 5 neurons are also reported to encode reach and arm information in hand-centred coordinates (Bremner & Andersen, 2012; Ferraina et al., 2009; Piserchia et al., 2017). During the instructed-delay period of instructed-delay reaching tasks – i.e. the planning stage of movement – neural activity specifies direction and depth (Crammond & Kalaska, 1989; Ferraina & Bianchi, 1994; Ferraina et al., 2009; Johnson et al., 1996), even when the movement is not overtly performed (Kalaska & Crammond, 1995). Further, inactivation of area 5 results in the inability to perform online reach corrections to jumping targets (Battaglia-Mayer et al., 2012), implicating the SPL in both the preparation and online guidance of reaching movements.

1.2.3 The parietal reach region

Regions in the dorsocaudal PPC, medial intraparietal area (MIP) and area V6A, are collectively referred to as the *parietal reach region* (PRR) (Snyder, Batista, & Andersen, 2000). The PRR is a functionally defined area, implicated specifically in the planning and control of arm and hand reaching movements (Andersen & Buneo, 2002; Buneo & Andersen, 2006; Galletti, Battaglini, & Fattori, 1991; Galletti, Fattori, Battaglini, Shipp, & Zeki, 1996; Galletti, Fattori, Kutz, & Battaglini, 1997; Snyder, Batista, & Andersen, 1997). Neurons are activated by reaching, grasping, and wrist orientation (Fattori et al., 2009; Fattori, Breveglieri, Raos, Bosco, & Galletti, 2012; Fattori, Gamberini, Kutz, & Galletti, 2001), implicating the PRR in both reaching and reach-to-grasp behaviour. It was recently shown that the planning activity within the

PRR can be differentiated according to the upcoming grasp versus reach movement requirements (Santandrea, Breveglieri, Bosco, Galletti, & Fattori, 2018).

Modulation of the PRR is related to the direction (Eskandar & Assad, 2002) and depth (Hadjidimitrakis et al., 2013) of hand movements, with specificity for the contralateral arm (Chang & Snyder, 2012; Savaki, Kennedy, Sokoloff, & Mishkin, 1993; Yttri, Wang, Liu, & Snyder, 2014) and space (Hadjidimitrakis et al., 2013). Similar to other reach-related regions of the PPC, the PRR synthesises target coordinates during movement planning and online control (Chang & Snyder, 2010; Hwang, Hauschild, Wilke, & Andersen, 2014; Kuang, Morel, & Gail, 2015). Unlike Area 5, where reach targets are commonly encoded in a hand- and body-centred frame of reference (Bremner & Andersen, 2012; Ferraina et al., 2009; Lacquaniti et al., 1995; Piserchia et al., 2017), evidence suggests that neurons in the PRR use a variety of eye- (Batista, Buneo, Snyder, & Andersen, 1999; Bhattacharyya, Musallam, & Andersen, 2009; Cohen & Andersen, 2002; Pesaran, Nelson, & Andersen, 2006), mixed hand/eye (Chang, Papadimitriou, & Snyder, 2009), or eye/head (Mullette-Gillman, Cohen, & Groh, 2005, 2008) reference frames. Interestingly, the reference frames in use within the PRR are shown to be dynamic. Cells activated by movements with either limb are encoded predominately in gaze-centred coordinates, while unimanual-limb cells incorporate gaze- and hand-centred reference frames (Chang & Snyder, 2012).

1.2.4 The dorsal premotor cortex

The dorsal premotor cortex (dPMC) constitutes a key node in the frontoparietal reaching network (for review see Wise, Boussaoud, Johnson, & Caminiti, 1997). Of particular relevance, evidence suggests that visual information and motor commands for action are integrated in the dPMC (Halsband & Passingham, 1985; Johnson et al., 1996). Action plans are sent for overt execution predominantly via interconnections between the dPMC and the primary motor cortex (Godschalk, Lemon, Kuypers, & Ronday, 1984; Johnson et al., 1996; Muakkassa & Strick, 1979). Response properties of dPMC cells indicate that visuospatial location of targets and directional signals related to movement are encoded during action preparation (Crammond & Kalaska, 1994; Wise et al., 1997; Wise, di Pellegrino, &

Boussaoud, 1996). The dPMC is also implicated in the context-dependent selection of actions, that is, under the conditions that involve arbitrary stimulus-response mappings (Shen & Alexander, 1997a, 1997b; Wise et al., 1996) (see also Section 1.4.1).

1.2.5 Attention versus intention in parietal cortex

It could be argued that parietal activity during the preparation of arm movements is attributable to processes of attention, rather than true motor planning. Indeed, attention-related processing is evidenced throughout the human PPC (Culham & Kanwisher, 2001). A critical role of the inferior parietal lobule is evidenced, in particular (Rushworth, Ellison, & Walsh, 2001). To dissociate these possibilities, Snyder, Batista, and Andersen (1997) recorded cell activity during the delay period of a single-movement task. In the task, animals were trained to perform a reach or saccade to a remembered target location, indicated by a spatial and colour cue. It was reasoned that, if modulated by attention, parietal activity would be comparable across reach and saccade trials toward the same target location. The delay-period activity was found to be dependent on the type of movement being prepared, and specific eye and arm cells were identified in the lateral and medial intraparietal areas, respectively (Snyder et al., 1997). Further, reflecting movement intent, eye- and arm-related cells are shown to encode the directional information relevant for the upcoming saccade or reach movement. Neuronal firing specifically increased when the location of the target overlapped with the receptive field of the cell. Targets lying outside the scope did not modulate cell activity (Andersen, Snyder, Bradley, & Xing, 1997; Snyder et al., 1997). These experiments demonstrate that the PPC, the SPL in particular, contains the relevant effector and movement information, reflective of true action intention.

1.2.6 Animal lesion perspective

Also in refute of the purely attentional account, lesion of the parietal reach network has considerable impact on reach behaviour. Peele (1944) was the first to perform ablations of distinct sub-regions of the PPC (S1, area 5, and area 7) and map the consequences on natural behaviour. Voluntary movements contralateral to

the lesion were significantly reduced in the most acute post-operative period. Ataxia or awkwardness of movement, hypotonia, and a slowness in movement of the contralateral limb was observed, particularly when movements were performed without vision (Peele, 1944). More recently, inactivation of the PRR has been shown to impact reaching, but not saccade, behaviour (Hwang et al., 2012). In this experiment, animals were trained to perform memory-guided reach and saccade tasks, performing a reach or saccade toward a visually cued target following a brief delay period. The PRR was reversibly inactivated using muscimol injection. Reach, but not saccade, amplitudes were significantly affected by the inactivation of the PRR, compared to control sessions. Misreaching, particularly falling short of the intended target location, or "hypometria", was present across all target locations and inactivation sessions. The effector-specific and target non-specific effects of PRR inactivation demonstrate that the results are not attributable to a deficit in spatial perception. That is, inactivation of the PRR led to the consistent and selective impairment of gross reaching behaviour. Further, accounting for the possibility that the altered reach behaviour may reflect impaired spatial memory, misreaching also occurred in a separate task without a delay period between target presentation and movement onset (Hwang et al., 2012). These data provide compelling evidence to demonstrate that PRR inactivation results in the inability to synthesise target location information required for effective reach behaviour.

Cooperation across all nodes of the reaching network produce the sensorimotor transformations that underpin hand-related visuomotor behaviour. Investigations with non-human primates have outlined distinct areas within the PPC that mediate reaching actions, the SPL and PRR in particular. These areas process the relevant visual cues from the environment, such as target location, and synthesise this information with a representation of the body to encode the appropriate action in motoric terms. Ongoing and reciprocal communication with the dPMC is suggested to monitor and integrate the sensorimotor inputs from the PPC to produce a movement plan, which is then sent via corticocortical connections with the primary motor cortex for execution.

1.3 The reaching network in humans

The aforementioned reaching areas, outlined on the basis non-human primate neurophysiology, have functional human counterparts. In this section, evidence from functional magnetic resonance imaging (fMRI), transcranial magnetic stimulation (TMS), and neuropsychology will be used to outline the putative human complements of the non-human primate reaching network.

1.3.1 Functional magnetic resonance imaging perspective

Functional MRI and, in particular, the blood oxygen level dependent (BOLD) signal, allow for the localisation of neural activity in response to a stimulus with relatively high spatial specificity (Logothetis, 2003; Logothetis & Wandell, 2004). Broadly, the BOLD signal is an indirect measure of neuronal discharge, and represents the displacement of oxygen-impoverished by oxygen-rich blood – the haemodynamic response – at a neuron-population level in response to a change in the rate of cell firing. Metabolic changes in response to a particular behavioural task, or exposure to a certain stimulus, can be localised by modelling the BOLD signal, to functionally "map" the brain (Logothetis, Pauls, Augath, Trinath, & Oeltermann, 2001). Functional MRI has been used across a plethora of scientific disciplines, and has been particularly informative to understand the relationship between non-human primate and human neurophysiology in the PPC (Culham & Kanwisher, 2001; Culham & Valyear, 2006; Gallivan & Culham, 2015).

Imaging the brain during reaching actions presents a unique set of difficulties, however, given that both arm- and corresponding induced head-movements are a considerable potential source of artifact. To circumvent this, participants can undertake pre-scanning training (e.g. Valyear & Frey, 2015), or perform "pointing", rather than "reaching", tasks, as seen in many fMRI studies (Culham, Cavina-Pratesi, & Singhal, 2006). While reaching requires the extension of the arm to touch a target, pointing refers to a finger extension in the direction of a target without an accompanying arm-movement (e.g. Astafiev et al., 2003). Also within the reaching task set, participants may be directed to perform reaching-to-point (with the index finger, e.g. Prado et al., 2005), reaching-to-touch (grossly, with the knuckles, e.g.

Culham et al., 2003), or reaching-to-grasp (e.g. Hinkley, Krubitzer, Padberg, & Disbrow, 2009) movements. The reaching circuit would certainly be modulated differently according to the task in use. For instance, reaching-to-touch and reaching-to-grasp are argued to encompass an element of hand pre-shaping, which could modulate nodes of the grasping circuit (Culham et al., 2006). Nevertheless, whilst acknowledging these limitations, the merits of fMRI in investigating reaching behaviour are considerable, and a general convergence with data yielded in primate neurophysiology experiments is seen.

1.3.2 Nodes of the parietal reaching network

Human neuroimaging studies have isolated two distinct reach-related sub-regions of the PPC. The first, with respect to the anterior-posterior axis, is located along the mid-section of the medial bank of the intraparietal sulcus (mIPS). A second module is located in the more posterior and medial region of the mIPS, encompassing the superior and anterior aspect of the parieto-occipital junction – coined the superior parieto-occipital cortex (SPOC).

Human neuroimaging outlines a role for the PPC in reaching behaviour and, further, offers an insight into the details of movement that this activation represents. During the planning phase of movement, activity within parietal regions is reflective of action intention (Gallivan, McLean, Valyear, Pettypiece, & Culham, 2011). In this study, participants performed reach-to-touch and reach-to-grasp actions with the right hand in a delayed-movement task. The spatial activity patterns within a number of parietal and premotor regions, including the mIPS, the SPOC, and the dPMC, reliably predicted the upcoming reach or grasp movement. Notably, the right-handed actions predominantly modulated activity in the left-hemisphere, suggesting contralateral effector encoding. While a level of effector-independent encoding has been reported (Gallivan, McLean, Smith, & Culham, 2011), recent evidence suggests action plans in the medial intraparietal and superior parietal cortices are encoded at a hand-specific level, with preference for the contralateral hand (Valyear & Frey, 2015). Neural activity in the mIPS and SPOC is also shown to reflect multiple, dynamic frames of reference, including gaze-, hand-, and body-centred coordinates, in order to encode the motoric goal for action (Bernier & Grafton, 2010;

Beurze, Toni, Pisella, & Medendorp, 2010), similar to observations in the PRR (Chang & Snyder, 2012). In the following sections, more detailed reviews of the mIPS and SPOC are presented.

1.3.3 The medial intraparietal area

Evidence suggests that the mIPS may be the human equivalent of the monkey area MIP (Grefkes & Fink, 2005); which, as discussed in Section 1.2.3, is a core component of the PRR. The mIPS is modulated by reaching (Prado et al., 2005) as well as pointing (DeSouza et al., 2000), indicating that this area transforms visuospatial information for coordinated movement. Grefkes, Ritzl, Zilles and Fink (2004) investigate this possibility using a joystick paradigm, similar to that employed previously with macaques (Eskandar & Assad, 1999, 2002). In the task, participants transported a square object between two points presented on a screen using a joystick. Transporting the square required the target location information to be encoded into a goal-directed motor command. Activation was compared against a condition where the participant responded to a visual cue with a directional movement of the joystick. Here, the participant was also required to execute a motor command, but no transformation of spatial coordinates was required. Controlling for additional visual and proprioceptive differences, the mIPS was preferentially modulated for movements requiring visuomotor coordinate transformation (Grefkes, Ritzl, Zilles, & Fink, 2004).

Other studies also support a role of the mIPS in transforming the spatial target coordinate information into an appropriate movement vector for overt action performance (Bernier & Grafton, 2010; Chen et al., 2014). In particular, employing a multivoxel analysis technique, the neural activity within the mIPS is shown to represent integrated target location and movement direction information (Barany, Della-Maggiore, Viswanathan, Cieslak, & Grafton, 2014); though the authors denote the mIPS region more broadly as the "superior parietal lobule". Here, the functional relationships between sensory- and motor-related features present in the neural activity of the motor network are examined. It was reasoned that the regions performing sensorimotor transformations for action would represent both the sensory and motor features in isolation, as well as an *interaction* between pairs of features.

Participants performed a number of movements with different wrist orientation, wrist angle, target location, movement direction, and movement amplitude demands. Accounting for the individual contributions of each condition in the observed activation separately, the mIPS displayed an interaction between sensory- and motor-relevant properties. That is, the interaction of target location (sensory) and movement direction (motor) features relevant for the upcoming action were represented. This interaction was not seen in other areas of the frontoparietal reaching network, such as the dPMC. These data are taken to evidence that the mIPS facilitates the visuomotor transformation computations of these stimulus features for movement (Barany et al., 2014).

1.3.4 The superior parieto-occipital area

The SPOC is suggested as a candidate homologue to the non-human primate PRR (Connolly et al., 2003; Pitzalis et al., 2013). Evidence suggests that the SPOC is involved in the preparation of reaching movements (Cavina-Pratesi et al., 2010), with specificity for the contralateral arm (Valyear & Frey, 2015; Van Der Werf, Jensen, Fries, & Medendorp, 2010). The SPOC has also been implicated in the planning of grasping movements (Gallivan, Cavina-Pratesi, & Culham, 2009), though neural activity associated with the arm-transport (reach) component can be reliably differentiated from grasping-related activity (Cavina-Pratesi et al., 2010). Areas within the SPOC are also specifically modulated by objects reachable by the hand (Gallivan et al., 2009), implying that a role of this region includes encoding the spatial location of movement goals. In line with this hypothesis, Fernandez-Ruiz and colleagues (2007) demonstrate that the SPOC performs the visuospatial transformations required for coordinated movement, rather than encoding the extrinsic movement direction. In this study, the participants performed a pointing task under two conditions; before and after undergoing visuospatial adaption (with a left-right reversing prism). Once adapted, the participants' *view* of the produced movement was reversed compared to the actual movement, i.e. the extrinsic direction of the movement remained constant, while the visual direction of the goal was adapted. The directional specificity within the SPOC was reversed in the

adapted condition, and remained tied to the visual direction of the movement goal (Fernandez-Ruiz, Goltz, DeSouza, Vilis, & Crawford, 2007).

In a complementary study, supporting a role of the SPOC in encoding and updating the spatial location of reach goals, activity was demonstrated to be highly sensitive to jumps in the location of a reach target (Diedrichsen, Hashambhoy, Rane, & Shadmehr, 2005). Here, the location of a reaching goal jumped 25° after movement onset for a subset of trials. The distance from the start point to the either the old or new endpoint location was equal. Activity evoked by the target jump condition was compared to a visual rotation condition, where visual feedback was rotated around the starting position by 25°. Alongside the mIPS, activity within the SPOC was increased during target jump conditions. This pattern suggests that the current reaching goal is represented in the medial superior parietal and parieto-occipital cortices, similar to what is observed in the non-human primate PRR (Battaglia-Mayer et al., 2000; Diedrichsen et al., 2005; Snyder et al., 2000).

1.3.5 Disruption of the reaching network

Damage to the PPC results in impaired reaching behaviour. For instance, the anatomic loci of reach- and point-related activity correspond well to the regions of infarct in patients with optic ataxia (Karnath & Perenin, 2005). Using a lesion subtraction analysis technique (Rorden & Karnath, 2004), where the lesions of PPC-damaged patients with and without optic ataxia are compared, Karnath and Perenin (2005) identified the most common regions producing the characteristic misreaching behaviour of optic ataxia. Damage to the medial parietal-occipital junction in both hemispheres was consistently seen in patients with optic ataxia, as well as the superior occipital gyrus, and the IPS. Left-hemisphere PPC lesion including the superior parietal lobule, while a damaged inferior parietal lobule following right-hemisphere lesion, was more commonly associated with optic ataxia. The medial parietal-occipital junction identified by Kernath and Perenin (2005) corresponds to areas within the SPOC. In line with the behavioural deficits reported in optic ataxia, where impairments are increased for reaches in the periphery, the SPOC shows specificity for extra-foveal, or peripheral, targets (Clavagnier, Prado, Kennedy, & Perenin, 2007; Martin, Karnath, & Himmelbach, 2015; Prado et al., 2005). Moreover,

misreaching in optic ataxia has been linked to an obscured representation of targets represented in gaze-centred coordinates (Khan et al., 2005), a function also mediated by the SPOC (Medendorp, Goltz, Vilis, & Crawford, 2003).

Perturbation approaches using TMS causally implicate the PPC in both the online control and planning of reach actions. To reiterate, the *online control* of actions refers to the integration of sensory (feedback) information with internal (feedforward) models of movement while the action is taking place. These processes are considered dissociable from the pre-movement specification of motor parameters, which relate to *action planning*.

TMS is a non-invasive neuromodulatory technique, and can be used to transiently manipulate neuronal discharge within the cortex underlying the coil (Walsh & Cowey, 2000). Briefly disrupting cell function can probe the role of a cortical region in the processing of a particular task (Cracco, Cracco, Maccabee, & Amassian, 1999). The cortical effects of TMS can be broadly categorised as excitatory or inhibitory, as well as transient, lasting milliseconds (e.g. Gandolfo & Downing, 2019), or persistent, lasting in excess of 30 minutes (e.g. Huang, Edwards, Rounis, Bhatia, & Rothwell, 2005). Transient after-effects of stimulation are usually the result of "online" TMS, where pulses are delivered while the participant is performing a task. On the other hand, in "offline" stimulation, the after-effects are maintained beyond the application of TMS pulses. The effects of TMS are determined by a combination of factors, including the frequency, intensity, and duration, of the protocol applied (for reviews see: Siebner, Hartwigsen, Kassuba, & Rothwell, 2009; Silvanto & Cattaneo, 2017).

Online TMS to the IPS impairs reach path corrections to target jumps, implicating a role for this region in online control of reaching movements (Desmurget et al., 1999). The disruptive effects of TMS are further shown to be linked to the initiation of online adjustments, rather than a gross impairment in executing online correction (Glover, Miall, & Rushworth, 2005). However, in a recent investigation TMS did not disrupt online correction to spatially perturbed targets (Marigold, Lajoie, & Heed, 2019), suggesting that the PPC may be primarily involved in action planning. TMS applied to the SPL during the preparatory phase of movement results

in increased endpoint errors, particularly for targets in the periphery (Striemer, Chouinard, & Goodale, 2011). Disruption of cell activity in the IPS deviates contralateral reaches, in particular (Smyrnis, Theleritis, Evdokimidis, Müri, & Karandreas, 2003; Van Donkelaar & Adams, 2005). Implicating a causal role of the mIPS in specifying the extrinsic direction vector of visually guided movements, TMS applied after target presentation, but prior to movement onset, increases variation in the initial reaching direction for targets in the contralateral hemifield (Davare, Zenon, Pourtois, Desmurget, & Olivier, 2012).

Vesia, Prime, Yan, Sergio, and Crawford (2010) demonstrate effector- (reach versus saccade) and limb- (left versus right hand) specificity within the PPC. Three parietal sites were interrogated; the SPOC, the mIPS, and the angular gyrus. Participants were cued to perform a reach or saccade movement to a visually presented target following a brief delay. Online bursts of TMS were applied at the onset of a mask, preceded directly by the reach target – i.e. during reach planning. TMS was shown to alter reach, but not saccade performance. Specifically, reach endpoint errors shifted toward fixation following stimulation of the SPOC, irrespective of hemisphere. TMS applied to the mIPS and angular gyrus produced a significant increase in endpoint variability for the contralateral hand. These effects were also strongest in the contralateral visual hemifield. Visual feedback of the hand was shown to rescue the TMS-induced effect on endpoint variability, while endpoint errors remained significantly perturbed. The authors suggest that TMS over the mIPS and the angular gyrus disrupts the planned reach vector, or hand position, information used for movement, which is corrected by visual feedback. Conversely, TMS applied to the SPOC disrupts the transformation of the visuospatial reach target, or movement goal, into motor parameters (Vesia & Crawford, 2012; Vesia, Prime, Yan, Sergio, & Crawford, 2010).

1.3.6 Comparison of reaching studies

Previous sections of this chapter have indicated important loci for the planning and online guidance of hand and arm actions. An overview of neuroimaging and TMS studies involving reaching and pointing is presented in Figure 1.3, compiled and synthesised for the purposes of this thesis. Specifically, the peak

activation/target coordinates were extracted from 14 fMRI, 3 Positron Emission Topography, and 7 TMS studies which investigated reaching behaviour (studies included are marked with an asterix in the References). In the case of whole-brain fMRI analyses, coordinate information related to activation within the PPC was used. Coordinates were transformed from Montreal Neurological Institute (MNI) to Talairach (Talairach & Tournoux, 1988) space where required, using the approach outlined by the Cambridge Brain Sciences Unit (Brett, 2017). This coordinate information was used to create 15mm-diameter spherical foci. These dimensions were arbitrarily chosen to provide a simple estimate of overlap across studies (this method extinguishes the associated magnitude- and extent-related activation information of each investigation). Akin to a probabilistic map, spherical foci were then used to compute the percentage overlap of reach-related activity to illustrate the parts of the brain that show the most consistency.

Reach-related activity is predominantly seen along the medial bank of the IPS in the SPL, and anterior to the parieto-occipital sulcus, the SPOC; aligned with areas of the dorsomedial pathway, and corresponding well with the regions outlined by primate neurophysiology (area 5 in the SPL, and the PRR), and those implicated by others in the human literature (Culham & Valyear, 2006).
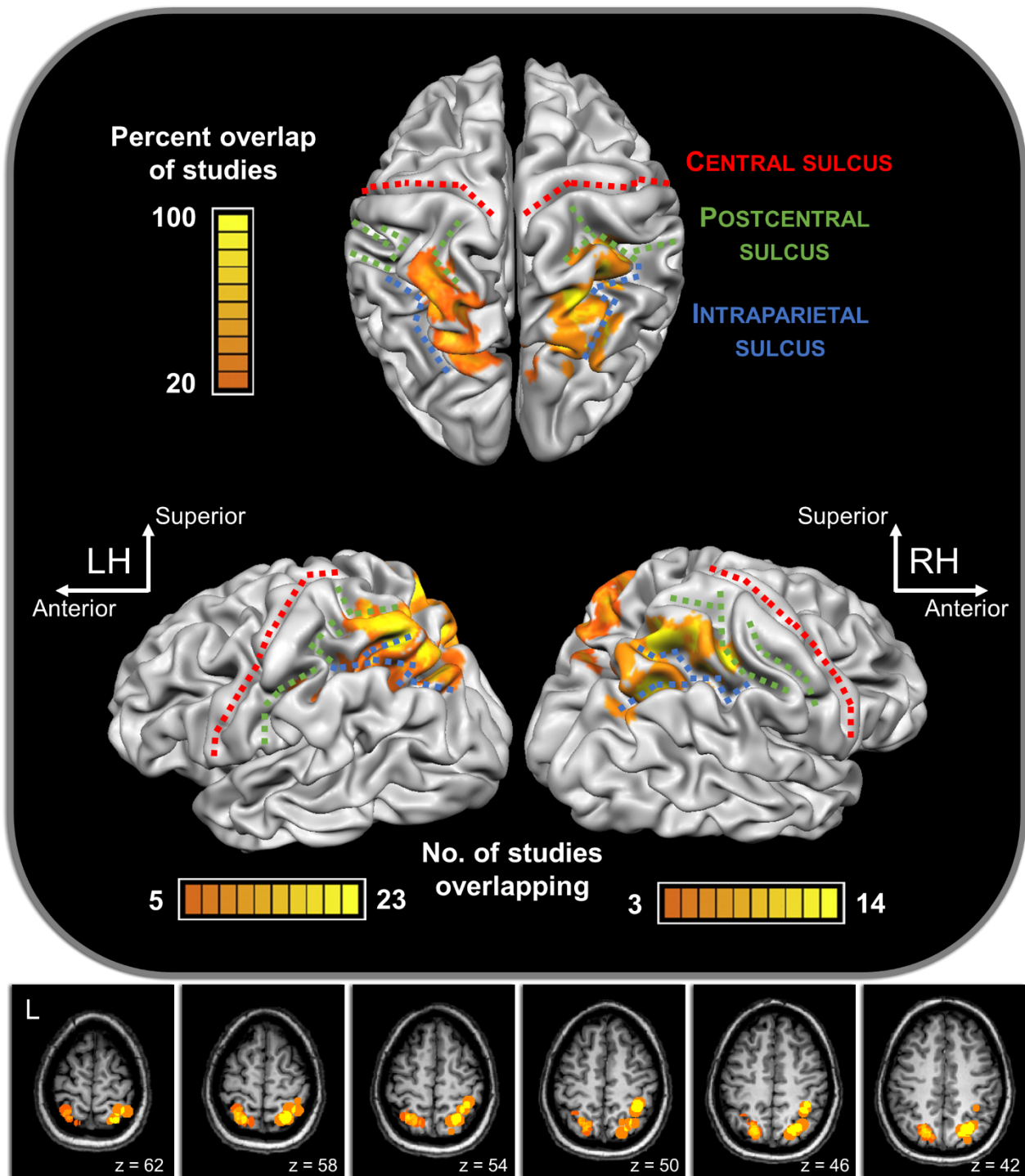
Figure 1.3. Comparison of reaching studies. The peak Talairach coordinates (converted from MNI space where required) of reported activity from published fMRI (14), PET (3), and TMS (7) studies involving reaching were used to create 15-mm-diameter spherical foci, and their voxel-wise overlap statistics. 23 and 14 studies reported coordinates in the left and right hemisphere, respectively. *Top:* Results are shown on a 3D cortical surface from a single subject in stereotaxic space. Dashed lines indicate the sulci. *Bottom:* Axial slice images show maximal overlap of studies. Only areas that were reported in >20% of studies are shown.

1.3.7 Summary

In humans, as in non-human primates, frontoparietal networks are shown to underpin visually guided reaching behaviour. In particular, neuroimaging investigations implicate regions encompassing the medial wall of the intraparietal sulcus, within the superior parietal lobule, and the more medial parietal-occipital area, in performing the sensorimotor transformations required for effector-specific movement planning. Patient lesion and TMS evidence demonstrate a causal role for the parietal cortex in mediating reaching actions. The mIPS is suggested to encode reaching direction and target location information required in both action preparation and online control, while evidence implicates the SPOC as predominantly involved in representing the reaching target, or movement goal, for hand and arm movements. For hand actions, these regions are shown to be organised with a contralateral limb preference.

1.4 Action selection

Previous portions of this chapter have outlined the cortical representation of hand movements, and indicate a dominant role of the distinct nodes of the PPC. In this section the notion that these regions, those associated with the *planning* and *online control* of hand action, are critically involved in *hand selection* is examined. Firstly, however, the role of the dorsal premotor cortex (dPMC) in action selection is introduced. As will be highlighted, the dPMC is considered the cortical hub of action selection. This description lends to a distinctive cognitive architecture for hand selection; the hypothesis that hand selection precedes action planning, and occurs outside of the sensorimotor areas of planning and control. However, motivated by the specific task conditions which have historically linked the dPMC with action selection, the differences in cued- versus free-choice tasks, and the consequences on both behavioural and neural measures, are discussed. These data are taken to indicate a disparity in the field that remains unaddressed. It is argued that true hand selection must be investigated in the absence of cued-selection, and in the context of dynamic choice. Following this, the cognitive and neural processes underpinning action selection are outlined, with particular reference to a multi-specification

framework and the *Affordance Competition Hypothesis* (Cisek, 2007). Finally, evidence in support and disagreement with this framework is presented.

1.4.1 The dorsal premotor cortex

The role of the dPMC in integrating visual information and motor plans has been highlighted previously (see Section 1.2.4). Alongside these functions, a dominant role of the dPMC specifically in the *selection* of appropriate motor actions has been outlined for decades (di Pellegrino & Wise, 1993; Halsband & Passingham, 1982; Kalaska & Crammond, 1995; Mitz, Godschalk, & Wise, 1991; Passingham, 1989; Rushworth, Johansen-Berg, Göbel, & Devlin, 2003; Toni, Thoenissen, & Zilles, 2001; Weinrich, Wise, & Mauritz, 1984; Wise, Weinrich, & Mauritz, 1983). Some of the most compelling evidence linking dPMC and action selection is presented by single-cell recording studies with non-human primates; where cells in the dPMC were shown to be preferentially modulated when the animal selected an appropriate motor response on the basis of an entrained, usually visual, cue (di Pellegrino & Wise, 1993; Halsband & Passingham, 1982; Mitz et al., 1991; Wise et al., 1983). Human neuroimaging also demonstrates modulation of the dPMC in associative visuomotor tasks, i.e. those involving definitive stimulus-response mappings (Thoenissen, Zilles, & Toni, 2002; Toni et al., 2001). Ablation of the dPMC results in the specific inability to learn stimulus-response associations, while visually cued object selection (Halsband & Passingham, 1985), and action repetition (Passingham, 1989) are not affected. The putative role of the dPMC in functions of action selection is also based on the cortical proximity and level of dense interconnections shared between the dPMC and primary motor cortex (Godschalk et al., 1984; Muakkassa & Strick, 1979; Taira, Tsutsui, Jiang, Yara, & Sakata, 2000).

The dPMC has since been theorised as the cortical hub of action selection, responsible for "selecting" an appropriate action from multiple plans received via reciprocal connections with the PPC, revising and consolidating a plan, before sending the chosen motor command to M1 (Gallese, Fadiga, Fogassi, Luppino, & Murata, 1997; Rizzolatti, Fogassi, & Gallese, 1997; Rizzolatti & Luppino, 2001; Taira et al., 2000). Neuroimaging evidence reveals that the Left-dPMC is active when participants select between movements executed with either hand, while actions with

the contralateral hand alone were shown to modulate activity in the Right-dPMC (Schluter, Krams, Rushworth, & Passingham, 2001). Further, TMS data demonstrate that stimulation of the dPMC disrupts movement selection, particularly the contralateral hand when applied to Right-dPMC, and either hand following Left-dPMC stimulation (Johansen-Berg et al., 2002; Schluter, Rushworth, Passingham, & Mills, 1998). Taken together, these data are argued to outline a dominant role of left-lateralised dPMC in action selection (Koch et al., 2006; Rushworth et al., 2003; Schluter et al., 2001).

1.4.2 Cued-selection versus free-choice

The context of action selection described above may, rather than choosing an action *per se*, moreso relate to selecting a learned visuomotor response on the basis of an arbitrary associated cue. Consequently, a leading role of the dPMC in selecting an action is emphasised, while the PPC is involved in the preparation of the associated motor plan. The notion that the dPMC is particularly concerned with action selection according to learned associations, as opposed to more organic reaching and grasping behaviour, is acknowledged (Rushworth et al., 2003). As will be described in this section, this selection behaviour differs fundamentally to situations where active and dynamic action options are available for selection, as in free choice paradigms. To clarify, cued-selection, cued-choice, and visuomotor association tasks are considered largely comparable. These tasks involve the "selection" of a *predetermined* or learned motor response. An important distinction is encapsulated in free choice tasks. Here, tasks explicitly lack a direct stimulus-response mapping, and selection closer reflects organic choice behaviour. There is a growing body of behavioural and neurophysiological evidence to support that movement-related frontoparietal activity is differently modulated by cued- versus free-choice tasks.

Firstly, behavioural evidence indicates that response times are significantly affected by volition, or the circumstances of selection (Oliveira, Diedrichsen, Verstynen, Duqué, & Ivry, 2010; Viswanathan et al., 2019). Oliveira and colleagues (2010) had participants perform unimanual reaches to targets presented in a semi-circular array in three conditions: predetermined left-hand use, predetermined right-

hand use, and free choice. Response times to initiate reaches were significantly increased in the choice condition, as compared to the collapsed left- and right-hand predetermined condition. This effect was observed around the locations in target space surrounding the point of subjective equality, which the authors associate with the highest degree of target and choice uncertainty. Similarly, Viswanathan et al. (2019) show an increase in the time-to-release for left- and right-hand button presses in free-choice versus cued-instruct conditions. These data indicate that there is a cost associated with choosing a hand, inciting the question: is there a difference in how these actions are generated neurally?

Viswanathan and colleagues (2019) also demonstrate a difference in the neural mechanisms that underpin freely chosen versus instructed actions using electroencephalogram (EEG). Their results reveal differences across both event-related potential (ERP) and EEG measures for cued versus freely chosen movements. Firstly, within the movement-related ERP component, the peak negativity assessed at ipsilateral sensorimotor electrodes was reached later in the free choice condition compared to the instructed. This temporal difference was evaluated using the phase relationship of δ-band oscillations. The dynamics of the δ-phase across conditions were near opposite. The authors suggest that this result signifies the differing motoric representations of these actions. Further, the timing of the contralateral β-rebound, a measure which characterises the termination of a movement, was affected by action condition. The onset of the β-rebound was linked to the "push" component of a button press in the cued condition only. The β-rebound was linked to the "release" component for freely chosen actions. The absence of push-evoked β-rebound in the choice condition is consistent with the notion of distinct sensorimotor organisation between the volitional contexts. The increases in time taken to reach peak negativity and β-rebound onset are suggested to represent the neural encoding of a competing, but not selected, action (Viswanathan et al., 2019).

Pesaran, Nelson, and Andersen (2008) demonstrate that free choice selectively activates a frontoparietal decision circuit. In this study, monkeys were trained to perform instructed search and free search tasks with visually presented

targets. These tasks map on to the cued- versus free-choice selection, defined above. In the instructed search task, objects of different shapes were presented in various configurations and the animal would perform the associated sequenced search. In the free search task, visually identical objects were presented and the animal could search in any sequence. As a control, the instructed sequences were matched to the choice behaviour in the free search task. Analyses of the searching behaviour revealed condition-related differences. Free search movement choices had high intratrial variability, while instructed searches had fixed behaviour in compliance with the cued sequence. Analyses of the spiking and local field potential activity between the PRR and dPMC were conducted, measuring the action and synaptic potentials at an individual neuron-level and population-level, respectively. Specifically, the spike-field coherency was estimated between the dPMC-PRR and the PRR-dPMC, separately. Spike-field coherency measures how well local field potential activity is predicted by action potentials. That is, the timing of spiking activity, or action potentials in one region, is correlated with changes in the local field potential activity in another area. A high and significant level of coherence was observed between spiking activity in dPMC and the local field potential activity in the PRR for both tasks, though stronger in free search. Coherence between spiking activity in the PRR and the local field potential activity in the dPMC was significant in the free, but not instructed, search task. These effects were maintained during a variation of the search tasks, which forced fixation, accounting for the possibility that the observed coherence was attributable to eye-movements. The level of activity-coherence across the frontoparietal circuit decreased dramatically in another control task, where the animal was instructed to move from a central location to a single peripheral target. Taken together, these data are interpreted to indicate that free-choice, but not instructed, search selectively activates the frontoparietal reaching circuit, and that decision making is distributed across nodes of the network (Pesaran, Nelson, & Andersen, 2008). Overall, these studies outline key differences in the how cued and freely selected actions are mediated by the brain, with both behavioural and neural consequences. What is considered to drive these differences, and the relation to action selection, is discussed in the proceeding section.

1.4.3 The multi-specification account

The data reviewed above establishes the existence of fundamental differences in the neural representation of action selection in cued-selection versus freely chosen contexts. Results implicate a reduced contribution of the greater frontoparietal reaching network in action selection for the former, association-based, selection, where the dPMC is evidenced to play an essential role. To date, action selection in free choice paradigms remains relatively under-investigated, though available data suggest that the PPC is involved. It is important to address this lack of empirical inquiry, and disentangle the role, if any, of the PPC in selection. In this section, data will be presented to outline that, in the absence of definitive stimulus-response mappings, multiple action plans are specified simultaneously within the reaching network; referred to here as "multi-specification". Further, the implication that these action plans are directly related to action selection is posed.

Psychophysical evidence shows that in speeded movement tasks, where a movement must be initiated prior to knowing which of the several targets is to be selected, spatial average behaviour is displayed whereby the initial aim of a reach or saccade is performed toward the midpoint of available options, consistent with the idea that the average of multiple competing actions is executed (Chapman et al., 2010; Ghez et al., 1997; Stewart, Gallivan, Baugh, & Flanagan, 2014; Van der Stigchel, Meeter, & Theeuwes, 2006). It was recently shown that additional motoric factors, outside of reach direction, are also encoded for competition. Specifically, the planned sensorimotor control policy, or *feedback gains*, of movements toward multiple targets corresponded to the average gains on trials with an unambiguous target (Gallivan, Logan, Wolpert, & Flanagan, 2016).

Multiple lines of neurophysiological evidence also reveal that several plans are specified in the frontoparietal reaching network in response to a single target, even when no overt action is performed (Andersen et al., 1997; Christopoulos, Bonaiuto, & Andersen, 2015; Cisek & Kalaska, 2005; Gallivan et al., 2016; Kalaska & Crammond, 1995; Kalaska, Scott, Cisek, & Sergio, 1997; Klaes, Westendorff, Chakrabarti, & Gail, 2011; Pastor-Bernier & Cisek, 2011a; Snyder et al., 1997; Suriya-Arunroj & Gail, 2019; Viswanathan et al., 2019). Though, in a cued-selection

reaching paradigm, evidence against a multi-specification account is also available (Dekleva, Kording, & Miller, 2018). Ultimately, this modulation suggests that, under certain task conditions, the PPC and interconnected premotor areas are interested in evaluating the motor significance of a sensory stimulus, irrespective of the likelihood of providing a response.

The significance of multi-specification has been linked to action selection (Cisek & Kalaska, 2005, 2010; Gallivan et al., 2018, 2016; Klaes et al., 2011). Cisek and Kalaska (2005) explicitly investigated this phenomenon. Here, cell recordings in the dPMC show that two separable populations of neurons are active during the instructed delay period of a two-target reaching task – i.e. during the planning phase of movement (Cisek & Kalaska, 2005). In the task, the animals were briefly presented two targets visually. Following a delay period, a non-spatial colour cue signalled which of the two cued targets was the selected target for movement. When two potential targets appeared in the visual cuing period, two distinct signals were modulated in the dPMC. Consistent with the hypothesis that these populations encode possible actions, cell activity was shown to reflect the preferred stimulus-response vector. When the colour cue specified the selected target, activity changed abruptly; cells attuned to the selected direction increased their firing, while the cells tuned to the alternative target location were rapidly suppressed (Cisek & Kalaska, 2005). Cell activity in the dPMC evoked by the movement information specified by the cued targets reveal that each population reflected motor intention; populations encoded the upcoming spatiotemporal parameters for reaching to a specific target. This neural activity is argued to signify the initial preparation of multiple executable actions toward the targets which, with the accumulation of task-relevant information, compete for overt execution (Cisek & Kalaska, 2005).

In another study, the dynamics of dPMC activation was further investigated (Pastor-Bernier & Cisek, 2011a). Specifically, whether decision-related variables, such as target-value and the spatial relationship between targets, had an effect on dPMC activity. When cued targets were associated with differing reward values, the cell population dedicated to a particular action was modulated by the value of their preferred target, *relative* to the value of the other target (Pastor-Bernier & Cisek,

2011a). This pattern was not observed in the absence of a prospective alternative, and is linked explicitly with choice behaviour. Further, the delay-period activity was also modulated as a function of *angular* distance between the cued targets. Targets presented at a closer angular distance evoke similar reaching parameters that compete for overt execution. In turn, this competition increases the level of recorded activity. Conversely, activity was weaker when the targets were presented further apart. The indication that targets presented in close angular proximity evoke an increased level of activity in the dPMC is in agreement with an underlying neuronal competition between potential action plans. Ultimately, these data support the notion that cell activity in the dPMC is influenced by the decision variables that are relevant for the action choice (Pastor-Bernier & Cisek, 2011a).

Klaes, Westendorff, Chakrabarti, and Gail (2011) address a persisting issue in the aforementioned studies – why are separate action possibilities represented in the dPMC, when the animal will eventually be cued to select a particular target? In other words, why is there action competition in a cued-choice paradigm? Using a reaching task which interleaved instructed and free choice trials, Klaes and colleagues (2011) demonstrate that the dPMC, as well as the PRR, are able to represent the potential *motoric goals* incited by a single cuing stimulus, rather than reflecting the *associated rule* (Klaes et al., 2011). In this task, animals are presented a target adjacent to a central fixation point. Following a memory-delay period, temporally jittered per trial, centrally presented colour cues signified two separate instruction contexts in 60-80% of trials; 1) move to the location of the initial target; 2) move to the location opposite the initial target. In a subset of trials (20-40%), no context information was provided, and the animal had free choice of movement. The subjective choice preferences of the animals were manipulated by varying the reward schedule in order to ensure a balance across the two potential motor goals. Under an explicitly rule-based hypothesis, it was argued that neural activity during the memory-delay period would reflect only one motor goal at a time. Under a goal-selection hypothesis, both potential actions would be encoded simultaneously. The response profiles displayed bimodal selectivity, and indicate that both motor goals are represented on a population level. This signifies that the brain is able to apply alternative rules to the same sensory cue, and that this information can be used to prepare separate action

plans within the frontoparietal reaching circuit, which compete for selection and overt execution (Klaes et al., 2011; Pastor-Bernier & Cisek, 2011b).

1.4.4 The Affordance Competition Hypothesis

The activation profiles exhibited in the neurophysiological data of Cisek and Kalaska (2005) and Pastor-Bernier and Cisek (2011a) are reliably reproduced in a computational model which stipulates that selection occurs via neuronal competition between the encoded potential actions within frontoparietal circuits (Cisek, 2006) (notably, Klaes et al. (2011) also comment that their data align with this framework). The model reliably simulated the activation patterns across the select brain areas relevant in the movement-decision tasks (i.e. the frontoparietal reaching circuit: dPMC, PPC, and M1), as well as the psychophysical properties of motor decision behaviour (Cisek, 2006). Taken altogether, these behavioural, neurophysiological, and computational data form the empirical basis of the *Affordance Competition Hypothesis* (ACH) (Cisek, 2007).

Briefly, the ACH outlines that selection may be viewed as continuous competition between viable action plans. Sensory information from the dorsal visual stream is used to specify the sensorimotor parameters of several potential actions in parallel. Here, the model borrows from the idea of *"affordances"*, referring to the internal representation of potential actions that are presented by the environment (Gibson, 1979). Action plans are simultaneously represented within frontoparietal circuits by cell populations which encode a preferred action. Populations do not encode a sole movement parameter, but rather can represent a distribution of potential values of movement parameters, such as movement direction; akin to a probability density function (Parzen, 1962). Plans compete for overt selection via a process of excitation and inhibition. Neurons encoding similar actions mutually excite each other, while in turn they exert an inhibitive influence on opposing populations encoding dissimilar actions. A variety of biasing signals are integrated into the preparation of plans, biasing the selection competition until a single response is selected. In the case of reaching actions, biasing inputs are received from prefrontal regions and the basal ganglia (Cisek, 2007).

Importantly, the ACH does not stipulate that every executable action plan is prepared, of which there would be near infinite. Rather, it is suggested that the relevant information processed by the dorsal visual stream, as well as the inputs from other brain areas, are used to construct a viable action plan, which is executable under the constraints of biomechanics, time, and space – which the authors pose is comparable to Gibson's *affordances* (Cisek, 2007; Cisek & Pastor-Bernier, 2014; Gibson, 1979). In line with this, neural activity within the frontoparietal reach network reflects the subjective decision *preference* of the behaving agent, instead of encoding every movement option (Klaes et al., 2011).

A core principle of the ACH can be characterised as follows: in a context demanding the simple selection of an action plan, action selection occurs in the same circuits that prepare and guide the execution of that action (Cisek, 2007; Cisek & Kalaska, 2010; Gold & Shadlen, 2007). Here, "simple" is referring to selection without explicit constraints and context – e.g. void of stimulus-response associations. The ACH, then, argues against a serial progression from action selection to the preparation of a motor plan for execution, similar to the terms outlined in theories of economic decision making (Padoa-Schioppa, 2011), or classic cognitive theories which outline that selection is a "higher order" function that is entirely independent of the sensorimotor system (Tversky & Kahneman, 1981). Instead, the ACH is applicable for the more instantaneous "moment-to-moment" demands of action selection (Cisek & Pastor-Bernier, 2014). Moreover, this view outlines that "selection" is not a singular abstract computation, but rather is a consequence of the intention to perform a particular action (Cisek & Thura, 2018, p. 92). For this thesis, the concepts outlined by the ACH are adopted and applied specifically to *hand* selection. That is, hand selection occurs in parallel with hand action planning, and is resolved via neuronal competition between potential action plans. Additional constraints are also applied to the current rationale, as will be outlined in *Chapter 2*. Importantly, the sensorimotor network critically and causally contributes to action selection. In the case of hand choice behaviour, selection depends on the functions of the key nodes of parietal reaching network outlined in Section 1.3.2.

In line with the ACH, accumulating evidence suggests that activity within the non-human primate reaching network is modulated by decision variables. Within dPMC, for instance, activity related to an action choice is modulated by the robustness of target location in formation (Dekleva, Ramkumar, Wanda, Kording, & Miller, 2016; Klaes et al., 2011; Pastor-Bernier & Cisek, 2011a; Ramkumar, Dekleva, Cooler, Miller, & Kording, 2016), urgency (Cisek, Puskas, & El-Murr, 2009; Thura, Beauregard-Racine, Fradet, & Cisek, 2012; Thura & Cisek, 2014, 2016), target-value (Pastor-Bernier & Cisek, 2011a), and reflects changes in mind (Pastor-Bernier, Tremblay, & Cisek, 2012). In the PRR, neural activity is also selective for motor goals (Gail & Andersen, 2006; Gail, Klaes, & Westendorff, 2009), and can predict reach, but not saccade, action choices to targets in the preferred direction of the cell (Scherberger & Andersen, 2007).

Recent evidence indicates a causal role of the PRR in action selection (Christopoulos, Bonaiuto, Kagan, & Andersen, 2015). In this study, animals were trained to perform memory-guided reaching and saccade tasks. Targets carrying equal reward were presented in opposite visual fields under two conditions. In the presence of a visual cue, animals were instructed to perform a reach or a saccade toward an intended target. Without a cue, animals freely selected between targets presented in the left and right visual field. Following reversible inactivation of PRR, performance in the reaching task was significantly altered compared to control sessions. Specifically, inactivation of the PRR selectively decreased freely-chosen reaches toward targets in the contralateral visual field, while instructed reaches to these targets were unaffected. Importantly, no significant alterations in saccade behaviour were evoked following PRR inactivation compared to control sessions. Given that saccade and instructed reaching behaviour were preserved, the decrease in freely-chosen contralateral reaches cannot be attributed to a deficit in spatial awareness or attention (Christopoulos et al., 2015). These results are the first to demonstrate a causal role of PRR in action selection, extending the role of parietal regions from reach planning to include selection.

In a subsequent study, Christopoulos and colleagues (2018) provide evidence of a double dissociation. Inactivation of lateral intraparietal area, an area strongly

implicated in the planning, selection, and control of eye-movements toward a target (Shadlen & Newsome, 2001), is shown to predominantly effect oculomotor, rather than reach, decisions (Christopoulos, Kagan, & Andersen, 2018).

1.4.5 The role of the posterior parietal cortex

In humans, evidence suggests that the sensorimotor system may also contribute to action selection (Ariani, Wurm, & Lingnau, 2015; Hamel-Thibault, Thénault, Whittingstall, & Bernier, 2016; Oliveira et al., 2010; Tosoni, Galati, Romani, & Corbetta, 2008). Perhaps most relevant for this thesis, Oliveira and colleagues (2010) applied single-pulse TMS to the PPC during reach-planning and assessed the effects of stimulation on hand selection behaviour. The experimental task of this study has been described previously in Section 1.4.2. Briefly, participants performed unimanual reaches to a semi-circular array of visually presented targets in both free and predetermined hand choice conditions. Their results reveal that TMS applied to Left-PPC led to decreased contralateral hand choices. TMS to Right-PPC, however, did not alter hand choice behaviour.

Conversely, it has been suggested that parietal modulation during action selection may reflect, rather than the action intention *per se*, abstract categorical outcomes linked with the experimental paradigm (Freedman & Assad, 2011). Also in refute of the parietal involvement in hand choice, Bernier, Cieslak, and Grafton (2012) suggest that action and effector selection precede reach planning. Here, in a visuomotor association task, the authors provide EEG and fMRI evidence to demonstrate that the activity within the dPMC and dorsomedial PPC was observed after target onset in the contralateral hemisphere only. The lack of ipsilateral modulation is taken to suggest that the alternative action, with the other hand, was not prepared in tandem. Further, the authors argue that the latency of evoked activation was delayed with respect to when the arm was required to be selected during movement planning. Taken together, these results imply that hand choice is determined prior to the specification of a singular motor plan (Bernier, Cieslak, & Grafton, 2012). However, as discussed previously (Section 1.4.2), visuomotor association tasks restrict selection behaviour, with behavioural and neural

consequences. The neural underpinnings of hand selection in a context free of stimulus-response associations has yet to be adequately assessed.

1.5 Thesis overview

In the previous sections of this chapter, an empirical summary is provided which outlines the role of the PPC in hand actions. The dorsomedial reaching circuit is highlighted, and the nodes subtending the computations necessary for visually guided reaching have been discussed. Regions encompassing the medial bank of the intraparietal sulcus, within the superior parietal lobule, and the superior parieto-occipital cortex are implicated specifically in performing the sensorimotor transformations critical for hand movements. Evidence has been presented to indicate that these regions are organised with a preference for the contralateral limb. The notion that the same neural mechanisms subtending hand action planning also mediate selection is posed; indicating a key role of the frontoparietal, dorsomedial, reaching circuit.

Whether the frontoparietal reaching network plays a causal role in hand choice, however, remains unclear. This thesis uses a multi-method approach to test the hypothesis that the same neural territories that specify the motoric parameters for movement causally contribute to hand selection. By virtue of this framework, hand choice is hypothesised to unfold in parallel with hand action planning via neuronal competition.

To date, there is no comprehensive dataset illustrating the contribution, if any, of the human PPC in hand selection. To address this, the first empirical chapter (*Chapter 2*) of this thesis investigates whether the PPC is indeed modulated in unimanual reaching decisions using fMRI. Here, a new neurobiological model of human hand selection is presented: the Posterior Parietal Interhemispheric Competition (PPIC) model. This model adopts the key features of the ACH (Cisek, 2007; Cisek & Kalaska, 2010) and additional constraints in order to specifically investigate hand selection. The PPIC model is used to outline the hypotheses in all empirical works of this thesis. As highlighted by Section 1.4.2, it is imperative that the neural mechanisms of hand selection are investigated in the context of free-choice

tasks. Free choice tasks have received a stark lack of empirical attention. In *Chapter 2*, a novel fMRI paradigm is also employed, which interleaves both instructed as well as free choice reaching trials in the scanner.

Secondly, in *Chapter 3*, the results of *Experiment 1* will be used to test whether the identified parietal regions are involved in hand choice, using fMRI-guided TMS. In a three-session repeated measures approach, changes in hand selection in a free-choice reaching task induced by TMS applied to the PPC are investigated.

The results of *Experiment 2* motivated a follow-up experiment. The outcome of this study is presented in *Chapter 4*. In particular, this investigation was conducted to corroborate the after-effects of the stimulation protocol applied in *Experiment 2*.

Finally, *Chapter 5* presents the general discussion. Results yielded throughout the empirical chapters of this thesis are synthesised and contextualised with respect to the current literature. The broader implications and future directions of this research are discussed with reference to both the scientific and clinical fields.

CHAPTER 2

This chapter is published as:

Acknowledgements

2.1 Abstract

The current study investigates a new neurobiological model of human hand choice: The Posterior Parietal Interhemispheric Competition (PPIC) model. The model specifies that neural populations in bilateral posterior intraparietal and superior parietal cortex (pIP-SPC) encode actions in hand-specific terms, and compete for selection across and within hemispheres. Actions with both hands are encoded bilaterally, but the contralateral hand is overrepresented. We use a novel fMRI paradigm to test the PPIC model. Participants reach to visible targets while in the scanner, and conditions involving free choice of which hand to use (Choice) are compared with when hand-use is instructed. Consistent with the PPIC model, bilateral pIP-SPC is preferentially responsive for the Choice condition, and for actions made with the contralateral hand. In the right pIP-SPC, these effects include anterior intraparietal and superior parieto-occipital cortex. Left dorsal premotor cortex, and an area in the right lateral occipitotemporal cortex show the same response pattern, while the left inferior parietal lobule is preferentially responsive for the Choice condition and when using the ipsilateral hand. Behaviourally, hand choice is biased by target location – for targets near the left/right edges of the display, the hand in ipsilateral hemispace is favoured. Moreover, consistent with a competitive process, response times are prolonged for choices to more ambiguous targets, where hand choice is relatively unbiased, and fMRI responses in bilateral pIP-SPC parallel this pattern. Our data provide support for the PPIC model, and reveal a selective network of brain areas involved in free hand choice, including bilateral posterior parietal cortex, left-lateralized inferior parietal and dorsal premotor cortices, and the right lateral occipitotemporal cortex.

2.2 Introduction

Deciding which hand to use to perform actions is one of the most fundamental choices humans make, and yet the brain mechanisms that mediate hand choice are poorly understood. According to traditional accounts of decision-making, the brain systems governing choices are separate from those that are responsible for the sensory guidance and control of actions (Padoa-Schioppa & Assad, 2006; Tversky & Kahneman, 1981). Numerous data from multiple domains challenge this view, however, at least with respect to those decisions that determine actions, and suggest that those brain areas important for the control of actions also contribute to action choices (Christopoulos, Bonaiuto, & Andersen, 2015; Cisek & Kalaska, 2010).

Convergent evidence implicates areas within the posterior parietal cortex (PPC), and interconnected premotor areas, as critical for the planning and control of actions (Culham & Valyear, 2006; Kalaska et al., 1997; Wise et al., 1997). These parietofrontal circuits are responsible for transforming sensory information to motor parameters for the control of actions (Jeannerod, Arbib, Rizzolatti, & Sakata, 1995; Rizzolatti & Luppino, 2001). This information is available in the neural response patterns within these areas before movements are initiated, and later within primary motor cortex, consistent with their necessary role in action planning and control (Crammond and Kalaska, 1996; Umilta et al., 2007; Schaffelhofer and Scherberger, 2016).

More recently, it has been suggested that these same parietofrontal areas causally contribute to action selection. The very same neural populations responsible for specifying the sensorimotor parameters necessary for the control of actions appear to mediate action choices (Cisek and Kalaska, 2005; Hanks et al., 2006; Scherberger and Andersen, 2007; Pesaran et al., 2008; Pastor-Bernier and Cisek, 2011; Thura and Cisek, 2014; Christopoulos et al., 2015b). These data form the bases of the Affordance Competition Hypothesis (Cisek, 2006, 2007; Cisek and Kalaska, 2010). According to this model, action choices are made by resolving competition between concurrently activated neural populations within parietofrontal areas that specify the spatiotemporal parameters of possible actions.

Motivated by the Affordance Competition Hypothesis, and on the basis of our recent fMRI evidence (Valyear and Frey, 2015), we propose a new systems-level model of human hand selection: The Posterior Parietal Interhemispheric Competition (PPIC) model (Figure 2.1). Our recent fMRI data suggest that specific areas within bilateral posterior intraparietal and superior parietal cortex (pIP-SPC) represent actions in hand-specific coordinates, and are predominantly contralaterally organized (Valyear and Frey, 2015). These response properties – hand-specific encoding and graded contralateral organization –, together with the population-level neural response principles defined by the Affordance Competition Hypothesis (Cisek, 2006), constitute the essential constraints of the PPIC model.

Neural populations within pIP-SPC are hypothesized to specify action plans in hand-specific coordinates, and compete for selection across and within hemispheres. Actions with either hand are represented bilaterally, but within each hemisphere a greater proportion of neural populations represents actions with the contralateral hand. Those populations encoding action plans with the same hand excite one another while those that represent actions with the opposite hand inhibit one another. When the activity levels of one population exceed a specific threshold, the parameters of the actions encoded – including the parameter 'hand' – are 'selected', and competing populations are inhibited.
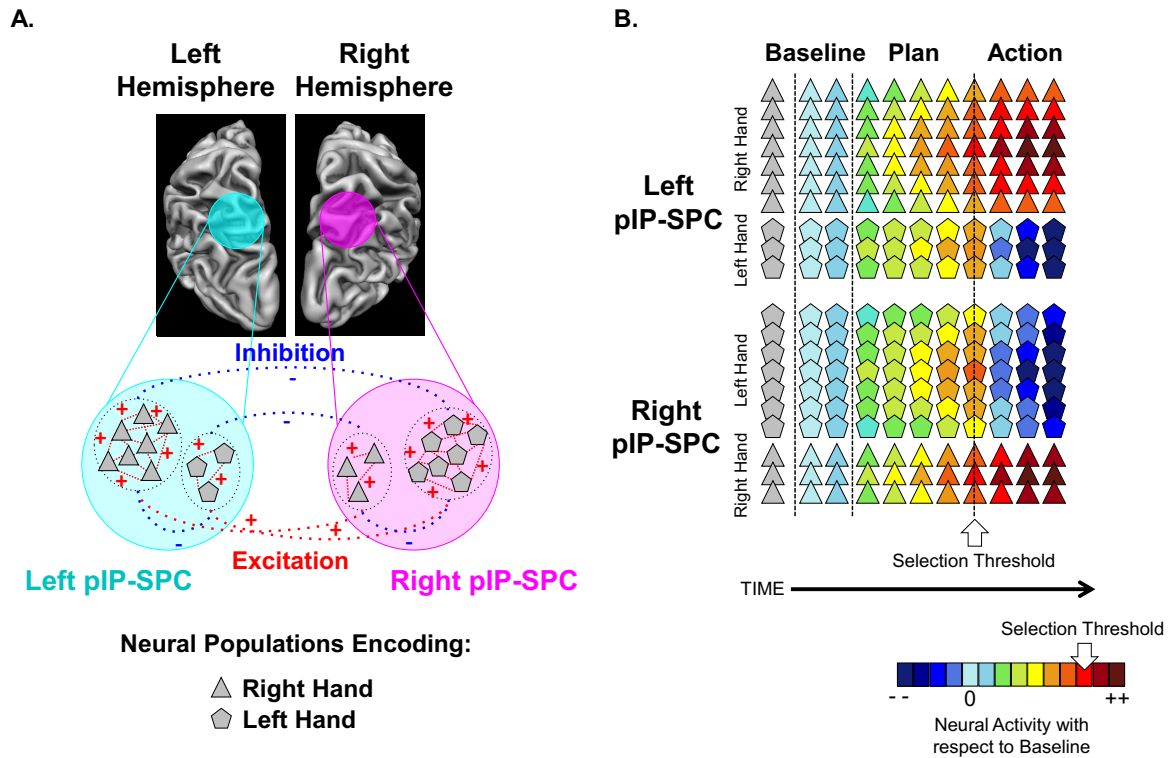
Figure 2.1. The PPIC model of hand selection. (A) Neural populations within pIP-SPC encode actions in hand-specific terms, and a greater number of cells encode actions with the contralateral hand. Cells encoding actions with the same hand excite one another while those that encode actions with the opposite hand inhibit one another. **(B)** Here we show an example of how activity changes in these areas over time in a case where the right hand is selected. During the planning phase the activity of all cell-types increase. The rate of increase depends on various factors, including target location. In this example, those cell populations encoding the right hand show a steeper rate of increase, and reach suprathreshold-activity-levels first. Once threshold is reached, the activity in these cell populations further increases and the spatiotemporal parameters of the actions they encode are selected, while opposing cell populations are robustly inhibited.

Distinct from the Affordance Competition Hypothesis, the PPIC model focuses on hand selection, and specifies interhemispheric competition between neural populations encoding hand-specific plans. The predominate contralateral organization of the underpinning neural architecture is an essential feature of the model. This organization drives the proposed interhemispheric competition, and imposes unique constraints on the predictions of the model. Areas within pIP-SPC should not only preferentially respond during conditions involving hand choice, but also for actions made with the contralateral hand.

Findings from a study by Oliveira et al. (2010) provide compelling evidence for the causal involvement of human PPC in hand choice, and suggest an underlying competitive process. Participants used either hand to reach to visual targets

presented in left and right hemispace, and the point in target space where the use of either hand was equally probable – the point of subjective equality (PSE) – was estimated. Consistent with a competitive process, response times to initiate actions were prolonged for reaches to targets near the PSE, and these effects were specific to when participants had to choose which hand to use. Further, TMS to the left hemisphere PPC increased the likelihood of reaches made with the left hand. Conversely, TMS to the right PPC did not influence hand choice. The data were interpreted as evidence that hand choice involves resolving competition between lateralized action plans localized within the PPC.

The current study tests the PPIC model, and the hypothesis that bilateral pIP-SPC plays an important role in choosing which hand to use to perform actions. Participants reach to visual targets while lying in the MRI scanner (Figure 2.2.A). In one condition, they are free to choose which hand to use (Choice), while in a second condition hand-use is instructed (Instruct). Targets are arranged symmetrically about the midline of the display, grouped near the centre (Central) and lateral edges (Lateral) of the display.

The PPIC model makes several specific predictions (Figure 2.2.B/C). First, bilateral pIP-SPC should respond preferentially for the Choice versus Instruct conditions. Critically, in-scanner videos are used to match subject's behaviour between Choice and Instruct conditions. Differences in activity levels between these conditions are not attributed to visual (or visual-attentional) or motor confounds. Second, bilateral pIP-SPC should respond preferentially for actions made with the contralateral hand – the left hemisphere pIP-SPC should respond more robustly for the selection and use of the right hand, and the right hemisphere pIP-SPC should respond more robustly for the selection and use of the left hand. Third, the anatomical specificity of these effects should correspond with areas previously implicated in the transformation of visual information to motor commands for the control of the arm for reaching.
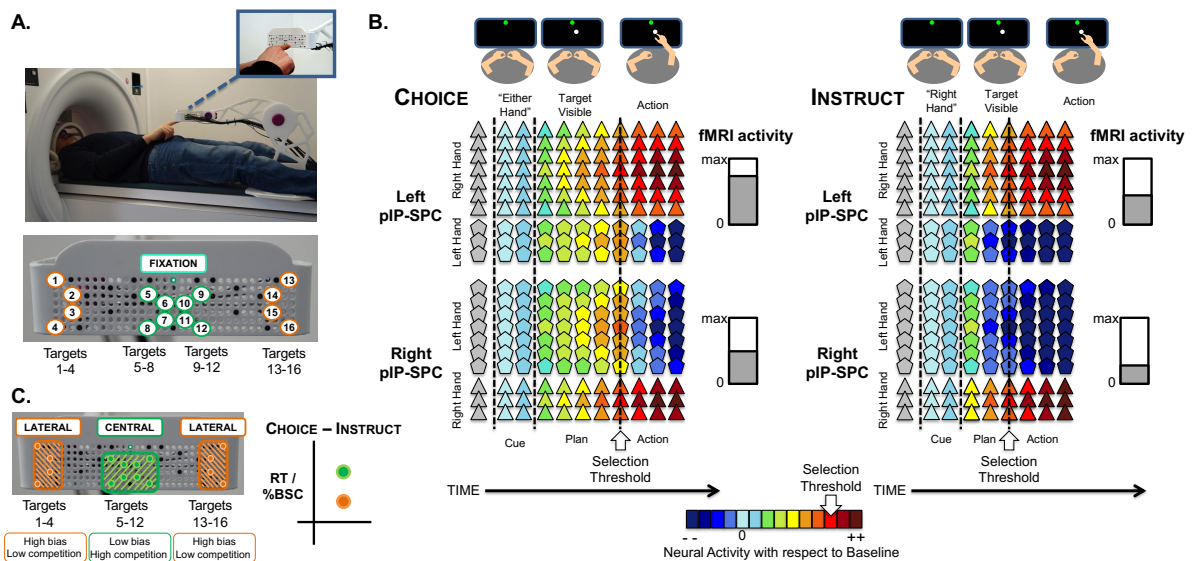
Figure 2.2. Methods and predictions. (A) Optical fibres are fitted to a display module and transmit light to provide 16 targets for reaching, arranged symmetrically around the midline of the display. Targets are presented at left/right Central or Lateral positions within the display. **(B)** The PPIC model predicts a main effect of Task (Choice > Instruct) and a main effect of Hand (Contralateral > Ipsilateral) within bilateral pIP-SPC. Neural populations encode hand-specific action plans, and within each hemisphere, the contralateral hand is overrepresented. Hand choice is determined by resolving competition between active populations. In this example, a Central target is presented and a right-hand response is selected. In the Instruct condition, the competitive process is supervened. This results in reduced fMRI activity levels and RTs relative to the Choice condition. Critically, Choice and Instruct conditions involve the same actions and visual stimuli. **(C)** Hand choice is biased by target location, as a consequence of differing biomechanical costs. Lateral targets represent a high bias, favouring the use of the ipsilateral hand. Stronger bias predicts weaker competition. Central targets represent similar biomechanical constraints for the use of either hand; low bias, and thus high competition. RTs and fMRI activity levels are expected to reflect this gradient: Greater choice-costs (Choice > Instruct) are predicted for Central versus Lateral targets.

A final set of predictions is tested. Intermanual differences in biomechanical and energetic consequences, related to the inertial properties of the arm (Gordon et al., 1994), bias both hand (Habagishi et al., 2014; Schweighofer et al., 2015) and arm-movement (Sabes and Jordan, 1997; Cos et al., 2011; Dounskaia et al., 2011) choices. When reaching to targets in either hemispace, the hand that is on the same side of space as the target is favoured, and this bias increases with target laterality (Stins et al., 2001; Oliveira et al., 2010; Valyear et al., 2018). As a consequence, Lateral targets in our display should favour the use of the hand in ipsilateral hemispace, while Central targets should represent more ambiguous choices. This gradient leads to specific predictions within the framework of the PPIC model. Lateral compared with Central targets are predicted to represent more sharply defined reach possibilities, and as a consequence, fewer competing neural populations will be activated and suprathreshold levels will be exceeded sooner – i.e. high- versus low-

levels of hand-choice-bias predict low- versus high-levels of competition (Figure 2.2C). These differences are expected to drive down choice-costs for reaches to Lateral versus Central targets. Both response times (RTs) and fMRI activity-levels are predicted to reflect this pattern: (Choice-Central > Instruct-Central) > (Choice-Lateral > Instruct-Lateral), and these fMRI effects should localize to bilateral pIP-SPC.

2.3 Materials and Methods

2.3.1 Participants

24 individuals participated in the study. One participant's data was excluded as they reported increasing levels of anxiety and discomfort during scanning, and discontinued testing after four functional runs. The remaining 23 participants (12 female; mean age = 23.2 ± 3.9 years, age range = 20 to 38) were right-handed according to a modified version of the Waterloo Handedness Inventory (Steenhuis and Bryden, 1989; scores range from -30 to +30) (mean score = 23.7 ± 6.2, range = 2 to 30). The experiment took approximately three hours to complete (including pre-scan training), and participants received financial compensation. An additional eight participants completed the pre-scan training (see Section 2.3.4).

All participants were naïve to the goals of the study, and had normal or corrected-to-normal vision, with no history of psychiatric illness. One participant reported prior clinical diagnoses of mild developmental dyspraxia, with no symptomology in adulthood. All participants provided informed consent in accordance with the Bangor University School of Psychology Research Ethics Committee.

2.3.2 Stimuli and presentation setup

Using a custom-built apparatus, targets for reaching were presented to subjects while lying supine in the MRI scanner (Figure 2.2.A). Optical fibres were fitted to the display module of the apparatus (17.5 cm x 6 cm), and used to transmit light to provide 16 targets for reaching, viewed via mirrors mounted to the scanner head coil. Active fibres were symmetrically configured within the display. This organisation ensured that target locations were represented equally across space. Specifically, 8 targets were positioned to the left and right of midline, and within each hemispace, four targets were positioned near the midline (Central), and four targets were positioned near the lateral edges (Lateral) of the display (see Figure 2.2.A). An additional 22 inactive fibres were included, pseudo-randomly arranged, and perceptually identical to the 16 active fibres. This was done to reduce the likelihood that participants would identify and memorize the active target configuration.

The display was adjusted so that all targets were comfortably reachable with either hand with minimal need to move the upper arm or shoulder. Depending on the participant's arm length, the display distance from the eyes was ~95 cm. Lateral targets were 7.6 cm (4.6°) and 6.6 cm (4.0°), and Central targets were 1.6 cm (0.97°) and 0.6 cm (0.36°) on either side of the display midline (visual angles are based on a display-to-eye distance of 95 cm, as calculated for one participant). Figure 2.3.A shows target distances from the midline of the display.

Participants held down response keys with the index finger of either hand in the rest position. The horizontal midline of the response pad was centred with the horizontal midline of the display module, and secured to the participant's abdomen near their waistline. In the rest position, the participant's left and right hands were 3.75 cm lateral to the horizontal midline of the display module. i.e., at rest, central targets were medial to either hand, and lateral targets were lateral to the nearest (ipsilateral) hand. Supplementary Materials include descriptions of in-scanner videos of participants performing the task (Appendix A, S1.1).

The apparatus remained outside the scanner bore with the participant localized to the isocenter of the magnetic field. Presentation software (Version 17.2, build 10.08.14) was used for stimulus presentation and behavioural response collection. An MR-compatible infrared-sensitive camera (MRC Systems GmbH) was used to record in-scanner behaviour for offline analyses (see Section 2.3.7.1).

2.3.3 Procedure

At rest, participants fixated a green coloured light-emitting diode (LED) transmitted via an optical fibre positioned in the middle and upper part of the display module (Figure 2.2.A). Trials began with a 600ms duration audio cue: "Left Hand", "Right Hand", "Choose". This was followed by a 200ms delay, and the illumination of a single target. Target illumination lasted for 1200ms. Participants were instructed to reach to targets as soon as they were illuminated, and to fixate targets during reaching. Actions were minimal-amplitude movements, involving mainly the wrist, fingers and thumb, and were approximately 1-3s in duration. Smooth movements, made at comfortable speeds were emphasized. Participants have full-vision

available during movements, and thus have visual feedback of their moving limb. Trials were separated by 10s intervals, from target illumination offset.

A slow event-related design was used for two main reasons. First, although perhaps more robust, a block design would be more susceptible to accumulative effects of fMRI-RS (or fMRI-adaptation) due to repeated use of the same hand, and in the case of the Instruct condition, repeated implementation of same rule. This would bias the Instruct condition to have reduced fMRI activity levels (fMRI-RS), and thus make interpretation of our predicted Choice > Instruct effects problematic. Second, a slow event-related design can reveal differences in baseline levels of activity between conditions that may arise prior to trial onsets, and otherwise complicate results interpretation. As such, we were able to rule out the possibility that such differences could account for our data (see Figures 2.5 and 2.6, event-related averaged time-course data).

Each run comprised 37 trials: 12 Choice, 12 Instruct Left Hand (Instruct-LHand), 12 Instruct Right Hand (Instruct-RHand), and lasted 7min and 30s (225 volumes). The first ("dummy") trial of each run was discarded from subsequent analyses, since its trial history could not be controlled. Runs included 6s (3 volumes) of rest to begin. Participants were asked to complete up to 8 functional runs, but were told that they could discontinue scanning if they became fatigued or uncomfortable. The majority of participants (N = 13) completed all 8 runs; 10 participants completed between 4 to 7 runs (mean = 5.4; mode = 6).

A custom Matlab (R2013b) script was used to create eight distinct run orders where trial history was balanced for each condition within runs. Specifically, 12 targets were presented per condition per run, balanced across Lateral and Central space, with an equal number of targets presented per hemispace, and the order of the presentation of each target position balanced across conditions. The presentation of run orders was pseudo-randomized across participants.

2.3.4 Pre-scan testing

Prior to scanning (mean = 5 ± 7 days, range = 1 to 27), participants took part in a behavioural training session. Training was performed in a mock scanner

designed to approximate the same physical constraints as the real MRI scanner but with no magnetic field. The same apparatus and materials used in the real MRI scanner were used for pre-scan testing (Figure 2.2.A). Participants completed a minimum of three, and maximum of four runs. A motion capture system, MoTrak (Psychology Software Tools Inc., 2012; version 1.0.3.4), was used to monitor participant head position during pre-scan testing.

The purpose of the pre-scan testing session was twofold. First, participants learned how to perform the task while keeping their head still. The problems associated with in-scanner head motion were thoroughly explained. Participants were told that their hand actions should involve minimal movements of the upper arm or shoulder, and that their head should be kept still at all times. Actions were trained to be performed smoothly. It is worth emphasizing here that the primary purpose of pre-scan training was to verify that participants could *keep their head still* while performing the task. Otherwise, the task was not difficult to learn or perform. For these reasons, we were unconcerned about large between-subject differences in timing between pre-scan and MRI testing.

Second, pre-scan testing was used to identify and exclude participants who either (1) moved their head too much, or (2) showed little variation in hand choice behaviour. Specifically, participants who showed evidence of excessive/abrupt head movements during the task, or who demonstrated > 75% use of the same hand during the Choice condition did not participate in fMRI testing. We recognize that these procedures introduce selection bias, and that this represents a limitation of our study. However, in the absence of sufficient variation in hand choice behaviour, we would be unable to test our current hypotheses.

Five participants (out of 34) were identified as showing > 75% use of the same hand during the Choice condition, and thus were excluded from fMRI testing. An additional five participants who completed pre-scan behavioural testing were later found to have (safety-related) contraindications for MRI testing, and were excluded.

2.3.5 Imaging parameters

Imaging was performed on a 3-Tesla Philips Achieva MRI scanner with a conventional 8-channel birdcage (SENSE) head coil. Functional MRI volumes were collected using a T2*-weighted single-shot gradient-echo echo-planar imaging (EPI) acquisition sequence: time to repetition (TR) = 2000ms; time to echo (TE) = 30ms; flip angle = 77°; matrix size = 64 by 64; field of view (FOV) = 256mm; slice thickness = 4mm; in-plane resolution = 4mm by 4mm; acceleration factor (integrated parallel acquisition technologies, iPAT) = 2 with parallel acquisition (SENSE). Each volume comprises 38 axial-oblique slices (0.1mm gap), spanning from the most superior point of cortex ventrally to include the entire cerebellum (i.e. whole-brain coverage). A T1-weighted anatomical image was collected using a multiplanar rapidly acquired gradient echo (MP-RAGE) pulse sequence: time to repetition (TR) = 1500ms; time to echo (TE) = 3.45ms; flip angle = 8°; matrix size = 224 by 224; field of view (FOV) = 224mm; 175 contiguous transverse slices; slice thickness = 1mm; in-plane resolution = 1mm by 1mm.

2.3.6 Functional MRI data preprocessing

Imaging data were preprocessed and analysed using Brain Voyager QX (BVQX) version 2.4.2.2070, 64-bit (Brain Innovation, Maastricht, The Netherlands). Each functional run was assessed for subject head motion by viewing cineloop animations and by examining Brain Voyager motion-detection parameter plots after running 3D motion correction algorithms on the untransformed two-dimensional data using BVQX trilinear (motion detection) and sinc interpolation (motion correction) options.

Functional data were preprocessed with linear trend removal and high-pass temporal frequency filtering to remove frequencies below three cycles per run. Functional data were aligned to anatomical volumes, and transformed to standard stereotaxic space (Talairach and Tournoux, 1988). Data were spatially smoothed for group analyses using a Gaussian kernel of 8mm (2 voxels) (full-width at half-maximum).

2.3.7 Data analysis

2.3.7.1 Matched Choice and Instruct conditions

In-scanner videos were used to match participant's motor responses between Choice and Instruct conditions. Specifically, for each target position presented within a given run, the hand used to respond during the Choice condition determined which of the two Instruct conditions – LHand/RHand – were defined as 'matched', and used for subsequent behavioural and fMRI analyses. For example, if target position 1 (see Figure 2.2.A) involved a left-hand response during the Choice condition, the corresponding Instruct-LHand trial for target position 1 was 'held' for analyses – defined as 'matched' –, while the Instruct-RHand trial for target position 1 from this same run was excluded from further analyses. This was an essential feature of our design. With this approach, comparisons between Choice and Instruct conditions, for both fMRI and RT data, are equated for motor and visual properties.

Videos were monitored and scored by an experimenter online, and independently scored by two additional experimenters, offline. Specifically, each observed participant performance and categorized the following errors: (1) Instruct trials were initiated with the incorrect hand; (2) movements changed abruptly during reaching; (3) no response was made. Errors in performing the task were scored (see Appendix A, Table S1.1), and these trials were excluded from RT analyses, and assigned a predictor of no-interest for fMRI analyses. Rater 1 scored all video data, while Raters 2 and 3 scored video data for the first 10 and 16 participants, respectively. We found no scoring differences between Raters, indicating that participant errors were unambiguous. For these reasons, it was deemed unnecessary to have all data scored by multiple Raters.

2.3.7.2 Behavioural data analysis

Hand choice: Point of subjective equality (PSE). Hand choice was coded online by an experimenter, and confirmed offline with video and button-release data. To quantify hand choice behaviour per participant, and at the group-level, target locations were reduced from 16 to 8 positions, depending on the lateral distance from midline (Figure 2.3.C), and the point in target space where the use of either

hand was equally likely was defined – the Point of Subjective Equality (PSE) (mean number of trials per target per participant = 20.5 trials, ± 0.91 SEM). Specifically, a psychometric function (McKee et al., 1985) was computed according to each participant's hand choice behaviour per target location, and the PSE was estimated by fitting a general linear model (as described in Valyear et al., 2018). The model contains target positions and a constant term, and uses a Logit link function to estimate the binomial distribution of hand choice responses (1 = right | 0 = left). Model coefficients are evaluated at 1000 linearly spaced points between the outermost values of the target array (i.e. ± 7.6 cm), and the value closest to a 0.50 probability estimate is defined as the PSE.

Pearson's *r* correlation analysis was used to test for a relationship between PSE and Waterloo handedness scores. A significant negative relationship was hypothesized. Positive Waterloo scores (max = +30) reflect (self-report) right-hand preferences, while negative PSE scores reflect right-hand choice preferences. Outliers were defined as ± 2.5 standard deviations from the group mean and removed from further analysis. Given the directional predictions of this test, we considered a one-tailed p < 0.05 as significant.

Response times. Response times (RTs) were defined as the time from the onset of target illumination to the release of (left/right hand) start buttons (i.e. times-to-movement onset). Data from pre-scan training trials were not included in these analyses.

We tested the effects of task instruction, hand used, and target location on RT with linear mixed-effects implemented using the lme4 package (Bates et al., 2014) for R (R Core Team, 2018). Statistical significance was tested for fixed effects by fitting the model with restricted maximum likelihood (REML), deriving degrees of freedom via Satterthwaite approximation using the lmerTest package (Kuznetsova et al., 2017). This approach has shown acceptable levels of Type I error for smaller datasets (<60 items; Luke, 2017). We contrasted levels of significant fixed effects with Tukey adjustment using the lsmeans package (Lenth, 2016).

We tested two models. Each model included the fixed effects of Task (Choice, Instruct) and Hand (LHand, RHand), but differed in how Target Location was defined. In the first model, Target Location was defined as Central (targets 5-12) and Lateral (targets 1-4 and 13-16) conditions. We refer to this model as RT-Central.

The second model was used to test for effects of Target Location defined according to individual-level PSE data. Specifically, Target Location was defined per individual as those targets nearest to the PSE, versus those in the far "extreme" lateral positions (ExLat; targets 1, 4, 13, 16) of the target display, corresponding with ±7.6 cm distances from the midline of the display (Figure 2.3.A). We refer to this second model as RT-PSE.

Both models permitted all possible interactions between fixed effects, and included a random intercept and slope for all fixed effects per subject and a random intercept per run.

We also analysed RT data using repeated measures analysis of variance (RM-ANOVA), and report these data in Supplementary Materials (Appendix A, S1.3).

2.3.7.3 Functional MRI data analysis

Analyses were based on a group-level random-effects (RFX) GLM with five predictors specified: Choice-LHand, Choice-RHand, Instruct-LHand, Instruct-RHand, and a predictor of no-interest (i.e. including the first trial of each run, unmatched Instruct trials, and errors). Predictors were modelled as two-volume (four second) boxcar functions aligned to the onset of each trial, convolved with the BVQX default two-gamma function designed to estimate the spatiotemporal characteristics of the Blood-Oxygen-Level Dependent (BOLD) response. Each run was percent-transformed prior to GLM analysis.

A group-level inclusion mask was defined, and used to constrain all subsequent tests. The mask comprised those voxels that were significantly identified by any of the following contrasts: (1) Choice-LHand > rest; (2) Choice-RHand > rest; (3) Instruct-LHand > rest; (4) Instruct-RHand > rest. The resultant statistical activation map was thresholded at $t(23) = 3.80$, $p < 0.01$ uncorrected, $p < 0.05$

cluster-size corrected (see Appendix A, Figure S1.1). The purpose of this method was to increase the sensitivity of subsequent statistical tests by reducing the number of voxels considered for correction for multiple comparisons to those that show task-related fMRI activity increases.

Voxel-wise conjunction contrasts. The PPIC model specifically predicts a main effect of Task (Choice > Instruct) and a main effect of Hand (Contralateral > Ipsilateral) within bilateral pIP-SPC (Figure 2.2.B). We use the following two conjunction contrasts to directly test these predictions:

> (1) (Choice-LHand + Choice-RHand) > (Instruct-LHand + Instruct-RHand)
> AND (Choice-LHand + Instruct-LHand) > (Choice-RHand + Instruct-RHand)

This conjunction tests for areas showing Choice > Instruct and LHand > RHand, predicted to identify the right hemisphere pIP-SPC (R-pIP-SPC).

> (2) (Choice-LHand + Choice-RHand) > (Instruct-LHand + Instruct-RHand)
> AND (Choice-RHand + Instruct-RHand) > (Choice-LHand + Instruct-LHand)

This conjunction tests for areas showing Choice > Instruct and RHand > LHand, predicted to identify the left hemisphere pIP-SPC (L-pIP-SPC).

Resultant activation maps were set to a statistical threshold of $t = 3.51$ ($p < 0.005$, one-tailed), corrected for multiple comparisons using Brain Voyager QX cluster-level statistical threshold estimator, found to indicate a minimum cluster size of (1) 298 mm³ and (2) 325 mm³ ($p < 0.05$) for each conjunction contrast defined above, respectively.

Region-of-interest (ROI) analyses. Multiple ROI-based analyses were performed. In all cases, mean percent BOLD signal change (%-BSC) values, represented as beta weights per condition of interest were extracted from each ROI, and tested. Hand specificity tests (Results Section 2.4.2.3) involved extraction of beta weights corresponding with unmatched Instruct trials from ROIs identified by voxel-wise conjunction contrasts, and comparisons between unmatched-LHand versus unmatched-RHand conditions using paired-samples t-tests, with $p < 0.05$ taken as significant. These data are independent of the data used to define ROIs.

Task by Target Location ROI-based analyses (Results Section 2.4.2.2) involved testing the RM-ANOVA interaction terms according to our a priori directional hypothesis: (1) (Choice-Central > Instruct-Central) > (Choice-Lateral > Instruct-Lateral); (2) (Choice-PSE > Instruct-PSE) > (Choice-ExLat > Instruct-ExLat). Here, we considered a one-tailed $p < 0.05$ as significant, given our predictions. These tests are orthogonal to the contrasts used to define ROIs.

Finally, we performed additional ROI analyses on the basis of our prior data showing fMRI repetition suppression for repeated hand actions within bilateral posterior parietal cortex (Valyear and Frey, 2015). Mean %-BSC values from the current data set were extracted from the complete set of active voxels identified from Valyear and Frey (2015) – comprising the ROIs: L-PPC, and R-PPC (Figure 2.6). This prior investigation involved an entirely different group of participants, and thus, these ROIs were defined independently from the current data.

2.4. Results

2.4.1 Behavioural results

Video data confirm that the task was performed correctly, and reveal very few errors (Appendix A, Table S1.1). Button release data is unavailable for four participants, due to technical errors.

2.4.1.1 Hand choice

Participants use both hands to respond to targets during the Choice condition, and there is a clear relationship between Hand and Target Position. Expressed as a function of quadrants of the target display (Figure 2.3.B) – left-Lateral (targets 1-4), left-Central (targets 5-8), right-Central (targets 9-12), right-Lateral (targets 13-16) –, the group data reveal that the left hand is typically used for targets in the left-Lateral quadrant, and the right hand is typically used for targets in the right-Central and right-Lateral quadrants, to the right of midline (Figure 2.3.B). Responses to the left-Central quadrant tend to involve a mixture of left- and right-hand responses. These differences were verified via a RM-ANOVA of arcsine transformed proportions of right-hand use (see Appendix A, S1.3.).

Subsequent analyses redefine target space as 8 conditions representing lateral distances from the midline, and reveal a group mean PSE – where the probability of hand choice is balanced between hands – of -1.30 cm, reflecting a leftward (right-hand) bias (Figure 2.3.C). The spread of individual-participant-PSE values includes -6.23 to 0.65, and for the majority of participants, overlaps with left- and right-central quadrants.

Correlation analyses between PSE and Waterloo handedness scores reveal a significant negative relationship ($r = -0.40$, $p < 0.05$). These results suggest that the leftward shift in PSE reflects the influence of hand preference – as a group, individuals are more likely to choose their preferred (right) hand to reach to targets.
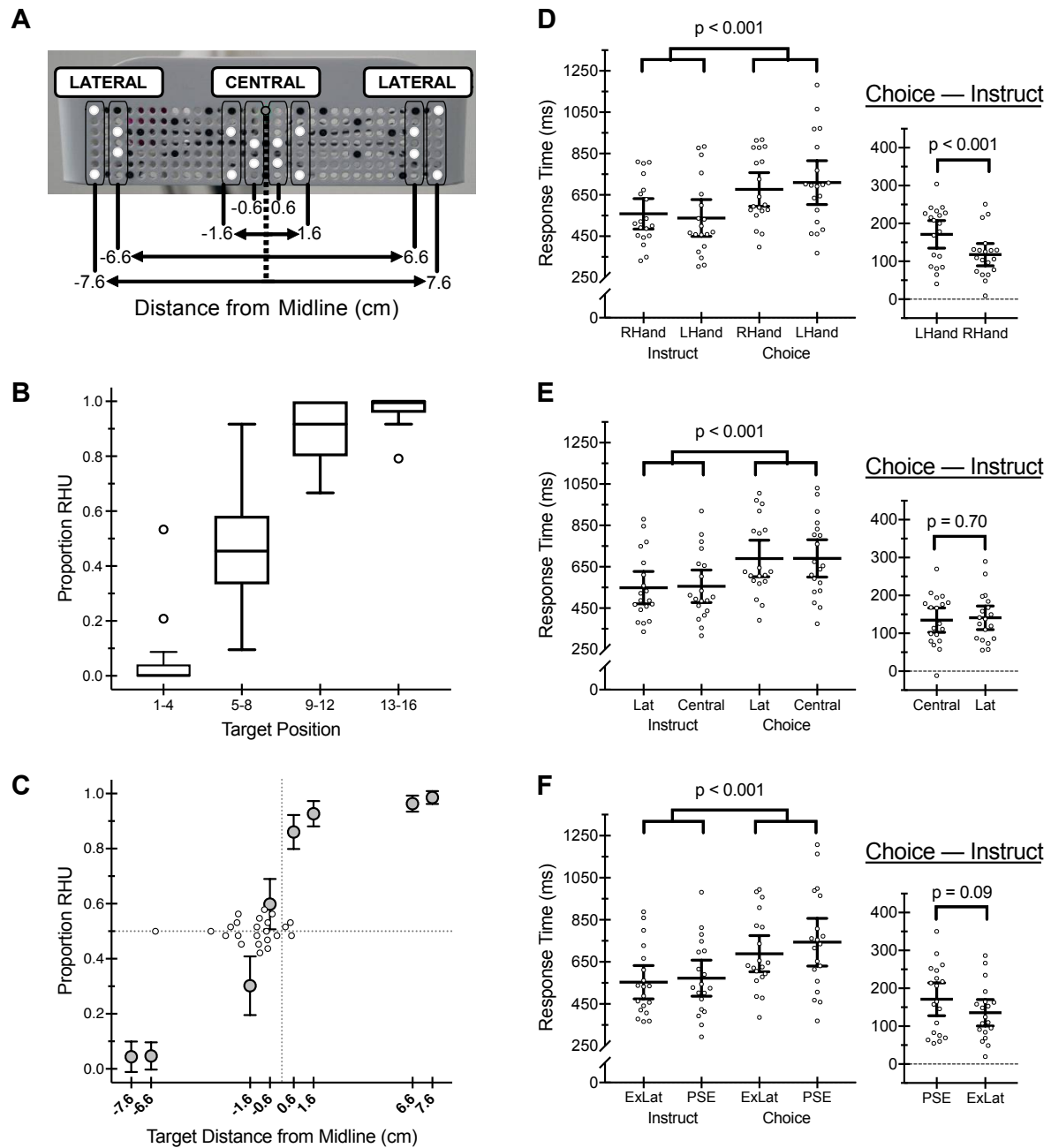
Figure 2.3. Behavioural results. (A) Target space defined as lateral distances from the midline of the display. **(B)** Boxplots showing the proportion of right hand use (RHU) per target quadrant. The lines within boxplots indicate the medians, the upper and lower edges indicate the third and first quartiles, respectively, and the error bars indicate the maximum and minimum data points (excluding suspected outliers). Suspected outliers (1.5*interquartile range above the third quartile or below the first quartile) are shown as unfilled circles. **(C)** Group mean proportions of RHU as lateral distances from the midline. Error bars reflect 95% confidence intervals (CIs). Individual-level PSEs are superimposed on this plot, indicated as unfilled circles. **(D)** Group (N=19) mean RTs as a function of Task and Hand (left), and group mean Choice – Instruct RT differences (right) are shown. Error bars reflect 95% CIs. Individual-level data are shown as unfilled circles. **(E/F)** Same as (D), but showing RTs as a function of Task and Target Location: (E) Central, Lateral; (F) PSE, ExLat.

2.4.1.2 Response times: Linear mixed-effects models

RT data are based on N = 19 participants.

The RT-Central model is a significantly better fit than a null model containing only its random effects (χ^2 = 76.0, p < 0.001), and reports a significant influence of Task (F(1, 19.9) = 112.9, p < 0.001). RTs are greater for the Choice versus Instruct condition (Figure 2.3.D/E/F), consistent with the additional time required to decide which hand to use – i.e. significant choice costs.

Two additional significant results are revealed. First, RTs are affected by an interaction between Task and Hand (F(1, 3108) = 17.0, p < 0.001). This reflects greater choice costs (Choice > Instruct) for the LHand, although choice costs are significant for both hands (Figure 2.3.D). Specifically, compared with the RHand, RTs are smaller with the LHand for the Instruct condition, yet larger with the LHand for the Choice condition.

Second, RTs are affected by an interaction between Hand and Target Location (F(1, 3104) = 12.1, p < 0.001). This result reflects a non-significant positive difference between LHand-Central – LHand-Lateral (p = 0.13) combined with a non-significant negative difference between RHand-Central – RHand-Lateral (p = 0.88). It is difficult to interpret these results, since the pairwise comparisons are both non-significant. No other significant effects are identified.

Contrary to our predictions, the interaction between Task and Target Location is non-significant (F(1, 3117) = 0.154 p = 0.695) (Figure 3E). These results indicate that the choice costs (Choice > Instruct) are similar for reaches to Central and Lateral targets.

We tested a second model – the RT-PSE model – instead defining Target Location per individual as those targets nearest to the PSE, versus ExLat (targets 1, 4, 13, 16; ±7.6 cm from the display midline). This model was also a significantly better fit for RTs than a null model omitting the fixed effects (χ^2 = 52.5, p < 0.001). Consistent with the results for RT-Central model, described above, these analyses

indicate that RTs are significantly influenced by Task ($F(1, 20.8) = 101.2$, $p < 0.001$), and by an interaction between Task and Hand ($F(1, 1508) = 8.04$, $p < 0.001$).

The results of the RT-PSE model also reveal a non-significant trend for the interaction between Task and Target Location $F(1, 1508) = 2.80$, $p = 0.09$) in the predicted direction: (Choice-PSE > Instruct-PSE) > (Choice-ExLat > Instruct-ExLat) (Figure 3F). Although not passing statistical significance, these results are consistent with the PPIC model, and other bounded-accumulation models (Cisek, 2006; Beck et al., 2008; Hanks et al., 2015), and are interpreted as evidence for a gradient of high (PSE) versus low (ExLat) areas of competition as a function of Target Location. No other significant effects are identified.

2.4.2 Functional MRI results

Participants were able to perform the task in the MRI scanner while keeping their head still (see Appendix A, Figure S1.2 for complete details).

2.4.2.1 Voxel-wise conjunction contrasts

The PPIC model predicts that bilateral pIP-SPC will respond preferentially to the Choice (> Instruct) and Contralateral (> Ipsilateral) conditions. Consistent with these predictions, the conjunction contrast Choice > Instruct AND LHand > RHand identifies significant activity within the right posterior intraparietal and superior parietal cortex (R-pIP-SPC), while the complementary conjunction contrast, Choice > Instruct AND RHand > LHand identifies significant activity within the left posterior intraparietal and superior parietal cortex (L-pIP-SPC) (Figure 2.4). Activity within the right hemisphere extends along the intraparietal sulcus, and includes distinct foci within the anterior intraparietal cortex (R-aIPC) and the superior parieto-occipital cortex (R-SPOC), medially, just anterior to the parieto-occipital sulcus. Activity within the L-pIP-SPC is comparatively more focal, largely restricted to intraparietal cortex.
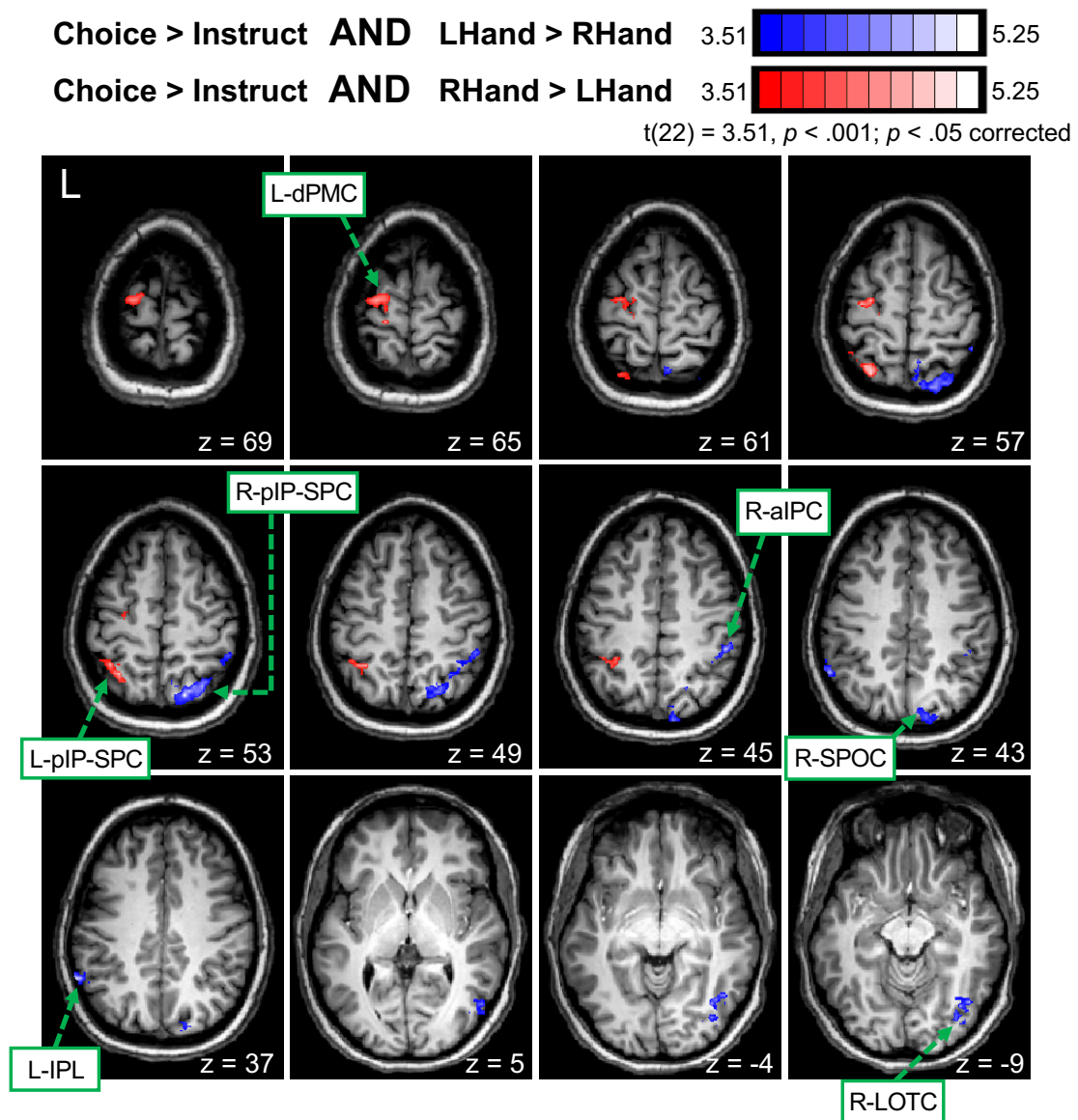
Figure 2.4. Functional MRI conjunction contrast results: Voxel-wise maps. Statistical activation maps showing significant responses for Choice > Instruct AND LHand > RHand (blue-to-white), and for the complementary conjunction contrast, Choice > Instruct AND RHand > LHand (red-to-white). Group data are shown on the anatomy of a single subject. Brain areas: left dorsal premotor cortex (L-dPMC); left posterior intraparietal and superior parietal cortex (L-pIP-SPC); right posterior intraparietal and superior parietal cortex (R-pIP-SPC); right anterior intraparietal cortex (R-aIPC); right superior parieto-occipital cortex (R-SPOC); left inferior parietal lobule (L-IPL); right lateral occipitotemporal cortex (R-LOTC).

The conjunction contrasts identify three additional brain areas (Figure 2.4). First, the contrast Choice > Instruct AND RHand > LHand reveals significant activity within the left dorsal premotor cortex (L-dPMC), at the junction of the precentral and superior frontal sulci. Second, the complementary conjunction contrast Choice > Instruct AND LHand > RHand identifies significant activity in two other areas: right lateral occipitotemporal cortex (R-LOTC), overlapping with the posterior middle

temporal gyrus, dorsally, and the fusiform cortex, ventrally; left inferior parietal lobule (L-IPL), at the intersection of the supramarginal and angular gyri. The L-IPL is the only area identified that shows stronger activity for responses made with the ipsilateral hand.

The event-related averaged %-BSC time-courses verify the timing of the effects within each area identified by the conjunction contrasts (Figure 2.5). This step is important to rule out possible differences between conditions that may arise prior to trial onsets; for example, related to previous trial history.

2.4.2.2 ROI results: Task by Target Location

A priori, we predicted that responses to Central versus Lateral targets would represent more ambiguous hand-use choices by virtue of the greater degree of inter-manual similarity in biomechanical and energetic costs associated with reaching to these target locations – relatively low bias, high competition (Figure 2.2.C). This difference would drive greater fMRI-activity-level differences between Choice and Instruct conditions in bilateral pIP-SPC.

Our fMRI data support these predictions. The patterns of %-BSC values extracted from four areas: L- and R-pIP-SPC, R-aIPC and R-SPOC are consistent with the predicted Task by Target Location interaction – i.e. (Choice-Central > Instruct-Lat) > (Choice-Lateral > Instruct-Lat) (Figure 2.5; Table 2.1). These effects reach statistical significance in R-aIPC, and near significance in areas R-SPOC ($p = 0.06$), L-pIP-SPC ($p = 0.09$) and R-pIP-SPC ($p = 0.08$). These results dissociate from our RT data, described above, where no statistical differences in choice-costs (Choice > Instruct) between Central and Lateral Target Locations are identified.
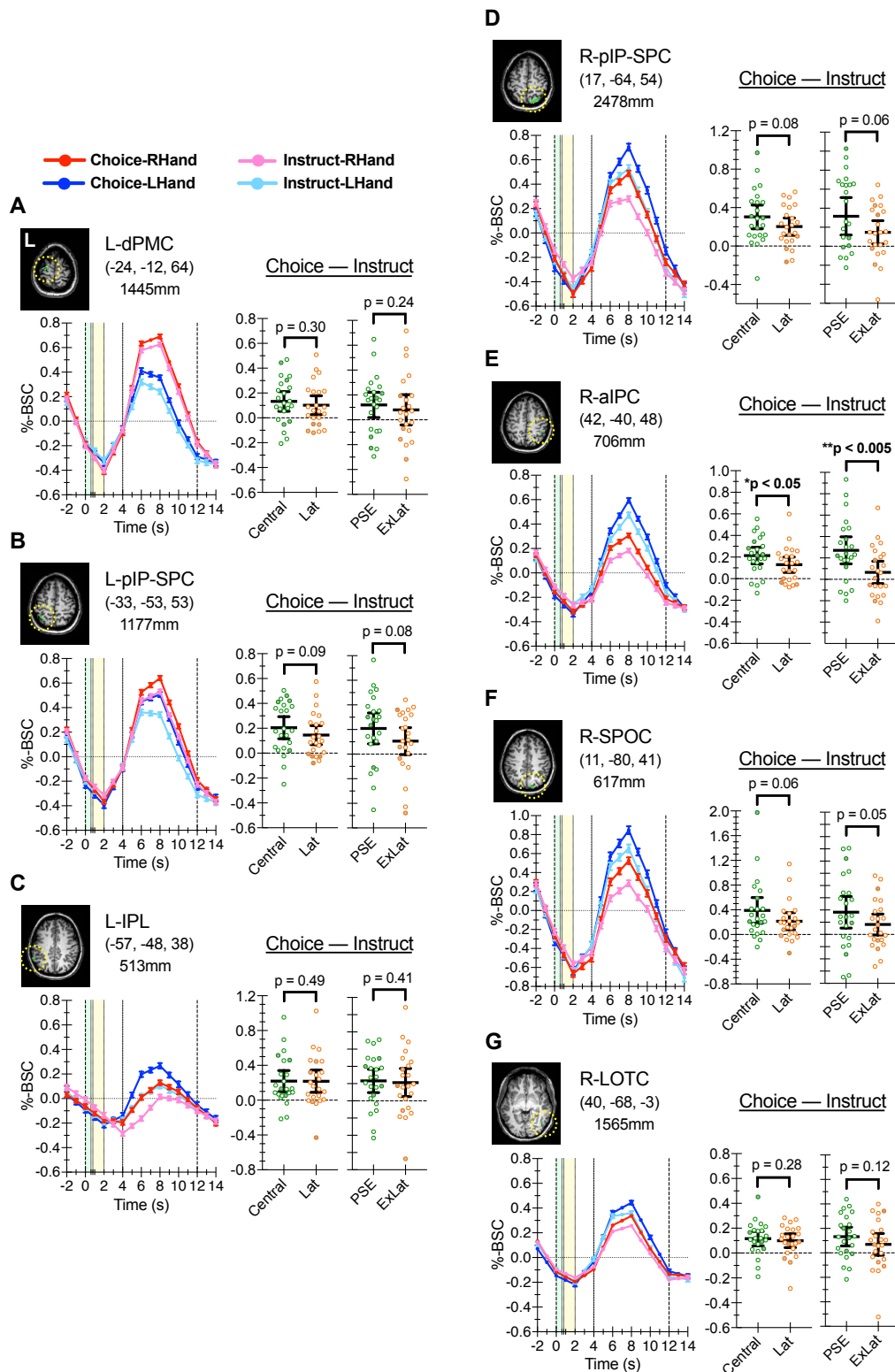
Figure 2.5. Functional MRI conjunction contrast results: ROI analyses. (A-G) Data extracted from areas identified via voxel-wise conjunction contrasts, as reported in Figure 4. Per area, time course data illustrate event-related averaged percent BOLD signal change (%-BSC) values per condition over time, aligned to the onset of the task instruction cue (green shading). The target illumination period is shown in yellow shading. Error bars in the time course data indicate SEMs. Scatter plots indicate %-BSC values expressed as difference scores between Choice – Instruct conditions as a function of Target Location: Central (green) versus Lateral (Lat) (orange); PSE (green) versus Extreme Lateral (ExLat) (orange). Open circles show individual participant scores. Participants without RT data are indicated as filled circles. Solid lines indicate group means with 95% confidence intervals. Brain area abbreviations are defined in Figure 2.4 caption.

When Target Location is defined per individual as those nearest to the PSE versus ExLat positions, similar findings are obtained. Again, fMRI response levels in bilateral pIP-SPC, R-aIPC and R-SPOC show the predicted Task by Target Location interaction: (Choice-PSE > Instruct-PSE) > (Choice-ExLat > Instruct-ExLat) (Figure 2.5; Table 2.1). This pattern of responses is specific to these brain areas, and is consistent with a competitive process underlying hand choice. Choice-costs are higher for responses made to targets near the PSE, where there is minimal bias in hand choice behaviour, and this is associated with significantly more pronounced differences in fMRI response levels between Choice and Instruct conditions. These fMRI data parallel our RT data, showing prolonged RTs for reaches to targets near the PSE for the Choice but not Instruct conditions (although as reported above, the RT data do not reach statistical significance; p = 0.09).

It is important to recognize that our tests involving the PSE versus ExLat conditions were unplanned, and in the case of our fMRI data, may be insufficiently powered; our experimental design provides limited numbers of trials per Task per Lateral Target Location per run. Low numbers of trials per condition per run is problematic for fMRI analyses. Given these limitations, these data should be interpreted cautiously. It is also possible, however, that these experimental-design limitations contribute to the relatively weak statistical significance of these effects.

2.4.2.3 ROI results: Hand specificity

Our voxel-wise conjunction contrasts identify areas showing both Choice > Instruct and Contralateral > Ipsilateral specificity (aside from the L-IPL, which shows stronger responses for actions with the ipsilateral hand). However, since hand-use and target location are tightly associated – i.e. the majority of left hand reaches are to targets in left hemispace, while the majority of right hand reaches are to targets in right hemispace –, interpretation of the Contralateral > Ipsilateral results is confounded. These effects may reflect specificity for actions/stimuli in contralateral hemispace.

To test this hypothesis, from each ROI identified by our conjunction contrasts we extracted data representing unmatched Instruct trials, and compared unmatched-

LHand versus unmatched-RHand conditions. Critically, these data are independent from those used to define the ROIs. The results reveal significantly greater fMRI responses for the use of the Contra- versus Ipsilateral hand, for all areas identified (aside from the L-IPL, which shows significantly greater fMRI responses for the use of the Ipsilateral – left – hand) (Table 2.1). Together with the conjunction contrast results, our data demonstrate hand specificity in these brain areas, independent of the spatial locations of targets in the display.

Table 2.1. ROI results for areas defined by the voxel-wise conjunction contrasts.

Brain Area	Hand Specificity (unmatched-Contralateral > unmatched-Ipsilateral)		Task by Target Location: Central/Lateral Interaction Term (1, 22)		Task by Target Location: PSE/ExLat Interaction Term (1, 22)	
	t	p	F	p	F	p
L-dPMC	8.90	<.001	0.53	0.24	0.53	0.24
L-IPL	-3.71	0.001	<.001	0.49	0.05	0.41
L-pIP-SPC	3.78	0.001	1.84	0.09	2.167	0.08
R-aIPC	3.44	0.002	4.55	0.02	8.73	0.004
R-LOTC	4.44	<.001	0.34	0.28	1.41	0.12
R-pIP-SPC	3.68	0.001	2.17	0.08	2.72	0.06
R-SPOC	4.28	<.001	2.55	0.06	2.80	0.05

2.4.2.4 ROI results: Independent tests of the PPIC model

Previous fMRI results from our lab (Valyear and Frey, 2015) constrain the anatomical specificity of the PPIC model to the posterior intraparietal and superior parietal cortex, bilaterally, and motivate two additional functional constraints: (1) hand-specific encoding, and (2) graded contralateral specificity. In other words, our model draws explicitly from these previous data; these same brain areas identified within bilateral posterior parietal cortex – labelled here as L- and R-PPC – are predicted to show both Choice > Instruct and Contralateral > Ipsilateral responses.

To test these predictions, we extracted the mean %-BSC values corresponding with Choice-LHand, Choice-RHand, Instruct-LHand, Instruct-RHand conditions from the complete set of active voxels identified within the L- and R-PPC on the basis of our previous study (Valyear and Frey, 2015), and entered these data

into a Task by Hand RM-ANOVA. As predicted by the PPIC model, the results reveal significantly stronger responses for both the Choice (> Instruct) and the Contralateral (> Ipsilateral) conditions within both the L- and R-PPC (Figure 2.6; Table 2.2).
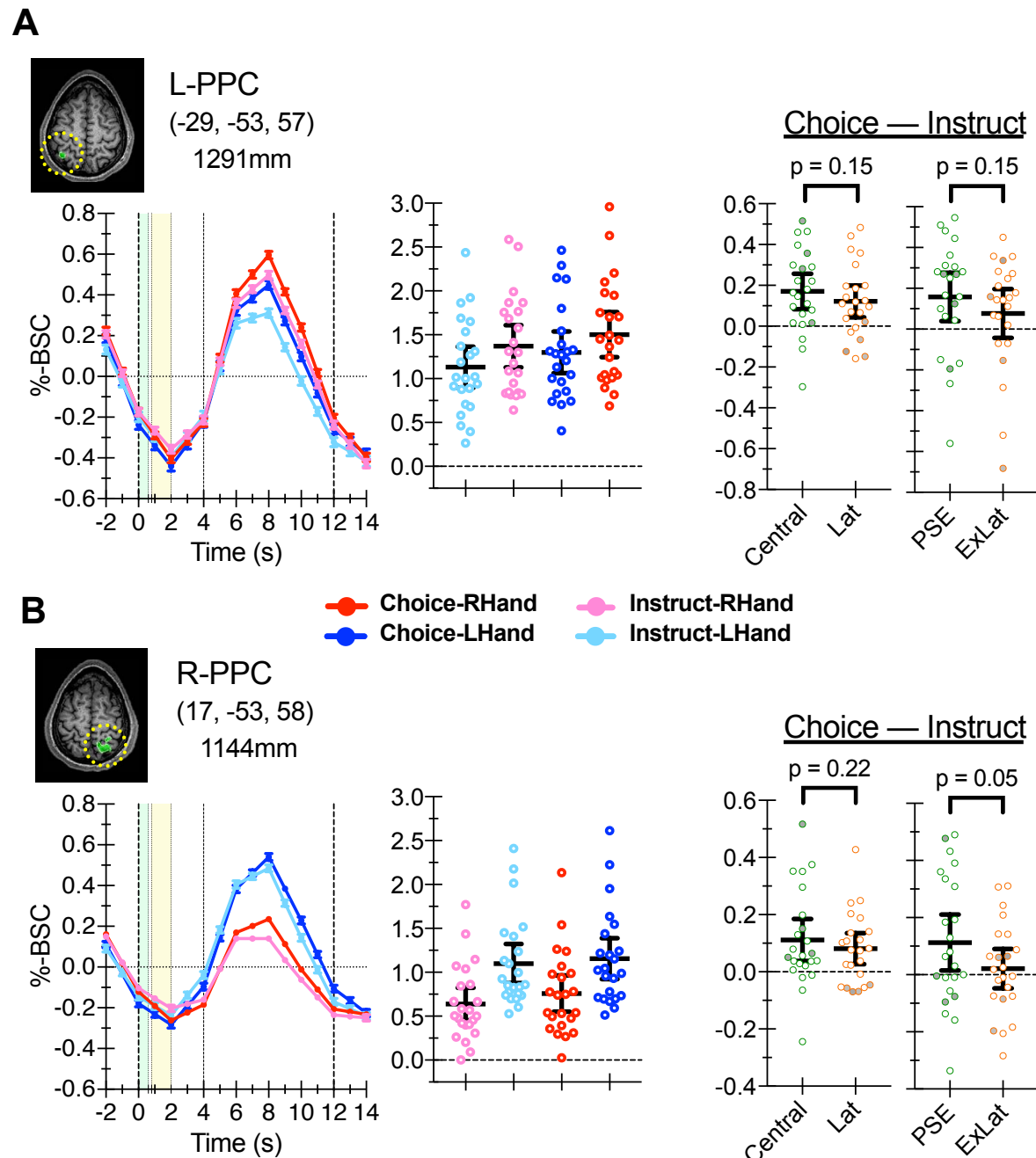
Figure 2.6. Functional MRI independent ROI results. (A/B) Functionally defined L- and R-PPC ROIs, respectively, independently defined on the basis of previous results from Valyear and Frey (2015). Time course data per ROI illustrate event-related averaged percent BOLD signal change (%-BSC) values per condition over time, aligned to the onset of the task instruction cue (green shading). The target illumination period is shown in yellow shading. Error bars in the time course data indicate SEMs. Scatter plots indicate %-BSC values per condition, with individual participant data shown as open circles. Solid lines indicate group means with 95% confidence intervals. The two leftmost scatter plots show %-BSC data expressed as difference scores between Choice – Instruct conditions as a function of Target Location: Central (green) versus Lateral (Lat) (orange); PSE (green) versus Extreme Lateral (ExLat) (orange). Participants without RT data are indicated as filled circles.

Post-hoc comparisons confirm greater responses for the Choice versus Instruct conditions for both Contra- and Ipsilateral conditions, within both L- and R-PPC (Figure 2.6). This is an important aspect of our findings, consistent with the PPIC model and the hypothesis that action plans for both hands are represented bilaterally within pIP-SPC.

Table 2.2. ROI results for areas independently defined on the basis of previous fMRI data (Valyear and Frey, 2015).

ROIs defined by Valyear and Frey (2015)	Hand by Task						Task by Target Location: Central/Lateral		Task by Target Location: PSE/ExLat	
Brain Area	ME Task (1, 22)		ME Hand (1, 22)		Interaction Term (1, 22)		Interaction Term (1, 22)		Interaction Term (1, 22)	
	F	p	F	p	F	p	F	p	F	p
LH-PPC	19.31	<.001	25.49	<.001	1.14	0.30	1.10	0.15	1.10	0.15
RH-PPC	11.32	0.003	126.73	<.001	4.70	0.04	0.60	0.22	2.91	0.05

We also tested for effects of Task by Lateral Target Location, according to both Central versus Lateral, and PSE versus ExLat conditions, respectively. The trends in both ROIs, though non-significant, are in the predicted directions, and in particular, reach near statistical significance ($p = 0.05$) in the R-PPC for the predicted (interaction) pattern of (Choice-PSE > Instruct-PSE) > (Choice-ExLat > Instruct-ExLat) (Figure 2.6; Table 2.2).

2.5 Discussion

The current data significantly advance our understanding of human hand choice behaviour. Few previous studies have investigated the brain mechanisms involved in 'free choice', and instead involve action selection on the basis of arbitrary rules. This is the first brain imaging study to investigate free hand choice in humans. Our findings reveal the selective involvement of a network of brain areas within bilateral posterior parietal cortex, left-lateralized inferior parietal and dorsal premotor cortices, and right lateral occipitotemporal cortex.

At the outset, we formulate a systems-level model of hand choice, the Posterior Parietal Interhemispheric Competition (PPIC) model. The model generates specific predictions, and provides a useful conceptual framework to constrain our results interpretations. We first evaluate our data within this framework, and then interpret the significance of our results revealing hand-choice selectivity in additional brain areas, not predicted by the model.

2.5.1 The PPIC model

According to the Affordance Competition Hypothesis (Cisek, 2007), the neural mechanisms that specify action possibilities in sensorimotor terms also play an important role in selecting among those possibilities. Areas within monkey superior parietal (Caminiti et al., 1996; Scherberger et al., 2005) and dorsal premotor (Scott et al., 1997; Hoshi and Tanji, 2004) cortices are necessary for the transformation of visual information to motor commands for reaching, and critically, the neural responses within these areas also reflect reach choices (Cisek and Kalaska, 2005; Scherberger and Andersen, 2007; Pesaran et al., 2008; Pastor-Bernier and Cisek, 2011; Thura and Cisek, 2014). Temporary inactivation of the "parietal reach region" – area PRR, located within the medial bank of the intraparietal sulcus – impairs reach (but not saccade) selection (Christopoulos et al., 2015b). These data provide powerful evidence for the causal involvement of the PPC in reach choices.

The PPIC model borrows from the neural population-level response dynamics specified by the Affordance Competition Hypothesis, and extends these principles to hand-specific encoding and hand selection. Neural populations within bilateral pIP-

SPC encode possible actions in hand-specific terms and compete for selection across and within hemispheres. Actions with either hand are represented bilaterally, yet within each hemisphere the contralateral hand is overrepresented.

Consistent with the PPIC model, our findings reveal the involvement of bilateral pIP-SPC in hand choice. Responses within pIP-SPC are significantly greater for the Choice versus Instruct condition, when hand use is freely selected. These effects are not attributable to motor or visual confounds, including potential differences in motor- or visual-response sensitivity to targets presented at different spatial locations. Choice and Instruct conditions are carefully matched for responses to each target location so that the contrast between these conditions is balanced for these features.

These same brain areas demonstrate a pattern of graded contralateral response specificity. Responses are strongest for actions made with the contralateral hand; although, actions with the ipsilateral hand also yield robust responses. Further, differences between Choice and Instruct conditions are not restricted to responses made with the contralateral hand. The Choice condition preferentially activates bilateral pIP-SPC, even for ipsilateral responses. This pattern is consistent with a role for the planning and selection of actions with either hand, as specified by the PPIC model.

The anatomical specificity of our data is consistent with the PPIC model, and the hypothesis that hand selection involves the same brain areas that are important for action planning. Bilateral pIP-SPC and R-SPOC showing preferential responses for the Choice condition closely overlap with areas implicated in the planning and sensorimotor control of the arm for reaching (Astafiev et al., 2003; Connolly et al., 2003; Medendorp et al., 2005; Prado et al., 2005; Culham and Valyear, 2006; Tosoni et al., 2008; Fabbri et al., 2010; Pitzalis et al., 2010; Vesia and Crawford, 2012; Andersen et al., 2014; Monaco et al., 2015). Consistent with our data, Beurze et al. (2007) demonstrate that during the planning phase of a reaching task, bilateral pIP-SPC integrates information about the spatial location of targets with the hand that will be used for reaching.

Finally, our results provide evidence for a competitive process underlying hand choice. Responses in bilateral pIP-SPC demonstrate increased levels of choice-specificity (Choice > Instruct) for reaches made to targets near the midline (Central) compared to the left/right (Lateral) edges of the display. These data are consistent with a gradient of increased levels of competition between neural populations representing hand-specific reach plans for targets near the midline, where inter-manual differences in the biomechanical and energetic costs associated with reaching are minimal.

Unexpectedly, however, our behavioural RT data reveal a more complex relationship between choice-costs and target location. Although RTs indicate significant choice-costs (Choice > Instruct), these costs are similar for reaches to Central and Lateral targets. Additional analyses indicate that for most participants the area in target space of maximal hand-choice ambiguity is shifted to the left of midline. This represents the theoretical point in target space where the use of either hand was equally probable – the PSE –, and a significant correlation between participant PSE and Waterloo handedness-preference scores suggests that this leftward shift reflects the influence of hand preference. Analyses of RT data indicate a non-significant (p = 0.09) trend in the predicted direction of greater choice-costs – greater Choice > Instruct differences – for reaches to targets near the PSE.

Complementary fMRI analyses reveal response patterns within bilateral pIP-SPC, R-aIPC, and R-SPOC that parallel these RT data – the strength of the Choice > Instruct differences in fMRI response levels in these brain areas are more pronounced for reaches to targets near the PSE. These particular aspects of our results should be interpreted cautiously, however. At this level, we may have too few trials per condition to reliably estimate fMRI responses. Notwithstanding these limitations, our PSE-level analyses reveal congruent fMRI and RT results that are consistent with the PPIC model, and a competitive process underlying hand choice. Choice-costs are higher for reaching to parts of target space where there is minimal bias in hand choice behaviour.

Although speculative, we suggest that our discrepant findings between RT and fMRI data regarding the influence of Central versus Lateral target locations

relate to differences in how biomechanical factors interact with hand preference to influence these measures. According to the PPIC model, Lateral versus Central target locations represent a narrower range of reach possibilities, and thus will activate fewer competing neural populations encoding those possibilities. As a consequence, the number of active neural units in competition, the time required for the activity of one population to reach suprathreshold levels, and the number of neural units that are actively inhibited after threshold is reached are reduced. All three of these factors will drive down fMRI response levels, while only the second factor – decreased times to reach threshold – will influence RTs. This can explain why, compared with RTs, fMRI data may show pronounced effects of target location.

According to these factors, however, RTs and fMRI activity-levels should nonetheless follow the same direction. Our Central-Lateral data do not. To explain this discrepancy, we suggest that hand preference influences hand choice by driving changes in the accumulation-to-threshold rates of competing neural units, and disproportionately influences RTs compared with fMRI activity levels. For Central targets in our display, increased accumulation-to-threshold rates in neural populations encoding the preferred (right) hand will reduce decision times and lead to the predominate use of the preferred hand. Despite these changes, however, the number of active neural units in competition, and the number of neural units that are actively inhibited after threshold is reached remain high. These differences, at least in principle, could explain why our fMRI data reveal greater Choice > Instruct effects for Central versus Lateral target locations while our RT data do not.

Other data are consistent with the current findings, and support the concept of simultaneously active reach plans competing for selection. When reaching to multiple potential targets, human behavioural (Gallivan et al., 2016; Gallivan et al., 2017), and monkey neurophysiological (Cisek and Kalaska, 2005; Scherberger and Andersen, 2007; Pastor-Bernier and Cisek, 2011) data suggest that parallel action plans are specified in motor (not visual) coordinates, and compete for selection. Further, although these studies tend to investigate reach choices involving the same effector, recent data suggest that similar "action-based" competitive models can explain effector-selection (Christopoulos et al., 2015a; Hamel-Thibault et al., 2018).

Using a free hand choice paradigm similar to that we use in the current study, trial-to-trial differences in pre-stimulus measures of cortical excitability over contralateral motor areas are shown to predict hand choice for reaching to targets near the PSE (Hamel-Thibault et al., 2018). Moreover, temporary inactivation of reach- (Christopoulos et al., 2015b) versus saccade-selective (Christopoulos et al., 2018) areas in monkey posterior parietal cortex (areas PRR, mentioned above, and the lateral intraparietal area, LIP, respectively) selectively impairs reach versus saccade choices, respectively, and these data can be explained by computational modelling that specifies competitive interactions between these brain areas (Christopoulos et al., 2015a). Conceptually, our PPIC model is consistent with this framework. In the PPIC model, parallel competitive interactions take place between brain areas in the PPC encoding hand-specific action plans, and mediate hand choice.

Our findings complement and extend those of Oliveira et al. (2010). Using single-pulse TMS, Oliveira et al. (2010) demonstrate a necessary role for the left PPC in hand choice. TMS to left PPC during the planning phase of a free-choice reaching task is shown to shift the probability of choices in favour of increased use of the left hand. Conversely, stimulation to the right PPC had no significant influence on hand choice. This asymmetry was unexpected, and the authors offered several possible explanations. Our new findings help to disentangle these interpretations.

First, Oliveira et al. (2010) speculate that perhaps the left- but not the right-hemisphere PPC represents action plans with both hands, and can therefore compensate for the disruptive effects of TMS to right PPC. Our data are inconsistent with this account, however. We find that both the L- and R-pIP-SPC respond preferentially when hand choice is necessary, and for both contra- and ipsilateral responses. If the right hemisphere PPC only represents action plans with the contralateral hand, preferential activity for the Choice condition for the ipsilateral hand is unexpected.

As another possibility, Oliveira et al. (2010) suggest that the critical functional area involved in hand choice may be more spatially restricted within the right PPC, and thus was not effectively disrupted via their TMS manipulation. Our data are inconsistent with this account, also. We find relatively widespread involvement of the

right hemisphere pIP-SPC in hand choice. If the critical area in right PPC was 'missed' by Oliveira et al. (2010), our data suggest that this was unlikely the consequence of spatially more circumscribed involvement of the right PPC in hand choice.

Finally, Oliveira et al. (2010) recognize that the absence of reliable right PPC TMS effects may relate to the strong right-hand bias present in their group of right-handers tested. This may have left little room for increased use of the right hand, following right PPC stimulation. Although our data do not directly address this possibility, this account remains tenable and represents an important hypothesis for future studies to investigate.

2.5.2 Visuospatial interpretations

Our data reveal the involvement of bilateral pIP-SPC in hand selection, and demonstrate that these areas show contralateral hand specificity, more robustly activated for actions made with the contralateral hand. Given that in our paradigm hand choice and space are closely associated, however, it is important to consider an account of the contralateral specificity of fMRI responses within bilateral pIP-SPC as attributable to visuospatial rather than (hand-specific) motor coding. Specifically, since reaches with the left hand are predominately made to targets in left hemispace, and vice-versa for right-hand reaches, contralateral specificity within bilateral pIP-SPC may reflect preferential neural responses for targets in contralateral hemispace, rather than the specification of hand-specific action plans.

Critically however, additional analyses controlling for target space confirm significant preferential fMRI responses for actions with the contralateral hand within L- and R-pIP-SPC. These data are not attributable to visuospatial coding, and instead reflect genuine contralateral hand-specificity. Also, preferential fMRI responses for the Choice condition in bilateral pIP-SPC are evident for actions made with the ipsilateral hand, a pattern that conflicts with a strictly visuospatial encoding account, but that is consistent with the PPIC model.

Notably, new behavioural data reveal that target space during a free hand choice reaching task similar to that used in the current study is represented in both

gaze- and head-centred reference frames (Bakker et al., 2018). Both gaze- and head-orientation are found to modulate hand choice. This raises the possibility that as part of the underlying brain mechanisms that mediate hand choice, spatial information about the targets of competing action plans is represented in multiple reference frames within bilateral PPC. Future work designed to investigate this hypothesis will be of value.

2.5.3 Additional brain areas

Alongside bilateral pIP-SPC, our results indicate the involvement of left dorsal premotor cortex (L-dPMC), left inferior parietal lobule (L-IPL), and right lateral occipitotemporal cortex (R-LOTC) in hand choice. All areas demonstrate significantly stronger activity for the Choice versus Instruct conditions. L-dPMC and R-LOTC are also more strongly activated for reaching with the contralateral hand, while the L-IPL is more strongly activated for reaching with the ipsilateral hand.

The dPMC is densely interconnected with intraparietal and superior parietal areas, and together these areas mediate the planning and online control of reaching (Scott et al., 1997; Wise et al., 1997; Vesia et al., 2005). The involvement of dPMC in the planning and selection of reaching actions is predicted by the Affordance Competition Hypothesis (Cisek, 2007), and supported by various data (reviewed above). Graded contralateral specificity within dPMC is also consistent with previous data (Medendorp et al., 2005; Beurze et al., 2007). The significance of the left-lateralization of these results is unclear, although previous findings indicate a predominant role for the left hemisphere in action selection (Schluter et al., 2001; Rushworth et al., 2003; Koch et al., 2006; Jacobs et al., 2010).

In the absence of advance predictions about the involvement of the R-LOTC and L-IPL in hand choice, we can only speculate as to the significance of these results. The importance of the LOTC in high-level visual processing is well established (Grill-Spector and Malach, 2004). Our activity in the R-LOTC likely includes the Extrastriate Body Area (EBA), a functionally-defined, predominately right-lateralized region within LOTC that is preferentially responsive to viewing human bodies (versus other object categories) (Downing et al., 2001). Although part

of the ventral visual pathway (Ungerleider, 1982; Goodale and Milner, 1992), and considered essential for body-part visual perception and recognition (Urgesi et al., 2004), other data suggest a role for the EBA in action planning. The spatial patterns of fMRI responses within EBA reliably distinguish between different types of upcoming actions performed with the hand (Gallivan et al., 2013), and the EBA is active during the performance of reaching actions in the absence of visual feedback (Astafiev et al., 2004; Orlov et al., 2010). These previous findings suggest that R-LOTC is not only important for high-level visual processing, but also plays a role in action planning. Our data extend this hypothesis to suggest that the R-LOTC is also important for hand choice.

The left supramarginal gyrus has long been associated with limb praxis and the performance of learned actions (Buxbaum, 2001; Goldenberg, 2009), including a specific role for action planning and selection (Buxbaum et al., 2005), while other data also implicate this area as important for visuospatial attention, and in particular, attentional reorienting (Corbetta et al., 2005). Our findings reveal the involvement of the L-IPL in hand choice, and in particular, during free choice actions made with the left hand. Although speculative, the preferential engagement of this area for reach-choices made with the left hand may reflect increased processing demands related to the selection and use of the non-preferred hand. Future studies involving free hand choice with both left- and right-handed participants will be of value.

These aspects of our results motivate changes to our proposed model. Alongside the involvement of bilateral posterior intraparietal cortex, our data indicate that the L-dPMC, L-IPL and R-LOTC are important for deciding which hand to use to perform actions. Further understanding how this network interacts to govern hand choice, and the potentially distinct functional contributions of these different brain areas, is an important goal for future research.

2.5.4 Concluding remarks

The brain mechanisms involved in 'free choice' have been scarcely studied; most previous investigations focus instead on rule-based action selection, where the mappings between stimuli and responses are arbitrary (e.g. respond with the left

hand when a stimulus is a particular colour). Here we identify a network of brain areas involved in selecting which hand to use to perform actions on the basis of 'natural' factors – e.g. target location –, similar to the conditions that commonly constrain these choices in everyday life. Our data reveal the specific involvement of bilateral posterior intraparietal and superior parietal cortex, left dorsal premotor cortex, left inferior parietal lobule, and the right lateral occipitotemporal cortex. Our findings provide support the PPIC model, and the hypothesis that hand-specific action plans are concurrently activated in bilateral posterior parietal cortex, and compete for selection. We suggest that, although incomplete, the PPIC model of hand choice is of continuing heuristic value, and warrants further investigation.

Fitzpatrick, A. M., Dundon, N. M., & Valyear, K. F. (in prep). Investigating the causal role of the posterior parietal cortex in hand choice using cTBS.

Acknowledgements

3.1 Abstract

In line with the Posterior Parietal Interhemispheric Competition model (PPIC), recent fMRI evidence suggests that the posterior parietal cortex is an important locus underpinning hand choice. The PPIC model outlines that, at a population level, hand selection unfolds via the resolution of neuronal competition within bilateral posterior intraparietal and superior parietal cortex (pIP-SPC). Cell populations within pIP-SPC prepare multiple actions at a hand-specific level. Within each hemisphere there is a dominant representation of the contralateral hand. An action is selected, and executed, when the associated plan reaches suprathreshold levels. In the current study, fMRI-guided continuous theta burst stimulation (cTBS) is applied to evaluate the PPIC model and the hypothesis that bilateral pIP-SPC is critically involved in hand choice. By virtue of the contralateral hand gradient outlined in the PPIC model, cTBS applied to pIP-SPC is expected to decrease the likelihood of selecting the hand contralateral to stimulation. Participants perform a reaching task after left pIP-SPC cTBS, right pIP-SPC cTBS, and Sham stimulation. Hand choice is quantified per individual and compared across the three stimulation sessions. Preregistered analyses reveal that measures of hand choice were not significantly biased by cTBS, and that the pattern of choice behaviour was similar irrespective of stimulation hemisphere. We performed additional analyses including a No-cTBS condition. Results show a significant reduction in the proportion of right hand use around the point of subjective equality following cTBS to right pIP-SPC compared to Sham stimulation. Overall, our hand choice data fail to provide support for the PPIC model, and suggest that hand selection is largely insensitive to cTBS to pIP-SPC.

3.2 Introduction

Hand actions are ubiquitous in human daily motor behaviour, though how the processes of hand selection and action preparation unfold in the brain is a topic of consistent debate among neuroscientists (Freedman & Assad, 2011; Gallivan et al., 2018). While traditional cognitive theories postulate that decisions are made in regions entirely separable from systems of perception and action (Padoa-Schioppa, 2011; Tversky & Kahneman, 1981), recent evidence spanning multiple domains implies that selection is underpinned by the same neural territories that govern the preparation and online guidance of actions (Ariani et al., 2015; Christopoulos, Bonaiuto, Kagan, et al., 2015; Christopoulos et al., 2018; Cisek & Kalaska, 2010; Oliveira et al., 2010).

Alongside the interconnected premotor areas, the posterior parietal cortex (PPC) is known to perform the critical sensorimotor transformations that subserve visually guided reaching behaviour (Culham & Valyear, 2006; Gallivan & Culham, 2015; Kalaska et al., 1997; Wise et al., 1997). Neurophysiological properties of parietal cells encode the motor parameters relevant for an upcoming action during the planning phase of movement (Crammond & Kalaska, 1994; Schaffelhofer & Scherberger, 2016) – often referred to as *motor intention* (Andersen et al., 1997; Snyder et al., 1997). Motor intention information is transmitted for overt execution via corticocortical connections to primary motor areas within distinct fronto-parietal circuits (Caminiti et al., 2017; Gamberini et al., 2019; Godschalk et al., 1984; Muakkassa & Strick, 1979; Rizzolatti & Luppino, 2001).

The information encoded in the PPC is critical for effective reach behaviour. In patients, damage to the PPC can result in characteristic reach deficits in a condition known as *optic ataxia* (Bálint, 1909; Hecaen & De Ajuriaguerra, 1954; Rafal, 2003). Selective ablation of the PPC in non-human primates manifests in a reduction of voluntary use of the contralateral limb and an awkwardness of movement (Andersen, Andersen, Hwang, & Hauschild, 2014; Grünbaum & Sherrington, 1902; Peele, 1944). In human subjects, transcranial magnetic stimulation (TMS) applied to the PPC, particularly in the superior parietal lobule, is shown to impair the preparation (Davare

et al., 2012; Striemer et al., 2011; Vesia et al., 2010) and online control (Desmurget et al., 1999; Glover et al., 2005) of reaching.

In recent years, the neuronal populations within fronto-parietal circuits dedicated to the specification of motor parameters for movement have been highlighted as important loci for action selection (Cisek & Kalaska, 2005; Klaes et al., 2011; Pastor-Bernier & Cisek, 2011a; Pesaran et al., 2008; Scherberger & Andersen, 2007). Neurophysiological evidence demonstrates that cell populations encode multiple action plans in parallel within the sensorimotor system (Cisek & Kalaska, 2005; Klaes et al., 2011; Pastor-Bernier & Cisek, 2011b; Suriya-Arunroj & Gail, 2019). Cell population activity is modulated by the decision variables relevant for action selection during the planning phase of movement (Dekleva et al., 2016; Klaes et al., 2011; Pastor-Bernier & Cisek, 2011b; Ramkumar et al., 2016; Thura et al., 2012; Thura & Cisek, 2016). The action plans encoded are suggested to compete for selection (and overt execution) via neuronal competition (Cisek, 2006; Cisek & Kalaska, 2010; Klaes et al., 2011; Pastor-Bernier & Cisek, 2011a, 2011b). These data form the empirical basis for the *Affordance Competition Hypothesis* (ACH) (Cisek, 2006, 2007; Cisek & Kalaska, 2010). A key principle of the ACH is that the same neural mechanisms that specify plans for action are also involved action selection. In the case of hand choice, this implicates a contributing role of the PPC.

To date, evidence from human behavioural studies is in line with the hypothesis that multiple action plans are specified in response to a singular stimulus (Chapman et al., 2010; Fitzpatrick, Dundon, & Valyear, 2019; Gallivan et al., 2016; Oliveira et al., 2010; Valyear et al., 2018; Viswanathan et al., 2019). Further, neuroimaging studies implicate a role of the same sensorimotor regions governing the specification and online control of actions in mediating their selection (Ariani et al., 2015; Fitzpatrick et al., 2019; Viswanathan et al., 2019). Alternatively, it has been proposed that action selection precedes planning (Bernier et al., 2012), and a dominant role of left-lateralised dorsal premotor cortex in mediating selection, in particular, is highlighted (Koch et al., 2006; Rushworth et al., 2003; Schluter et al., 2001).

A recent investigation with non-human primates provides causal evidence for the role of the parietal reach region (PRR) in action selection (Christopoulos, Bonaiuto, Kagan, et al., 2015). Animals were trained to perform memory-guided reaching or saccade tasks. The tasks required a choice between two targets carrying equal reward, presented simultaneously in opposite visual fields. On some trials, a peripheral visual cue instructed a particular eye- or arm-movement toward one of the targets. Without a cue, the animals freely selected an eye- or arm-movement response. Inactivation of the PRR affected performance in the reach, but not the saccade, task. Specifically, PRR inactivation resulted in a significant reduction in arm-movement choices to targets in the contralateral visual field, compared to control sessions. Instructed arm-movements to these targets were not altered. Given that saccade behaviour and instructed reaches were unaffected, the observed changes in the internally guided reaching decisions cannot be attributed to impairments in visual acuity or gross motor ability. The authors argue that the PRR is critically involved in reach decisions, and not just reach planning (Christopoulos, Bonaiuto, Kagan, et al., 2015). In a subsequent study, Christopoulos and colleagues (2018) provide evidence for a double dissociation. Oculomotor, rather than reach, decisions are shown to be predominantly affected by the inactivation of lateral intraparietal area (Christopoulos et al., 2018). Taken together, these experiments provide compelling evidence in support of the hypothesis that the neural systems that underpin action specification also mediate their selection.

In human subjects, the role of the PPC in hand choice has been assessed using transcranial magnetic stimulation (TMS). Oliveira and colleagues (2010) applied single-pulse TMS the PPC while participants performed a reaching task. Specifically, TMS was applied after target onset and before movement initiation, during the planning phase of movement. Stimulation of the left PPC significantly reduced the likelihood of reaches made with the right hand – i.e. the hand contralateral to stimulation. These data provide causal evidence for a role of the PPC, particularly in the left-hemisphere, in human hand selection. Further, this study suggests that hand selection is resolved via a competitive process. Response times to initiate actions in a free choice condition were prolonged compared to when hand choice was predetermined. This effect was seen in regions of target space

surrounding a participant's point of subjective equality, corresponding to the most uncertain region of space, or highest competition, compared to the targets in the periphery (Oliveira et al., 2010).

Motivated by the evidence introduced above, we recently developed an action-based model of human hand selection we call the Posterior Parietal Interhemispheric Competition (PPIC) model (Figure 3.1.A). The PPIC model makes two assumptions: (1) there are populations of neurons within the posterior intraparietal and superior parietal cortex (pIP-SPC) of both the left and right hemispheres that specify motor parameters for actions in hand-specific coordinates, and (2) within each hemisphere, more of these neurons code for actions with the contralateral hand.

Otherwise, the mechanics of the model are taken directly from the Affordance Competition Hypothesis (Cisek, 2006, 2007). Populations of neurons encoding similar actions with the same hand excite one another while those encoding actions with the opposite hand (and those encoding dissimilar actions) inhibit one another, and the strength of influence of a given neural population scales nonlinearly with its current level of activity. Hand (and action) selection is determined when the activity of one of these neural populations reaches a specific (suprathreshold) level. At this point, the activity within this neural population further increases and the spatiotemporal parameters encoded by these neurons, including which hand to use, are selected while opposing cell populations are inhibited.

We recently tested the PPIC model using functional MRI, and found supporting evidence (Fitzpatrick et al., 2019). Areas within pIP-SPC were significantly more active during reaching actions involving free choice of which hand to use compared to when hand use was instructed; and critically, these conditions were balanced for visual and motor factors. This pattern of choice-selectivity was found bilaterally in pIP-SPC for actions made with either hand, yet within each hemisphere, actions with the contralateral hand evoked the strongest responses. Moreover, consistent with a competitive process, fMRI activity levels were elevated for responses to targets that represented more ambiguous choices. These findings

are consistent with the PPIC model, and the hypothesis that pIP-SPC plays an important role in deciding which hand to use to perform actions.

In the current study, we used a high-frequency repetitive TMS protocol known as continuous theta burst stimulation (cTBS) to evaluate the PPIC model and the hypothesis that bilateral pIP-SPC is causally involved in hand choice. When applied to primary motor cortex, cTBS has been shown to reduce cortical excitability for up to 60 minutes (Huang et al., 2005). These suppressive effects are thought to reflect reduced synaptic efficacy (Huang, Chen, Rothwell, & Wen, 2007).
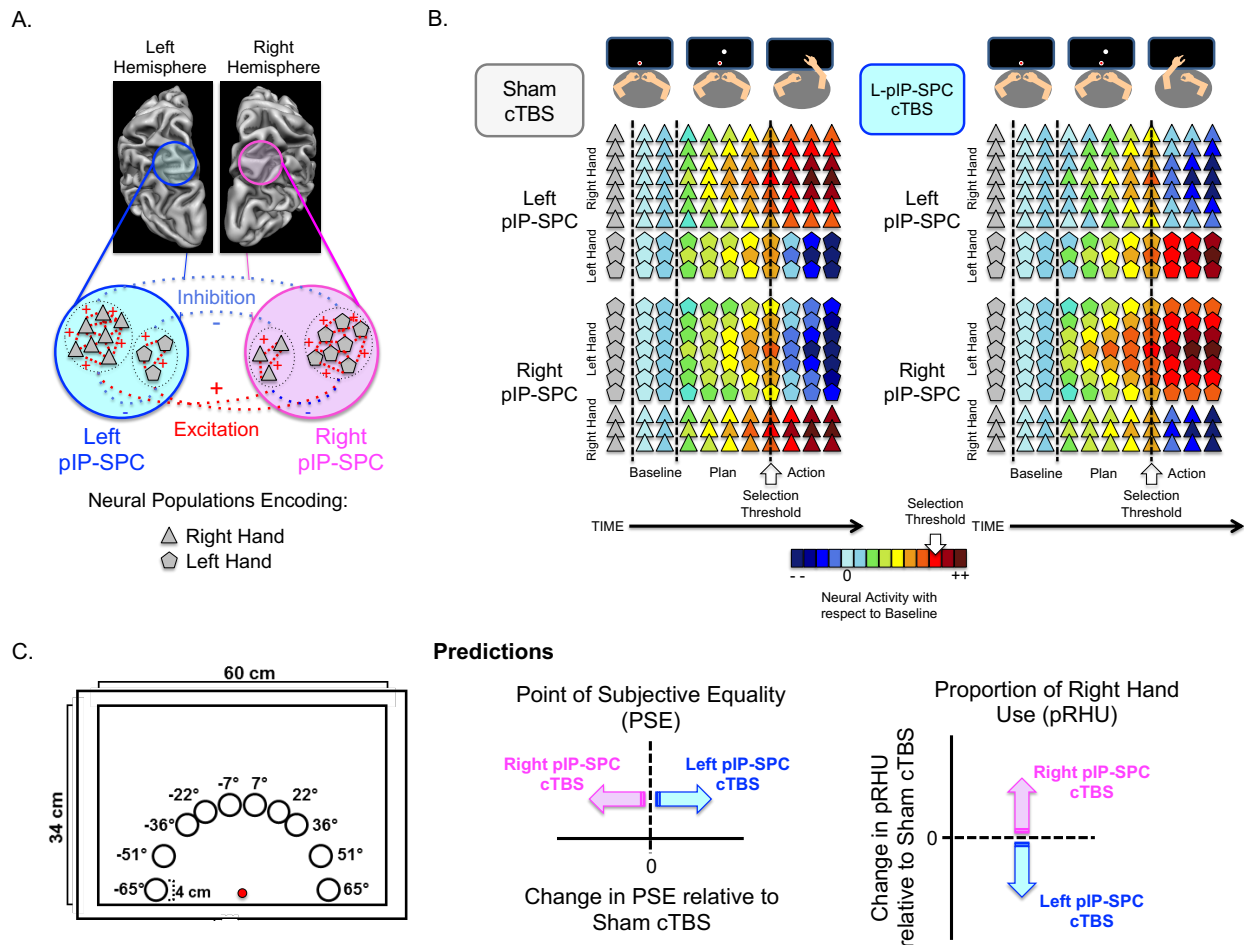
Figure 3.1. The PPIC Model, methods and predictions. (A) *The PPIC model.* Populations of cells in bilateral pIP-SPC encode actions in hand-specific terms. Within each hemisphere, the contralateral hand is overrepresented. Cells encoding actions with the same hand excite one another while those that encode actions with the opposite hand inhibit one another. **(B)** An example of how activity in pIP-SPC changes over time following Sham and left pIP-SPC stimulation as hypothesised by the PPIC model. During the planning phase the activity of all cell-types increase. The rate of increase depends on various factors, including target location. In the Sham cTBS condition, cell populations encoding the right hand show a steeper rate of increase, and reach suprathreshold activity-levels first. Once threshold is reached, the activity in these cell populations further increases and the spatiotemporal parameters of the actions they encode are selected, while opposing cell populations are robustly inhibited. Following cTBS to left pIP-SPC, excitability of underlying cell populations is reduced, and their extent of influence on populations in the right pIP-SPC is decreased. Cells dedicated to the left hand in the right pIP-SPC now reach suprathreshold activity-levels first. **(C)** *Experimental set-up.* Schematic representation of 10 circular targets for reaching, arranged symmetrically around the midline of a display (screen dimensions: 34cm x 60cm). The red dot indicates the fixation point. *Predictions.* The PPIC model predicts that cTBS to pIP-SPC will reduce the likelihood of choosing the hand contralateral to stimulation. Relative to Sham stimulation, a leftward (positive) shift in the point of subjective equality (PSE) and a decrease in the proportion of right hand use is predicted following cTBS to left pIP-SPC (indicated in blue). The opposite is predicted for cTBS to right pIP-SPC (indicated in pink).

According to the PPIC model, cTBS applied to unilateral pIP-SPC will decrease the probability of selecting the hand contralateral to stimulation. Two aspects of the PPIC model motivate this hypothesis. First, the model stipulates that a greater proportion of cells in pIP-SPC encode the selection and use of the contra- vs.

ipsilateral hand (Figure 3.1.A). The dampening effects of cTBS on synaptic efficacy are expected to disproportionately impact these cells, and as a consequence, decrease the likelihood of selecting the hand contralateral to the site of stimulation (Figure 3.1.B). Second, as the excitatory potential is reduced in these cells their activity-dependent inhibitory drive on those (opponent) cells encoding the ipsilateral hand, found predominately in the opposite hemisphere, will also be reduced. These effects combine to reduce the likelihood of using the hand contralateral to the site of stimulation.

Continuous TBS to the left hemisphere pIP-SPC (L-pIP-SPC) is predicted to decrease the proportion of reaches to targets that are made with the right hand, reflected as a positive (rightward) shift in the PSE, while the opposite pattern – a negative (leftward) shift in the PSE, and an increase in the proportion of right hand use – is predicted following cTBS to the right hemisphere pIP-SPC (R-pIP-SPC) (Figure 3.1.B and C).

3.3 Methods

3.3.1 Pre-registration

The study was pre-registered via aspredicted.org (Appendix B). Pre-registration included predictions and analyses plans.

A power analysis using G*Power (Faul, Erdfelder, Lang, & Buchner, 2007) was used to estimate sample size on the basis of the effect size (d = 0.76) calculated on the basis of Oliveira et al. (2010), discussed above. The results suggest that a sample size of 20 participants is needed to detect an effect-size of d = 0.76, with 95% power using a paired-samples t-test with alpha at 0.05.

3.3.2 Participants

Twenty-six individuals (14 males, 12 females, M = 22.54 years ± 3.24 SD) participated in the experiment. Data from six participants were excluded: three left-handers, two self-reported strategy-users (see Section 3.3.4.2), and one individual who experienced adverse effects of TMS. The final dataset reported here includes 20 right-handed participants (10 males, 10 females, M = 22.90 years ± 3.48 SD). Analyses including all data are presented in the Supplementary Materials (Appendix C, Table S3.1 and Table S3.2). Handedness was qualified using a modified Waterloo Handedness Inventory (Steenhuis & Bryden, 1989; scores range from -30 to +30).

All participants provided informed consent in accordance with the Bangor University School of Psychology Ethics Board, and were naïve to the goals and predictions of the study. All participants had normal or corrected-to-normal vision, with no MRI/TMS contraindications. Participants completed three sessions of TMS and behavioural testing, separated by a minimum of 1 week (M = 7.60 days; SD = 2.26). A single MRI session was performed prior to TMS and behavioural testing. Altogether, the study took approximately five hours to complete, and participants were financially compensated.

3.3.3 Experimental setup and materials

Participants were seated ~50cm from a 65cm x 45.5cm vertical touchscreen monitor (1920 x 1080 resolution), centred with respect to their mid-sagittal plane. At the start of a trial, the left and right index fingers held two start keys (2.2cm x 3.3cm) depressed, fixed to a table 30cm from the monitor, aligned with the centre of the monitor. Targets were 4cm-diameter white circles presented against a uniform black background. Targets were presented at 10 positions relative to midline: -65, -51, -36, -22, -7, 7, 22, 36, 51, and 65 degrees, jittered by a 2D Gaussian kernel (SD = 0.5cm). A central fixation point (0.2cm x 0.2cm) was displayed at 5cm from the base of the monitor screen (Figure 3.1.C). All targets were presented equidistant (30cm) from the centre of start-keys and were comfortably reachable with either hand. The experiment was controlled in Matlab (r2015b) using the Psychophysics Toolbox extensions (Brainard & Vision, 1997; Kleiner, Brainard, & Pelli, 2007; Pelli & Vision, 1997).

3.3.4 Procedure

3.3.4.1 Transcranial magnetic stimulation

TMS was delivered using a Magstim Rapid Plus stimulator with a 70mm figure-of-eight coil. Coil localization was performed using the BrainSight frameless stereotaxic neuronavigation system (BrainSight Software, Rogue Research Inc., Montreal, Quebec, Canada, version 2.3.10; Polaris System, Northern Digital Inc., Waterloo, Ontario, Canada) and individual participant MRI data.

T1-weighted anatomical MRI data were collected on a 3T Philips Achieva scanner using a multiplanar rapidly acquired gradient echo (MP-RAGE) pulse sequence: time to repetition (TR) = 1500ms; time to echo (TE) = 3.45ms; flip angle = 8°; matrix size = 224 by 224; field of view (FOV) = 224mm; 175 contiguous transverse slices; slice thickness = 1mm; in-plane resolution = 1mm by 1mm.

High-frequency repetitive continuous theta burst stimulation (cTBS) was used to evaluate the PPIC model and the hypothesis that bilateral pIP-SPC is critically involved in hand choice. Continuous TBS involved the application of bursts of three

TMS pulses presented at 50Hz, with an inter-burst frequency of 5Hz for 40s (600 pulses). First, active motor thresholds were defined per individual subject. The participant's anatomical MRI was used to estimate the location of the hand area in the primary motor cortex of the left hemisphere. With the coil held tangentially on the scalp surface with the handle oriented posteriorly and angled laterally at approximately 45° from the midline, single TMS pulses were delivered while electromyographic recordings were measured from the contralateral first dorsal interosseous (FDI) muscle. If necessary, the coil was then repositioned to where the maximal motor evoked potential (MEP) was observed; the 'motor hotspot'. Active motor thresholds were then defined as the minimum stimulator intensity wherein peak-to-peak MEP amplitudes of greater than 200μV were elicited in 5/10 consecutive trials while the subject was voluntarily contracting their FDI muscle at 20% maximal force using visual feedback (Rossini et al., 1994). For subsequent cTBS, the intensity of the stimulator was set to 80% of the participant's active motor threshold. When applied to primary motor cortex, this protocol has been shown to reduce cortical excitability for up to 60min (Huang et al., 2005).

To target the L- and R-pIP-SPC for cTBS, we used a combination of functional and anatomical guidelines. First, we used the results of our previous fMRI study identifying hand-choice-selective responses in L- and R-pIP-SPC (Fitzpatrick et al., 2019). Specifically, for L- and R-pIP-SPC stimulation, the TMS coil was moved to the coordinates of the hotspots of activity identified by the group-level contrast of Choice > Instruct, controlled for visual and motor confounds. Second, if necessary, we then adjusted the coil position per individual so that the target trajectory passed through the medial bank of the intraparietal sulcus, within the superior parietal cortex. On the basis of our fMRI results, the R-pIP-SPC target was marginally more posterior and medial than the L-pIP-SPC target. The estimated group-average distances (mm) from the coil on the scalp to the targets within the cortex were as follows: L-pIP-SPC = 25.80 (5.39); R-pIP-SPC = 22.90 (2.62). The coil-handle orientation was posterior and approximately parallel with the midline.

To facilitate comparison between our stimulation sites and prior data, we also performed a meta-analysis of previous published fMRI and TMS studies involving

reaching (see Figure 1.3). The reported locations of reach-related fMRI activity and TMS-targeted brain areas, respectively, were used to estimate the hotspots of maximal overlap between studies. Good correspondence is revealed between these results and our fMRI activity used to guide coil localization in the present study.

Sham cTBS involved positioning the coil over either the L- or R-pIP-SPC using the same approach described above, counterbalanced for area across participants, yet with coil surface angled 90° from the scalp during stimulation. The cTBS protocol was otherwise the same. With this approach, the feeling of the coil on the surface of the head, and the sounds made from discharging the coil are similar to active cTBS, yet any stimulation that penetrates the scalp (via the 'wing' of the coil) is presumed ineffective – i.e. unlikely to meaningfully influence underlying neurophysiology (Duecker & Sack, 2013; Lisanby, Gutman, Luber, Schroeder, & Sackeim, 2001).

3.3.4.2 Behavioural testing

Trials began with participants in the start position, holding down each of the start keys with their index fingers. Participants were instructed to fixate the central fixation point. When both start keys were depressed, a 400ms-duration tone was played to alert participants that the trial had started. This was followed by a variable delay (200/400/600/800ms, randomly ordered). Next, a target appeared at one of the 10 positions of the target array. Participants were instructed to reach to contact the target with the index finger of one hand, as quickly and accurately as possible. They were also told that they may move their eyes freely during reaching. Target onset was coincident with the removal of the fixation point. Reach targets were removed after movement onset, triggered by the release of a start key. The next trial began as soon as the participant returned to the start keys.

Two additional types of trials were included: two-target and fixation-catch conditions. In the two-target condition, two targets were presented at the most peripheral edges of the target array (i.e. at -65/65 degrees ± jitter). Participants were instructed to use both hands to contact targets, and to move each hand together, at the same time. The fixation-catch condition involved the presentation of a single

target near fixation, and participants were instructed to use both hands to contact this target, and to move each hand together. These conditions were included to minimize the likelihood that participants would always use the same hand for single-target conditions. The fixation-catch condition should also reinforce the likelihood that participants will maintain fixation at trial onset.

Participants completed six blocks of 145 trials per session. Two blocks were completed pre-cTBS, and four blocks were completed post-cTBS. A custom Matlab (R2011b) script was used to create trial sequences wherein trial (t) history (t – 1) is balanced according to condition, and target position for single-target conditions. Thus, each experimental block comprised 120 single-target trials, 12 per target position, and 24 two-target and fixation-catch trials, balanced for condition history. A unique trial sequence was generated per block. The first trial of each block was an additional, randomly selected trial, not controlled for condition history. Data from two-target and fixation-catch conditions were excluded from analyses. Unless specified, pre-stimulation data were excluded from analyses.

After the final cTBS-behavioural session, participants completed (1) the Waterloo Handedness Inventory, and (2) were asked if they "used a specific strategy, or rule" to decide which hand to use during behavioural testing.

3.3.5 Dependent measures and analyses

Study pre-registration included outlier removal procedures: Outliers are defined as ± 2.5 standard deviations from the group mean, per statistical test, and removed from further analyses (Appendix B). Results from non-outlier-removed analyses are reported in the Supplemental Materials (Appendix C, Table S3.1 and Table S3.2).

All results are considered significant at $p < 0.05$. Where violations of sphericity were identified, Greenhouse-Geisser correction was applied. Where appropriate, Bonferroni correction was applied to post hoc follow-ups, with a corrected $p < 0.05$ considered significant.

3.3.5.1 Hand choice

Hand choice was measured using button-release data, and, if unclear (e.g. trials involving multiple button releases), confirmed using video data. For each participant, a psychometric function (McKee, Klein, & Teller, 1985) was computed according to their hand choice behaviour (on single-target conditions) per target location, and the theoretical point in space where the participant was equally likely to use either hand – the point of subjective equality (PSE) – was determined. Specifically, PSE values were estimated by fitting a general linear model to each participant's hand choice data. The model included target positions and a constant term, and used a logit link function to estimate the binomial distribution of hand choice responses (1 = right ǀ 0 = left). Model coefficients were evaluated at 1,000 linearly spaced points between the outermost values of the target array (i.e. ± 65 degrees), and the value closest to a 0.50 probability estimate was defined as the PSE. The model was fitted separately per individual, per TMS condition. Resultant PSEs per TMS condition were evaluated using a repeated measures ANOVA (rmANOVA).

Two additional analyses were performed. Hand-choice data expressed as proportions of right-hand use were first arcsine transformed, calculated as the arcsine square root of the proportions. The arcsine transformation stretches the upper and lower ends of the data. This makes the distributions more symmetrical and reduces problems with violations of the assumption of normality. The transformed proportions were then tested using two rmANOVAs: (1) to test for TMS effects on the mean proportions of right-hand use across all target locations, and (2) to test for effects on the mean proportions of right-hand use at those targets that bound the PSE as defined per individual on the basis of Sham-cTBS, consistent with the approach used by Oliveira et al. (2010).

3.3.5.2 Response time

Response time (RT) was measured using button-release data, and defined as the time taken to initiate a reach after target onset in milliseconds (ms). Bimanual catch trials confounded the RT of targets at ± 65 degrees, and these targets were

removed from analyses. We did not pre-register analyses and predictions regarding response times. The push-pull characteristics of the PPIC model, however, make the following predictions.

By reducing the excitatory potential of cells underlying the site of stimulation, cTBS to unilateral pIP-SPC is predicted to slow the rates of excitation to reach selection-threshold-levels for the contralateral hand, since cells representing the contralateral hand are overrepresented within each hemisphere pIP-SPC. As such, response times to initiate reaches with the contralateral hand will be prolonged. Further, as a consequence of the rivalry between hemispheres, these effects are also predicted to result in relatively faster response times to initiate reaches with the limb ipsilateral to stimulation. Reduced excitatory potential of cells in one hemisphere will also reduce their inhibitory drive on cells in the opposing hemisphere. Response times per hand per TMS condition were evaluated using a rmANOVA.

3.4 Results

Data reported include right-handers without strategy use (N=20). Results from the complete dataset, including left-handers (N=3), right-handers who reported strategy use (N=2), and non-outlier-removed analyses are provided in the Supplementary Materials (Appendix C, Table S3.1 and Table S3.2).

Participants made few errors, affecting <1% of the total number of trials (see Table 3.1 for details). Two types of errors were performed; 1) A button release prior to target onset – *negative response time*. 2) Both buttons released in response to a single-target trial – *double button response*.

Table 3.1. Participant errors.

Participant	Total	Percent of Participant's trials	Negative response time	Double button response
1	2	0.10	0	2
2	15	0.75	3	13
3	10	0.50	9	1
4	6	0.30	2	4
5	12	0.59	3	9
6	7	0.35	4	3
7	14	0.69	4	10
8	17	0.84	13	4
9	13	0.64	6	7
10	15	0.74	4	11
11	6	0.30	0	6
12	12	0.60	7	5
13	13	0.64	7	6
14	1	0.05	1	0
15	22	1.09	12	10
16	7	0.35	2	5
17	6	0.30	3	3
18	7	0.35	4	3
19	9	0.45	7	2
20	11	0.55	7	4

3.4.1 Hand choice

Figure 3.2.A shows the inter-participant distribution of hand choice data expressed as the mean proportions of right-hand use (RHU) for L-pIP-SPC, R-pIP-SPC, and Sham cTBS conditions. At the group-level and independent of stimulation condition, participants typically use their left hand to contact targets on the left side of

space and their right hand to contact targets on the right side of space, and target -7°
shows the most variation in hand choice behaviour.

The results of a rmANOVA of PSE measures of hand choice reveal no
significant differences between cTBS conditions ($F(2, 36) = 0.56$, $p = 0.58$, $\eta^2 = .03$)
(Figure 3.2.C). The group mean PSEs are near target -7° for all conditions. Both L-
and R-pIP-SPC stimulation conditions show a small ($< 2°$) and inconsistent right-
ward (positive) shift in group mean PSE values relative to Sham-cTBS. In other
words, these results reveal no evidence for effects of cTBS on hand choice
behaviour.

Individual-level data with resultant curve-fits per condition, used to estimate
PSE values, are shown for two participants, for illustrative purposes (Figure 3.2.B).

Figure 3.2. Hand choice. (A) Violin plots depict the distribution of hand choice data across target locations expressed as the proportions of right-hand use (RHU) for L-pIP-SPC (blue), R-pIP-SPC (pink), and Sham (grey) cTBS conditions. Within each violin plot, the median, and upper and lower quartile values are indicated by solid lines. Vertical dashed line depicts the midline of the display (0°). Horizontal dashed line shows the point of equal proportion (0.50) of left- and right-hand use. **(B)** For illustrative purposes, individual-level data for two participants with resultant curve-fits per stimulation condition, used to estimate PSE values, are shown as continuous lines. Filled circles represent the proportion RHU per target location, per condition. **(C)** Horizontal violin plots illustrate the group mean point of subjective equality (PSE) values per condition. Solid black lines indicate group means with 95% confidence intervals. Orange lines represent target locations at -7° and 7° from midline. *Inset.* PSE values are represented as the difference score for active stimulation conditions minus Sham. Horizontal dashed line indicates the group mean PSE value in the Sham cTBS condition.

Analyses of arcsine transformed proportions of RHU reveal similar results. First, considering responses to all targets, we find no significant differences in hand choice as a function of cTBS condition ($F_{(2, 36)} = 0.71$, $p = 0.50$, $\eta^2 = 0.04$) (Figure 3.3.A). At the group-level, participants show a small yet reliable preference to use their right hand in the Sham-cTBS condition (mean proportion of RHU = 0.549; compared with 0.5, $t_{(18)} = 5.36$, $p < 0.001$), and this preference is statistically unchanged following cTBS to either L-pIP-SPC (mean proportion of RHU = 0.540) or R-pIP-SPC (mean proportion of RHU = 0.537).

Figure 3.3. Hand choice: Proportion of right hand use. (A) Violin plots depict the distribution of hand choice data collapsed across targets expressed as the proportions of right-hand use (RHU) for L-pIP-SPC (blue), R-pIP-SPC (pink), and Sham (grey) cTBS conditions. Within each violin plot, median, and upper and lower quartile values are indicated by solid lines. Solid black lines indicate group mean proportion RHU values with 95% confidence intervals. Horizontal dashed line depicts the point of equal proportion of left- and right-hand use. *Inset.* Proportion of RHU expressed as the difference score, relative to Sham cTBS. **(B)** Violin plots depict the distribution of hand choice data collapsed across targets expressed as the proportions of right-hand use (RHU) around the point of subjective equality (PSE) for stimulation conditions. *Inset.* Proportion of RHU at the PSE expressed relative to Sham cTBS.

Second, restricting our analyses to those data that bound the PSE values as defined per individual and on the basis of the Sham-cTBS condition, we also find no significant differences between cTBS conditions ($F_{(2, 38)} = 1.09$, $p = 0.35$, $\eta^2 = 0.05$) (Figure 3.3.B). Here, again, we find that real cTBS reduces the use of the right hand after application to either L- or R-pIP-SPC, yet these effects are statistically unreliable. Altogether, our results are inconsistent with the predictions of the PPIC model, and with the findings from Oliveira et al. (2010).

3.4.1.1 Additional exploratory analyses: No-cTBS baseline

We decided to perform a separate set of analyses using No-cTBS as a baseline measure of hand choice behaviour, defined by the pre-stimulation data from Sessions 2 and 3. Pre-stimulation data from Session 1 were excluded, as these data are considered practice trials.

Our motivations for these additional exploratory analyses are twofold. First, we wanted to address the possibility that Sham-cTBS may have influenced hand choice, perhaps as a consequence of changed participant expectations – i.e. placebo effects. Some participants reported experiencing Sham-cTBS as real stimulation, and, likewise, reported post-stimulation-related sensations (see Supplementary Materials, Appendix C Table S3.3). If Sham-cTBS had an influence on hand choice behaviour this may have dampened our ability to detect differences between conditions, at least in principle (e.g., if all conditions were to shift hand choice in a similar direction). Second, some of the TMS effects reported by Oliveira et al. (2010) involved comparison with a baseline condition involving no TMS. Including analyses of No-cTBS in our study promotes comparison with these previous results.

We performed three sets of analyses, as above, but with four stimulation conditions included: (1) No-cTBS; (2) Sham-cTBS; (3) L-pIP-SPC; (4) R-pIP-SPC. First, we examined PSE measures. The results reveal no significant differences between conditions ($F(3, 54) = 0.48$, $p = 0.70$, $\eta^2 = 0.03$) (Figure 3.4.B). The group mean PSE values for No-cTBS and Sham-cTBS are similar (-6.7° and -7°, respectively). These results suggest that, at least at the group-level, the use of Sham-cTBS as a baseline measure of hand choice is unproblematic, unconfounded by placebo effects. Sham- and No-cTBS provide comparable estimates of hand choice behaviour.
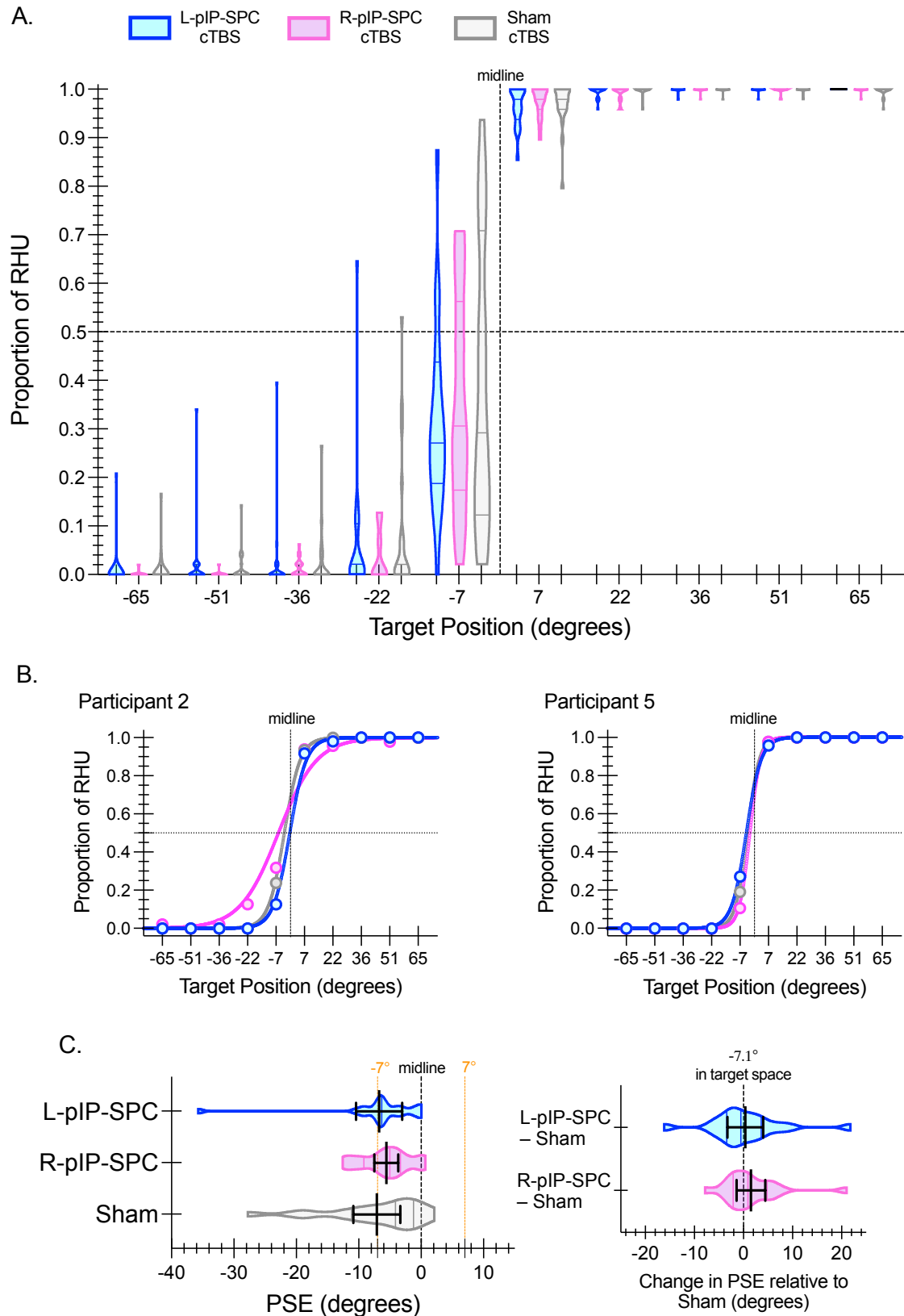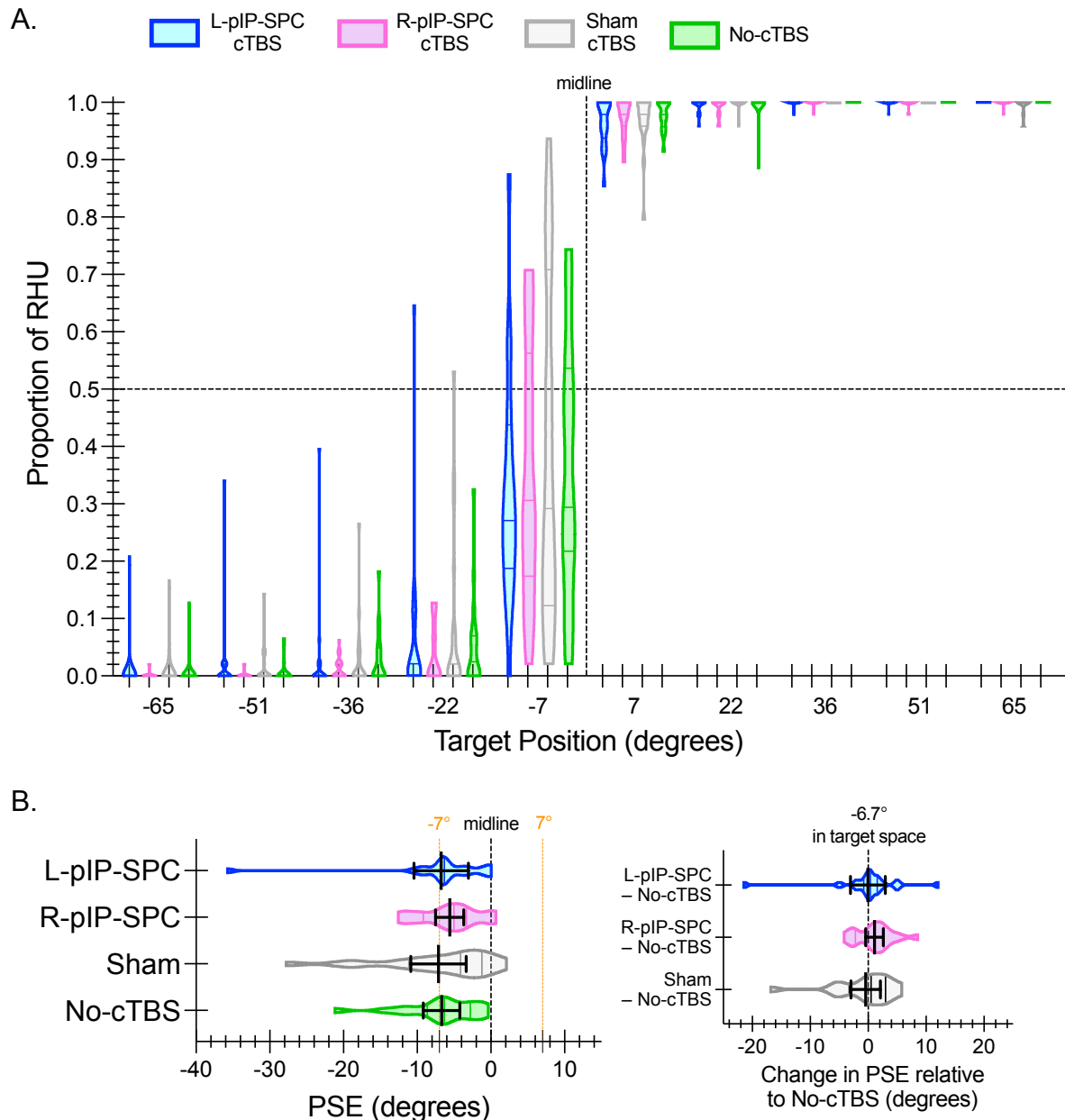
Figure 3.4. Hand choice: No-cTBS. (A) Violin plots depict the distribution of hand choice data across target locations expressed as the proportions of right-hand use (RHU) for L-pIP-SPC (blue), R-pIP-SPC (pink), Sham (grey), and No-cTBS (green) stimulation conditions. Within each violin plot, median, and upper and lower quartile values are indicated by solid lines. Vertical dashed line depicts the midline of the display (0°). Horizontal dashed line shows the point of equal proportion of left- and right-hand use. **(B)** Horizontal violin plots illustrate the group mean point of subjective equality (PSE) values per condition. Solid black lines indicate group means with 95% confidence intervals. Orange lines represent target locations at -7° and 7° from midline. *Inset*. PSE values are represented for stimulation conditions relative to the No-cTBS condition. Horizontal dashed line indicates the group mean PSE value in the No-cTBS condition. ±51 degrees

Second, we examined arcsine transformed proportion RHU across all target locations. These results reveal no significant differences between conditions $F(3, 54)$ = 0.60, p = 0.62, η^2 = 0.03) (Figure 3.5.A). Third, we isolate targets that bound the PSE as defined per individual participant according to the No-cTBS condition and

compare proportion RHU at these target locations as a function of stimulation condition. These results, different from all other analyses outcomes reported above, yield significant effects of cTBS condition ($F_{(3, 57)} = 2.96$, $p < 0.05$, $\eta^2 = 0.14$) (Figure 3.5.B). Follow-up tests indicate that these effects reflect significant differences between R-pIP-SPC and Sham-cTBS conditions. The likelihood of right-hand selection is reliably decreased after cTBS to the R-pIP-SPC relative to Sham-cTBS. This same pattern of decreased proportion RHU after cTBS to R-pIP-SPC is evident when compared with No-cTBS, yet these differences do not survive correction for multiple comparisons.
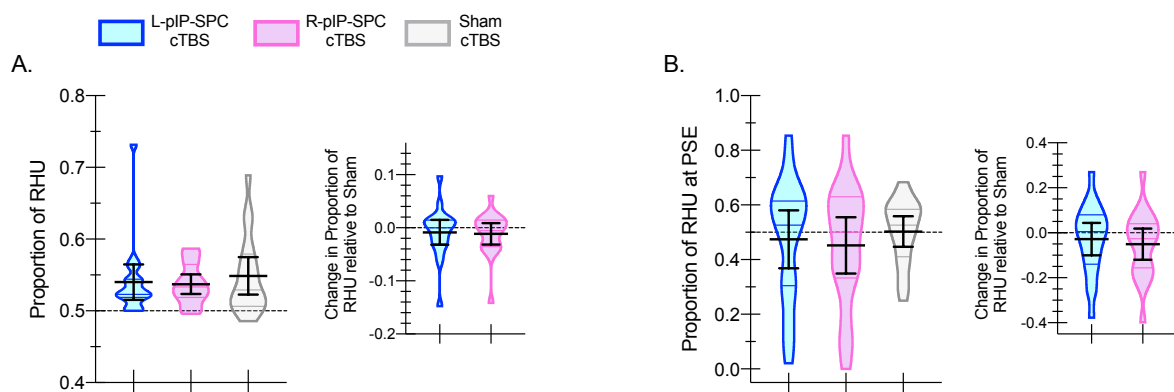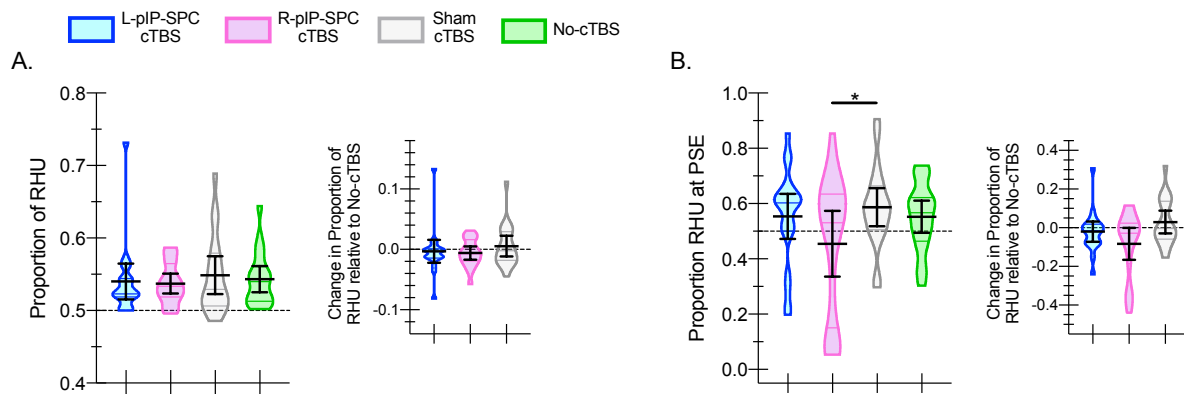

Figure 3.5. Hand choice: Proportion of right hand use: No-cTBS. (A) Violin plots depict the distribution of hand choice data collapsed across targets expressed as the proportions of right-hand use (RHU) for L-pIP-SPC (blue), R-pIP-SPC (pink), Sham (grey), and No-cTBS (green) stimulation conditions. Within each violin plot, median, and upper and lower quartile values are indicated by solid lines. Solid black lines indicate group mean proportion RHU values with 95% confidence intervals. Horizontal dashed line depicts the point of equal proportion of left- and right-hand use. *Inset.* Proportion of RHU expressed relative to No-cTBS. **(B)** Violin plots depict the distribution of hand choice data collapsed across targets expressed as the proportions of right-hand use (RHU) around the point of subjective equality (PSE) as defined in the No-cTBS condition. Asterix indicates a significant reduction in the proportion of RHU at the PSE following R-pIP-SPC cTBS compared to Sham cTBS. *Inset.* Proportion of RHU at the PSE expressed relative to No-cTBS.

Inspection of individual-level data shows that the differences in outcomes between these exploratory analyses and our pre-planned analyses reflect a change in PSE estimates, and corresponding PSE-bounding targets for six (of 20) participants. In all cases, the PSE-bounding targets are positively shifted, rightwardly in target space. Specifically, in five participants the PSE shifts from between targets -22˚ and -7˚, as defined by Sham-cTBS, to between targets -7˚ and +7˚, as defined by No-cTBS. The sixth participant shows a shift from targets -36˚ and -22˚, Sham-cTBS, to targets -22˚ and -7˚, No-cTBS.

Less clear, however, is how to interpret these different outcomes. Our secondary exploratory results involving No-cTBS to define baseline estimates of hand choice suggest that cTBS does have an influence on subsequent hand choice behaviour. In particular, the probability of right-hand selection and use is reduced following cTBS to the right hemisphere pIP-SPC. The effects are subtle, restricted to the area of target space where participants are most willing to use either hand, and show considerable inter-subject variability. Other analyses fail to yield similar statistically significant outcomes, although the general pattern of comparatively reduced right-hand selection following cTBS to R-pIP-SPC is observed. These results are both inconsistent with the predictions of the PPIC model, and the findings from Oliveira et al. (2010).

3.4.2 Response times

Figure 3.6.A shows the group mean RT for the left- and right-hand for L-pIP-SPC, R-pIP-SPC, and Sham cTBS conditions. Irrespective of hand and stimulation conditions, RT is equitable. The results of a rmANOVA of RT measures reveal no significant differences in the time taken to initiate reaches with the contralateral hand as a function of cTBS condition ($F(2, 36) = 0.41$, $p = 0.66$, $\eta^2 = 0.02$) (Figure 3.6.A). Overall, results reveal no evidence for effects of cTBS on motor performance.
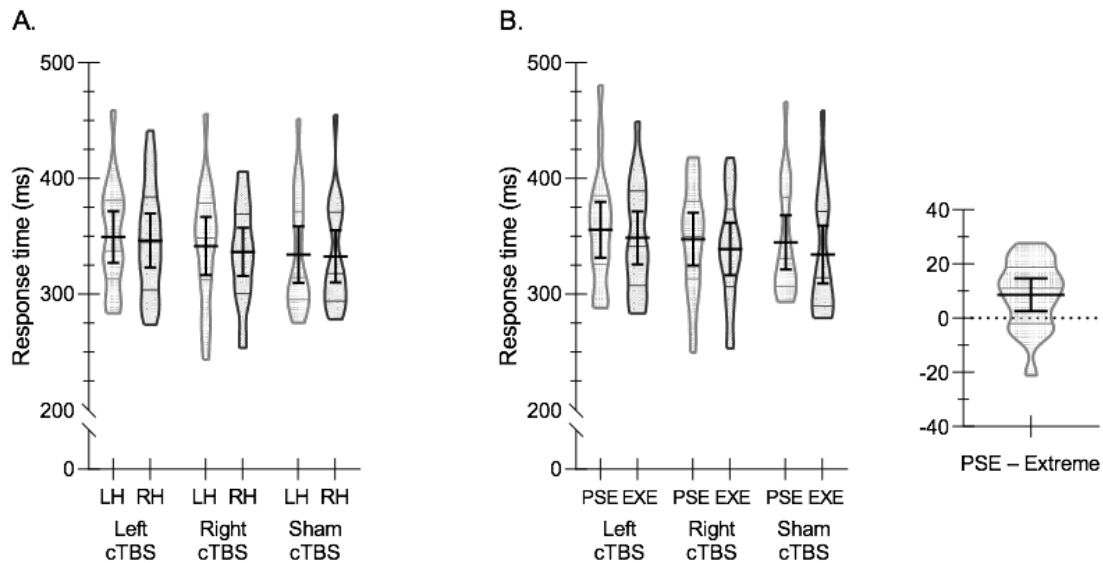
Figure 3.6. Response times. (A) Violin plots show the group mean distribution of response times (RT) for the left hand (LH) and right hand (RH) for L-pIP-SPC (Left cTBS), R-pIP-SPC (Right cTBS), and Sham (Sham cTBS) conditions. Within each violin plot, median, and upper and lower quartile values are indicated by solid lines. Solid black lines indicate group mean proportion RHU values with 95% confidence intervals. **(B)** Violin plots show the group mean distribution of RT for targets at the point of subjective equality (PSE), as defined by the Sham-cTBS condition, and targets in the lateral periphery (EXE) of the display (±51 degrees) per stimulation condition. *Inset.* Significant main effect of target location illustrated as a difference score of RTs to PSE bound targets minus Extreme lateral targets.

3.4.2.1 Additional exploratory analyses: Choice costs

In a separate exploratory set of analyses we assessed the RT cost associated with reaches to the point of subjective equality, or space of high competition and low bias. Here, RTs to the targets bounding the PSE value are compared to targets in the lateral periphery (targets ± 51 degrees) of the display. The PSE bounds were calculated on the basis of the Sham-cTBS and No-cTBS PSE values, separately.

Our motivations for these additional exploratory analyses are, firstly, to corroborate previous literature, in which a "cost" associated with reaches toward uncertain or low bias space is reported (Oliveira et al., 2010). Secondly, we reasoned it is important to substantiate that, under the current task demands, behavioural evidence of a choice cost is observable. Although speculative, failure to observe a behavioural effect of choice in this reaching paradigm could indicate that participants adopted a rule-based selection procedure. In this circumstance, cTBS to pIP-SPC may not necessarily induce changes in hand choice.

The results reveal a significant difference in RT between target locations ($F_{(1, 18)} = 9.05$, $p < 0.01$, $\eta^2 = .34$) (Figure 3.6.B). Consistent with increased choice costs, an increased RT (8.63ms) is observed in group mean PSE-bound targets relative to Extreme targets (Figure 3.6.B inset). A main effect of target location is also observed using the PSE bounding targets on the basis of No-cTBS-defined PSE values ($F_{(1, 18)} = 10.75$, $p < 0.01$, $\eta^2 = .37$). In other words, participants show a reliable increase in time taken to initiate their reaches for targets at the PSE, unaffected by PSE calculation (on the basis of Sham-cTBS or No-cTBS). At a group level and independent of stimulation condition, these results are consistent with the notion of a choice cost associated with hand selection, and the results of Oliveira et al. (2010).

3.5 Discussion

This study investigates the role of the posterior parietal cortex (PPC) in human hand choice. We apply continuous theta burst stimulation (cTBS) to reduce the excitability of neurons in the posterior intraparietal and superior parietal cortex (pIP-SPC) and assess the effects on hand choice behaviour. Our hypotheses are guided by the principles outlined in the Posterior Parietal Interhemispheric Competition (PPIC) model (Fitzpatrick et al., 2019). Across three measures of hand choice, no significant alterations in hand choice are found. Additional analyses reveal that right hand use is significantly reduced following R-pIP-SPC stimulation as compared to Sham stimulation. This effect is observed in the region of space surrounding the point of subjective equality (PSE), associated with high competition and low bias, which was calculated on the basis of a No-cTBS condition. Otherwise, comparable estimates of hand choice behaviour are observed across Sham- and No-cTBS conditions. This effect is in contrast with the predictions of the PPIC model. Continuous TBS to R-pIP-SPC was expected to reduce the likelihood of choosing the left hand, contralateral to stimulation. Taken together, the current data do not provide support for the PPIC model of hand selection.

3.5.1 The role of the posterior parietal cortex

The PPC and interconnected premotor regions are considered critical for the sensorimotor transformations that underpin visually guided reaching behaviour (Culham & Valyear, 2006; Gallivan & Culham, 2015). Multiple lines of evidence have also indicated that the PPC is causally involved in action selection (Christopoulos, Bonaiuto, Kagan, et al., 2015; Klaes et al., 2011; Oliveira et al., 2010). The stimulation sites used in the current study were informed by human functional MRI data (Fitzpatrick et al., 2019) and a meta-analysis of reaching studies (Figure 1.3). Led by this, we assess the role of cortical regions important for the planning and control of reaching movements in hand selection. In the present study, participants did not alter their hand choice following cTBS to pIP-SPC relative to Sham stimulation, considered as a baseline. Ultimately, the results suggest that hand choice is largely insensitive to cTBS applied to pIP-SPC. Failure to implicate pIP-SPC in selection can be considered consistent with previous accounts, which

highlight that the mechanisms involved in action selection are localised to left-lateralised dorsal premotor cortex (Rushworth et al., 2003; Schluter et al., 2001).

However, the results of additional analyses indicate a role of R-pIP-SPC in hand choice. Specifically, participants chose their right hand significantly less in the target space surrounding the PSE following cTBS to the R-pIP-SPC compared to Sham stimulation. Changes in hand choice are also observed in this region of space by Oliveira and colleagues (2010). In their study, stimulation of left-PPC led to a significant decrease in right hand use for targets around the PSE. While the observed effect in the current study refutes the predictions of PPIC model, it does suggest that hand choice was affected by manipulation of pIP-SPC.

3.5.2 Hand choice behaviour

Participants displayed systematic choice behaviour for the majority of target locations (Figure 3.2.A). The distribution of hand choice irrespective of stimulation condition shows that the target just left of midline (-7°) has the highest variability in hand use. In contrast, the frequency of choosing the hand ipsilateral to a target is near, if not at, maximum for most other target locations. This effect is unsurprising, given that previous work has extensively shown that people tend to choose the hand ipsilateral to a target (Bishop, Ross, Daniels, & Bright, 1996; Bryden, Pryde, & Roy, 2000; Bryden & Roy, 2006; Gonzalez & Goodale, 2009; Helbig & Gabbard, 2004; Mamolo, Roy, Rohr, & Bryden, 2006; Stins, Kadar, & Costall, 2001).

However, we also considered the possibility that the task demands extinguished true choice behaviour. In other words, participants may have performed a near binary selection procedure, based on the location of a target in left- or right-hemispace. On the contrary, response time analyses indicate a "cost" associated with hand selection in regions of target space with the highest level of competition uncertainty, and low bias. Bias in hand choice, here, refers to the mechanical and energetic advantage associated with reaching to a particular target location. The preference to use the hand ipsilateral to a target increases with target eccentricity (Valyear, Fitzpatrick, & Dundon, 2018). Observing a choice cost at this space is in line with previous reports (Oliveira et al., 2010). We take this evidence to corroborate

the ability of the reaching task to adequately assess hand selection behaviour. Further, that participants did not arbitrarily assign specific selection rules to specific targets.

3.5.3 Stimulation protocol

It could be argued, given the extent of parietal modulation in a free-choice condition (Fitzpatrick et al., 2019), that regions of the intraparietal sulcus unaffected by stimulation overcome the bias induced by cTBS. The data of Oliveira and colleagues (2010) refute this, and illustrate that focal stimulation of PPC is sufficient to evoke changes in hand selection (Oliveira et al., 2010). However, it is important to note that the shift from online to offline TMS is non-trivial.

Continuous TBS to pIP-SPC did not induce changes in hand selection, while online TMS applied to PPC has been shown to alter hand choice behaviour (Oliveira et al., 2010). The mechanics of "disruption" between online TMS and cTBS protocols are separable. Online TMS operates under the idea that indiscriminately activating neurons with a pulse introduces additional noise to neural processing (Silvanto & Cattaneo, 2017). Reducing the signal-to-noise ratio of a cell population involved in a particular cognitive process leads to impaired performance in a related task (Miniussi, Harris, & Ruzzoli, 2013; Silvanto & Cattaneo, 2017). Online TMS, therefore, compromises the encoding of relevant information within an activated cell population by adding random noise in-time with the pulse applied. On the other hand, cTBS is considered to modulate cortical physiology (Cárdenas-Morales, Nowak, Kammer, Wolf, & Schönfeldt-Lecuona, 2010), and, in particular, reduces the excitability of underlying cells by affecting synaptic efficacy (Huang et al., 2005; Huang, Rothwell, Edwards, & Chen, 2007).

We elected to apply cTBS as the most appropriate test of the PPIC model, which outlines that, at a systems-level, hand choice is determined by an interhemispheric competition between action plans in bilateral pIP-SPC. Suppressed excitability is essential in order to assess the predictions of the PPIC model; it is under these conditions that we can manipulate the interhemispheric neuronal competition underpinning hand choice. The PPIC model would not predict a change

in hand choice behaviour under sustained, unchanged, or the inconsistent suppression of cortical excitability. Following this, a critical assumption held for this investigation lies in the reliability of inducing and maintaining a reduction in the cortical excitability of pIP-SPC using cTBS.

We performed a follow-up investigation in order to evaluate whether cTBS had the expected, suppressive, after-effects on cortical excitability. This experiment will be presented in full, here, before returning to discuss the results with the current experiment in tandem.

CHAPTER 4

Assessing the efficacy of induced cortical inhibition following cTBS to M1.

4.1 Abstract

Continuous theta burst stimulation (cTBS) is an offline, high frequency, repetitive protocol used in transcranial magnetic stimulation, reported to supress the excitability of underlying cells. In *Experiment 2,* cTBS was applied to reduce the excitability of bilateral posterior intraparietal and superior parietal cortex and investigate changes in hand choice. No effects of cTBS compared to Sham stimulation were found. In this experiment, the efficacy of cTBS in suppressing the excitability of cells is investigated. Ten participants were re-recruited from *Experiment 2*. Participants (N = 21) received Active or Sham cTBS, applied to the left primary motor cortex (M1). The percent change in the average motor evoked potential (MEP) elicited in the contralateral hand muscle was compared across groups. Continuous TBS was expected to supress cells in the M1 and reduce the amplitude of the post-stimulation MEP relative to pre-stimulation for the Active group only. Contrary to this hypothesis, Active cTBS led to a significant increase in the group MEP compared to the Sham cTBS group. Results also show a high level of inter-individual variability. In a sample recalled from *Experiment 2,* cTBS is shown to have a variable, yet group-level facilitative, effect on M1 excitability.

4.2 Introduction

Modern methods used in cognitive neuroscience to probe and manipulate cortical excitability have predominantly relied on transcranial magnetic stimulation (TMS) (Allen, Pasley, Duong, & Freeman, 2007). TMS is a non-invasive neuromodulatory technique, when applied on the surface of the scalp can alter the firing rate of underlying cells (Barker, Jalinous, & Freeston, 1985; Pascual-Leone, Walsh, & Rothwell, 2000). In the following paragraphs, methods in assessing and altering cortical excitability using TMS will be discussed. In particular, the characterisation and use of the motor evoked potential (MEP) as a measure of corticospinal excitability. Further, the application and reliability of repetitive TMS protocols, with particular reference to continuous theta burst stimulation (cTBS), will be outlined. This investigation is conducted as a follow up to *Experiment 2* in *Chapter 3* of this thesis. In the experiment, cTBS was applied to the posterior parietal cortex in order to assess the hypotheses of the Posterior Parietal Interhemispheric Competition (PPIC) model. Here, the aim is to corroborate and assess the induced cortical suppression of the cTBS protocol in a sample recalled from *Experiment 2*.

TMS applied to primary motor cortex (M1) induces a response in the contralateral muscle, recorded electromyographically as a *motor evoked potential* (MEP) (Rothwell et al., 1987). The TMS pulse applied to M1 activates corticospinal neurons with monosynaptic connections to spinal motoneurons for the contralateral upper limb (Day et al., 1989; Palmer & Ashby, 1992). Accordingly, characteristics of the elicited MEP, particularly the amplitude, can offer a direct insight into the integrity of corticospinal conduction (Bastani & Jaberzadeh, 2012; Rossini & Rossi, 1998). The amplitude of an MEP, an index of size, is variable across individuals, though research has shown specificity within the hand muscles (Ziemann, Ilić, Alle, & Meintzschel, 2004), and high intraindividual test-retest reliability (Bastani & Jaberzadeh, 2012; Christie, Fling, Crews, Mulwitz, & Kamen, 2007; Doeltgen, Ridding, O'Beirne, Dalrymple-Alford, & Huckabee, 2009; Kamen, 2004).

The MEP profile is modulated by the state excitability of the corticospinal pathway. Decades of research have taken advantage of this relationship, and MEPs have been used to diagnose and treat patient groups with compromised corticospinal

connectivity (Di Lazzaro et al., 1999; Traversa, Cicinelli, Bassi, Rossini, & Bernardi, 1997), and to study cortical plasticity and re-organisation (Cohen, Bandinelli, Findley, & Hallett, 1991; Traversa et al., 1997). For instance, in stroke, the state of the MEP profile can inform the extent of damage and cortical reorganisation caused by the infarct (Cicinelli et al., 2005; Murase, Duqué, Mazzocchio, & Cohen, 2004; Trompetto, Assini, Buccolieri, Marchese, & Abbruzzese, 2000; Ward et al., 2006). In healthy individuals, contraction of a muscle increases the elicited MEP amplitude. This is achieved as the discharge of motorneurons in the primary motor cortex synchronises the firing activity of spinal motoneurons (Day et al., 1989; Rossini et al., 2015). In line with this, MEPs are facilitated during (Hess, Mills, & Murray, 1987; Stedman, Davey, & Ellaway, 1998; Tinazzi & Zanette, 1998) and immediately after (Brasil-Neto, Araújo, & Carneiro, 1999) contraction of hand muscles.

The size of an MEP is also influenced by other factors. In particular, the waveform and directionality of the TMS pulse applied (Di Lazzaro et al., 2001; Kammer, Beck, Thielscher, Laubis-Herrmann, & Topka, 2001; Mills, Boniface, & Schubert, 1992; Rossini et al., 2015; Sommer et al., 2006), as well as the intensity of the induced current (Capaday, 1997; Chen et al., 1998; Devanne, Lavoie, & Capaday, 1997; Rossini et al., 2015) influence MEP amplitude. On a trial-by-trial basis, MEPs can vary in size and shape even when these stimulator parameters are maintained as constant during stimulation (Ellaway et al., 1998; Kiers, Cros, Chiappa, & Fang, 1993). It is suggested that intrinsic fluctuations in neural excitability can contribute to this MEP variability (Rossini et al., 1994; Wassermann, 2002). In order to ensure that any change in the MEP is a result of a change corticospinal excitability, rather than state-variability and sampling noise, the relationship between TMS pulse and MEP is determined by averaging the muscle response across multiple samples (Rossini et al., 2015). Taking the average of twenty TMS pulses has been reported to provide a reasonable estimate of corticospinal excitability (Goldsworthy, Hordacre, & Ridding, 2016). Taken together, the MEP, when sampled appropriately, offers insights to corticospinal conduction and represents a physiological marker of cortical excitability.

TMS, specifically repetitive TMS (rTMS), can be used to induce temporary changes in cortical excitability. During rTMS, multiple TMS pulses are regularly applied to a single scalp position (Wassermann, 1998). The resultant changes in cortical excitability are expected to arise from the manipulation of long-term potentiation- or depression-like mechanisms at the level of cell synapse (Cárdenas-Morales et al., 2010). Depending on the protocol of stimulation applied, the induced after-effects of rTMS on cortical excitability are classified as excitatory or inhibitory (Maeda, Keenan, Tormos, Topka, & Pascual-Leone, 2000; Pascual-Leone, Valls-Solé, Wassermann, & Hallett, 1994; for review see Fitzgerald, Fountain, & Daskalakis, 2006). Low-frequency rTMS at a stimulation rate of 1Hz, for instance, is shown to reduce the cortical excitability of M1 and decrease MEP amplitudes (Chen, Classen, et al., 1997; Maeda et al., 2000; Muellbacher, Ziemann, Boroojerdi, & Hallett, 2000), while high-frequency rTMS facilitates MEPs and increases cortical excitability at 5Hz (Berardelli et al., 1998), 10Hz (Pascual-Leone et al., 1998), or 20Hz (Maeda et al., 2000).

Theta burst stimulation (TBS) is a variant of rTMS, where high-frequency, sub-threshold, bursts of stimulation are applied at theta frequencies (Huang et al., 2005). When applied continuously, in a protocol referred to as continuous TBS (cTBS), to primary motor cortex, a reduction in cortical excitability is reported (Huang, Edwards, Rounis, Bhatia, & Rothwell, 2005; Huang, Rothwell, Edwards, & Chen, 2007; for review see Wischnewski & Schutter, 2015; Chung, Hill, Rogasch, Hoy, & Fitzgerald, 2016). The cTBS protocol is particularly advantageous in its ability to induce long lasting effects over less stimulation time and lower stimulation intensity, as compared with alternative rTMS protocols (Cárdenas-Morales et al., 2010; Huang et al., 2005), leading to tremendous clinical interest (Di Lazzaro et al., 2006; Paulus, 2005; Talelli, Greenwood, & Rothwell, 2007; Talelli et al., 2012; Yamada et al., 2014). Similar to other rTMS protocols, cTBS is also hypothesised to act upon intrinsic mechanisms of long-term potentiation or long-term depression within the circuitry of motor cortex (Di Lazzaro et al., 2005), by inducing plasticity-like changes at synaptic connections (Huang, Chen, et al., 2007). Support for this account is provided as cTBS after-effects are shown to be dependent on activity in

N-Methyl-D-Aspartate receptors (Huang, Chen, et al., 2007; Teo, Swayne, & Rothwell, 2007).

In the original study detailing the cTBS protocol, Huang et al. (2005) illustrate the time course of suppressive after-effects. A reliable reduction in cortical excitability within 5 minutes post-cTBS is seen, though the data suggest a stability in suppression at ~20 min time-point (Huang et al., 2005). Subsequent investigations have replicated these effects, at ~20 minutes post-cTBS MEP amplitudes are reliably decreased with moderate-to-large effect sizes of d = -0.62 (Chung et al., 2016) and 1.37 (Wischnewski & Schutter, 2015) across 53 and 24 datasets, respectively. This effect translates to a mean reduction of 21.94% ± 3.27 SEM in MEP amplitude (Wischnewski & Schutter, 2015).

A high level of inter-individual variability in the response to TBS is reported within the literature (Brownjohn, Reynolds, Matheson, Fox, & Shemmell, 2014; Hamada, Murase, Hasan, Balaratnam, & Rothwell, 2012; Hinder et al., 2014; Lakhani, Bolton, Miyasike-daSilva, Vette, & McIlroy, 2014; Player, Taylor, Alonzo, & Loo, 2012; Rocchi et al., 2018; Vernet et al., 2014). In particular, Hamada and colleagues (2012) compare the after-effects of two forms of TBS; cTBS and intermittent TBS (iTBS), a protocol reported to induce a transient increase in cortical excitability (Huang et al., 2005). According to Hamada and colleagues (2012), 25% of participants presented the expected after-effects of TBS after stimulation (iTBS – facilitatory; cTBS – inhibitory), and 31% displayed the inverse (iTBS – inhibitory, cTBS – facilitatory), while 27% and 17% of participants were facilitated and inhibited, respectively, irrespective of the type of TBS applied.

A conversation surrounding the factors that may modulate the variability of cTBS after-effects has considered brain-derived neurotrophic factor polymorphisms (Antal et al., 2010; Cheeran et al., 2008; Lee et al., 2013), baseline excitability (Gentner, Wankerl, Reinsberger, Zeller, & Classen, 2007; Huang, Rothwell, et al., 2007; Iezzi et al., 2008), individual differences in I-wave recruitment (Hamada et al., 2012), and the intensity of single-pulse TMS for MEP measurement assessing the after-effects of TBS (Goldsworthy et al., 2016). Despite the acknowledged variability,

the cTBS protocol is widely applied in cognitive neuroscience and clinically as a method of inhibiting the targeted cortical region.

As previously stated, a critical assumption of *Experiment 2* lies in the efficacy of cTBS in reducing cortical excitability. Continuous TBS is expected to consistently depress the excitability of cells in the posterior parietal cortex across participants. Under conditions of reduced excitability, the predictions of the PPIC model and hand selection are assessed. It is important to explore, to the best of our ability, that the suppressive effects of cTBS are observable in our sample of participants. Unlike the relationship shared between primary motor cortex and MEPs, the posterior parietal cortex lacks the corresponding direct measure to qualify changes, if any, following application of cTBS. Therefore, the current investigation aims to assess the efficacy of cTBS in reducing the cortical excitability of M1 using MEPs in a sample recalled from *Experiment 2*.

Continuous TBS applied to M1 is expected to reduce the cortical excitability of underlying neurons. A decrease in baseline excitability of these cells is expected to translate to measures of corticospinal excitability. Specifically, a reduction in average post-stimulation MEP amplitude is expected, as compared to pre-stimulation.

4.3 Materials and Methods

4.3.1 Participants

Twenty-one individuals (8 males, 13 females, M = 24.05 years ± 4.82 SD) participated in the experiment. All participants were self-reported right-handed, corroborated by a modified version of the Waterloo Handedness Inventory (Steenhuis and Bryden, 1989; scores range from -30 to +30). Ten individuals (4 males, 6 females, M = 24.00 years ± 3.87 SD) were re-recruited from the sample of *Experiment 2*.

Participants were split into two groups, receiving Active (N = 11; 4 males, 7 females, M = 24.00 years ± 3.87 SD) or Sham (N = 10; 5 males, 5 females, M = 24.10 years ± 5.92 SD) stimulation. This study was conducted to explore and assess the cTBS-induced cortical suppression in participants of *Experiment 2*. All re-recruited participants were allocated the Active cTBS group. Participants were in good health with normal to corrected-to-normal vision. Through self-report, no contraindications to TMS were identified. All participants provided informed consent in accordance with the Bangor University School of Psychology Research Ethics Committee. The experiment took approximately 2.5 hours to complete.

4.3.2 Procedure

During the experiment, participants sat comfortably in a chair with their right forearm (the limb contralateral to stimulation) fully supported along the ulnar plane while their hand lay relaxed. Surface electromyography (EMG) data was collected from the first dorsal interosseous (FDI) muscle using two Ag/AgCl electrodes arranged in a belly-tendon configuration. Skin was prepared with a scrub and cleared with an alcohol wipe. EMG was amplified (4444 V/V), filtered with a band-pass filter (16-470Hz), digitized and sampled at a rate of 3000Hz to a computer using the BrainSight interface. EMG was collected with a 200ms window around the TMS pulse (50ms pre- to 150ms post-TMS pulse).

4.3.3 Stimulation and recording

Frameless stereotaxic neuronavigation (BrainSight Software, Rogue Research, Montreal, Quebec, version 2.3.10; Polaris System, Northern Digital Inc., Waterloo, Ontario, Canada) was used to monitor TMS coil position during stimulation for all participants. Individual MRI anatomical scans were used to identify the hand area in left primary motor cortex of the participants re-recruited from *Experiment 2* (see Section 3.3.4.1 for MRI acquisition details). The remaining participants were co-registered with the MNI template (Copyright 1993–2009 Louis Collins, McConnell Brain Imaging Centre, Montreal Neurological Institute, McGill University) in BrainSight.

4.3.3.1 Motor hotspot

Monophasic single-pulse stimulation was applied to the primary motor cortex (M1) using a 50mm figure-of-eight coil using a MagStim BiStim stimulator to define the motor hotspot. The coil was hand-held tangentially to the scalp, the handle orientated posterolaterally at 45° angle to the central sulcus, with a posterior-anterior current flow across M1. The M1 hotspot was identified by applying single pulses at a suprathreshold stimulator intensity with small spatial variations in the coil position on the scalp. The scalp location eliciting the most reliable and highest-in-amplitude motor evoked potential (MEP) was identified as the hotspot. The location and trajectory information required to stimulate the hotspot was saved as a target location in BrainSight. The BrainSight software provides online feedback relating to the coil position and orientation with respect to a target, offering real-time visual feedback to the experimenter. This information was used for all subsequent stimulation, to ensure the same site was interrogated for the remainder of the experiment.

4.3.3.2 Resting motor threshold

Monophasic single-pulse TMS pulses were delivered over the M1 hotspot during resting motor threshold (RMT) calculation using a Magstim BiStim stimulator and a 50mm figure-of-eight coil. RMT was defined as the minimum stimulator

intensity required to elicit a MEP in the relaxed FDI muscle of $\geq 50\mu$V peak-to-peak amplitude in 5 out of 10 consecutive stimuli, separated by $\geq$10s (Rossi et al., 2009).

4.3.3.3 Cortical excitability

Motor cortical excitability was defined across twenty trials of monophasic single-pulse TMS, applied to the M1 hotpot at 120% RMT using a Magstim BiStim stimulator and a 50mm figure-of-eight coil. Trials were separated by an inter-pulse-interval (IPI) (Min = 9.9s, Max = 29.7s, M = 11.6s $\pm$ 3.0 SD). The average MEP elicited from the 20 pulses was calculated at baseline and again 20mins after Active or Sham cTBS. MEP amplitude information was not visible to the TMS operator during the collection of pre- and post-stimulation cortical excitability. Participants wore ear protection during measurement of cortical excitability, as per the published TMS safety recommendations (Rossi et al., 2009). Previous experiments have shown that activation of the target muscle during or following cTBS can alter the after-effects of the intervention (Huang, Rothwell, Edwards, & Chen, 2007; Iezzi et al., 2008; see also Gentner, Wankerl, Reinsberger, Zeller, & Classen, 2007). In line with previous investigations (Hamada et al., 2012; Hsu et al., 2011), participants were therefore instructed to keep their hand completely relaxed during the 20 pulses and during a 20min post-cTBS period.

4.3.4 Continuous theta burst stimulation

4.3.4.1 Active motor threshold

Biphasic single-pulse stimuli were delivered over the M1 hotspot during active motor threshold (AMT) calculation using a Magstim Rapid[2] stimulator and a 70mm figure-of-eight coil. AMT was defined as the minimum stimulator intensity required to elicit a MEP in the partially contracted FDI muscle of $\geq 200\mu$V peak-to-peak amplitude in 5 out of 10 consecutive stimuli, separated by $\geq$10s (Oberman, Edwards, Eldaief, & Pascual-Leone, 2011). Participants performed a contraction of the FDI muscle of their right hand at 20% voluntary maximum during AMT calculation. Participants received visual feedback of their exerted force applied to a force transducer device during FDI contraction. A gauge depicted the strength of contraction using numerical (percentage of maximum) and colour-bar information.

Contraction around the desired 20% (±2%) was illustrated in green, over- or under-contraction was illustrated in red.

4.3.4.2 Continuous theta burst stimulation

Continuous theta burst stimulation was applied as per Huang et al. (2005); three pulses at 50Hz, repeated at 200ms intervals for 40s (total of 600 pulses). Continuous TBS was delivered with biphasic waveform at 80% of AMT using a MagStim Rapid² stimulator and a 70mm figure-of-eight coil. The coil was hand-held in position tangentially on the scalp surface, with the handle pointing posterolaterally from the central sulcus at ~45°. Participants wore ear protection during the 40s of stimulation.

4.3.5 Data analysis

The effects of stimulation (Active, Sham) on MEP peak-to-peak amplitude were assessed using an independent samples t-test. Specifically, we compare the percent change in MEP amplitude post- minus pre-stimulation, calculated per participant, per group. The percent change in the MEP is calculated as:

$$Percent\ change_{MEP} = \left(\frac{MEP_{post} - MEP_{pre}}{MEP_{pre}} \right) \times \frac{100}{1}$$

To test that observed differences are not attributable to baseline differences in cortical excitability or threshold, we also compared baseline MEP amplitudes and RMT values per group using independent samples t-tests. All results are considered significant at $p < 0.05$. Shapiro-Wilk test of normality was used to assess the distribution of the data. Levene's test is used to assess for the homogeneity of variances.

4.4 Results

Participants reported no adverse sensations following stimulation (see Appendix D, Table S4.1).

4.4.1 MEP amplitude

Figure 4.1.A indicates the inter-group difference in MEP expressed as the mean peak-to-peak amplitude across time for Active and Sham group conditions. At the group level, MEPs are unchanged in the Sham cTBS group and increased following Active cTBS. An independent samples t-test reveals a significant difference in the percent change in MEP amplitude for Active versus Sham participants $t(19) = 2.17$, $p < 0.05$. Following Active cTBS, the percent change in MEP amplitude (M = 49.43% ± 72.27 SD) is significantly greater than changes observed following Sham stimulation (M = -3.88% ± 30.20 SD) (Figure 4.1.B).
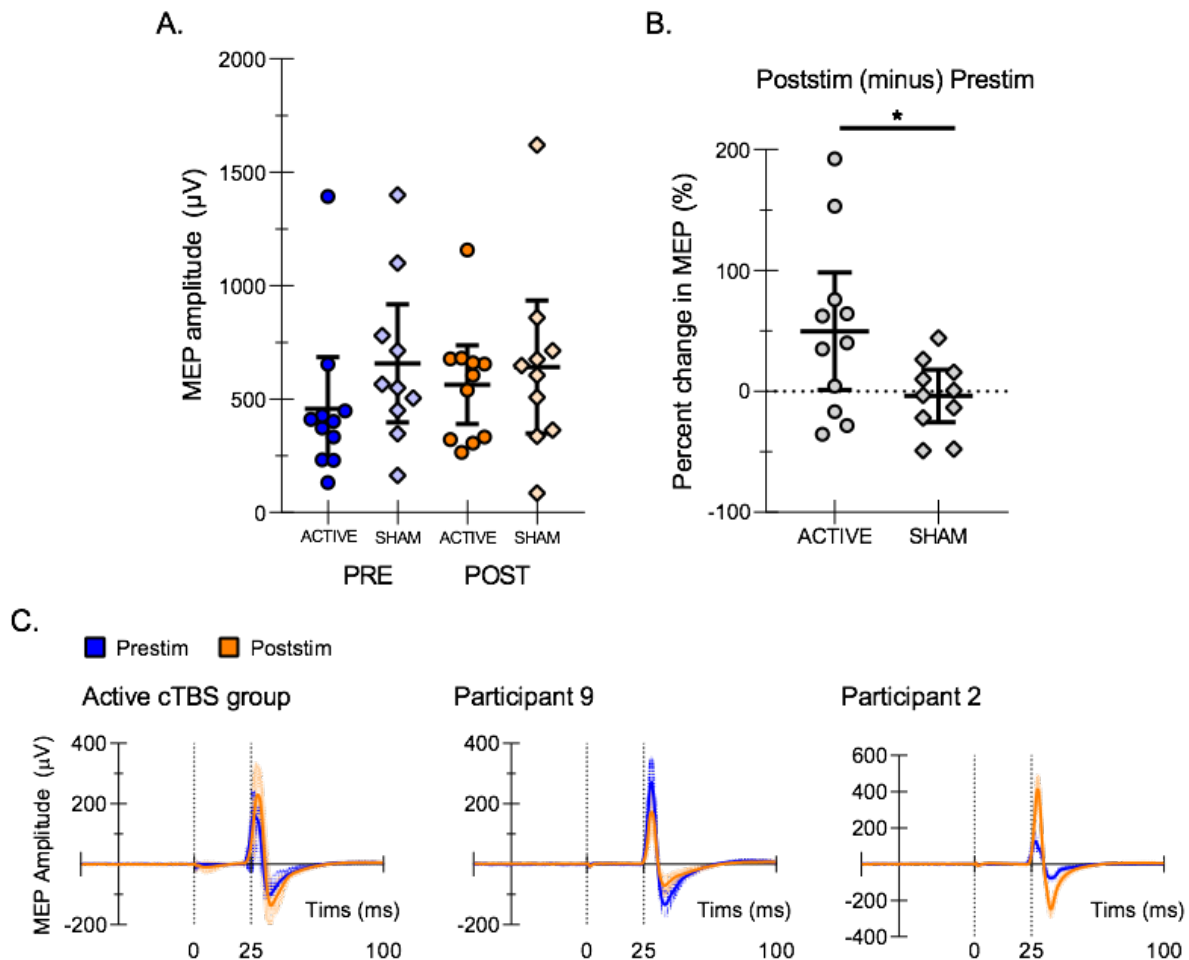
Figure 4.1. Motor evoked potentials. (A) Scatter plots indicate individual-level and group mean MEP peak-to-peak amplitude values in microvolts (µV) per cTBS group (Active, Sham) per time point (Pre – Pre-stimulation; Post – Post-stimulation). Black lines indicate group mean values. Error bars are 95% confidence intervals (CIs). **(B)** Scatter plots indicate percent change in MEP values expressed as difference scores between Post-stimulation minus Pre-stimulation as a function of Pre-stimulation baseline per cTBS group (Active, Sham). Black lines indicate group mean values. Error bars are 95% CIs. **(C)** *MEP recordings*. Average of 20 MEP trials used to assess cortical excitability for Pre-stimulation (purple) and Post-stimulation (orange). Shaded area indicate 95% CI bands. Illustrated for the Active cTBS group, and two exemplar participants demonstrating MEP suppression and excitation following cTBS.

The group-level MEP before and after Active cTBS, and individual-level data shown for two participants, for illustrative purposes (Figure 4.1.C).

4.4.2 Baseline measures

An independent samples t-test reveals that average baseline MEP amplitudes, calculated across 20 single-pulses applied to the M1 hotspot, did not differ across stimulation group, $t(19) = -1.30$, $p = 0.21$. Similarly, RMT values, calculated at baseline, did not significantly differ across stimulation groups, $t(19) = -1.39$, $p = 0.18$.

These data illustrate that participant groups are comparable pre-stimulation across threshold and cortical excitability measures, implying that subsequent between-groups differences are not attributable to differences at baseline.

4.5 Discussion

Continuous TBS is widely applied in cognitive neuroscience as a suppressive TMS protocol, with after-effects lasting for up to 60 minutes post-stimulation (Huang et al., 2005). However, a high variability in the after-effects of the cTBS is also reported in the literature (Do et al., 2018; Jannati, Block, Oberman, Rotenberg, & Pascual-Leone, 2017; Rocchi et al., 2018). A critical assumption of *Chapter 3* of this thesis relates to the consistent induced inhibition of the posterior intraparietal and superior parietal cortex (p-IP-SPC) after cTBS across participants. The efficacy of cTBS in supressing the cortical excitability of a subgroup of participants recalled from *Chapter 3* is examined in this experiment. We compare the change in cortical excitability across groups of participants who received Active or Sham cTBS. Changes in excitability are measured as percent changes in the peak-to-peak amplitude of the motor evoked potential (MEP) before and after stimulation. At a group level, participants who received Active cTBS show a significant increase in MEP amplitude compared to the Sham stimulation group. A high-level of inter-individual variation in the response to cTBS is also shown in the Active group. Contrary to the hypothesis, this result indicates that cTBS had a significant *facilitatory* effect on cortical excitability. These results will be firstly be discussed with respect to other studies detailing the after-effects of cTBS, and then with focus on the ramifications for *Chapter 3* of this thesis.

4.5.1 Variability in the cortical response to cTBS

4.5.1.1 Cortical response

The data show an increase in cortical excitability following cTBS. This result fails to reconcile with the wider literature, in which a reduction in cortical excitability induced by the cTBS protocol is commonly reported (Bonni et al., 2015; Conte et al., 2012; Goldsworthy, Vallence, et al., 2016; Hartwigsen et al., 2013; Huang et al., 2005; Kaulmann, Hermsdörfer, & Johannsen, 2017; Obeso et al., 2013; Ross, Iversen, & Balasubramaniam, 2018; Staines & Bolton, 2013). Instead, the data support the notion of high inter-individual variability in the cortical response to cTBS, similar to the results of Hamada and colleagues (2012). Hamada et al. (2012) report

facilitation of the MEP following cTBS in 58% of participants. In line with the data of Hamada et al. (2012), participants in the current study show facilitation of MEPs after cTBS (63.63% of the total sample); seven participants overall, though five participants which have a greater percent change compared to that seen in the Sham group. This facilitation represents the *inverse* of the expected after-effects of cTBS, consistent with Hamada and colleagues (2012). Three participants in the current dataset show the expected modulation, and are supressed (27.27% of the total sample), compared to 42% as seen in the study of Hamada and colleagues (2012). Overall, the group-wise consensus seen in the current sample is opposite to that expected following cTBS (Huang et al., 2005), though consistent with others (Do et al., 2018; Hamada et al., 2012; Jannati et al., 2017; Rocchi et al., 2018).

4.5.1.2 MEP amplitude

Hamada et al. (2012) split their data according to those who were *facilitated* and *inhibited* following cTBS. Performing the same post-hoc split on our sample, the results yielded from the Active cTBS group corroborate previous reports of percent changes in MEP amplitude. In a review of 24 studies, totalling 372 participants, Wischnewski and Schutter (2015) report that the average percent reduction in MEP following cTBS was 21.94% ± 3.27 SEM. The results yielded here are comparable, participants showing a suppressive effect of cTBS (N = 3) have a mean reduction of 26.96% ± 5.43 SEM in MEP amplitude. A comparison of amplitude changes with the participants who demonstrate a facilitation of M1 is less straightforward, considering that group-wise inhibition is predominantly reported in the literature. However, on the basis of induced changes post-iTBS, a mean increase of 28.51% ± 3.82 SEM in MEP has been reported (Wischnewski & Schutter, 2015). Our results indicate an average increase of 88.96% ± 22.66 SEM.

Whether these percent changes are truly meaningful is another question. For instance, splitting the Sham stimulation group in the same way; positive versus negative percent change in MEP as indicative of facilitation or suppression, a mean increase of 24.05% ± 7.50 SEM and decrease of 27.13% ± 9.19 SEM is evidenced. Participants in the Sham group, after no active stimulation, display a similar level of "inhibition" to a proportion of participants in the cTBS cohort. It is therefore difficult to

ascertain whether the participants in the Active group who illustrate suppression (N = 3) are truly supressed, or simply non-responsive to cTBS.

4.5.2 Potential considerations for the experimental use of cTBS

Given that cTBS presents variable after-effects (Hamada et al., 2012), the use of this stimulation protocol presents concerns for data integrity. This could suggest that the cortical response of any participant to cTBS should, where possible, be assessed a priori, and used as an inclusion criterion. Such a procedure has recently been adopted in the field. Derosiere and colleagues (2019) examine the percent change in MEP amplitude after cTBS delivered to M1 across seven time points (Range: 1 – 37 mins post-cTBS) for all participants in their experiment (N = 19). Any participant demonstrating a percent change in MEP in excess of +2.5 SD above the group at any time-point was excluded from subsequent analyses (Derosiere, Thura, Cisek, & Duqué, 2019). Following this exclusion criterion, data from three participants were not included. This procedure ensures that the main analyses of the experiment included only the data of cTBS-inhibited participants.

Corroborating the physiological effects of cTBS on brain areas outside of M1 is a more difficult task, and ultimately, this information is not yet known. The mechanisms of action in cTBS are a relatively new area of study. However, one avenue of potential promise is a combined EEG-TMS approach (Opitz et al., 2015). Here, the authors measure fronto-parietal phase coupling and the amplitude of somatosensory evoked potentials to investigate the effects of active and sham cTBS to the dorsolateral prefrontal cortex. Of course, combined EEG-TMS is not feasible for all studies. However this information, alongside other future investigations, will illustrate the regional response-pattern of cTBS that is necessary to inform use of this technique outside of M1.

In an alternative approach, the variability in inter-individual response to cTBS could be used as a determinant in power analyses. A power analysis was conducted a priori to *Experiment 2* to inform the sample size required for the detection of effects with 80% power. On the basis of a stimulation experiment assessing hand choice behaviour conducted by Oliveira and colleagues (2010), a sample of N = 20 was

determined. However, the inter-individual variability in response to cTBS was not considered as a factor when calculating the sample size. As such, the sample in *Experiment 2* may not be sufficient to assess changes in hand selection behaviour in conjunction with cTBS. The data here, alongside others (Hamada et al., 2012), provide an estimate of the proportion of participants who may respond 1) as expected, 2) inverse to the expected, or 3) non-responsive to cTBS. Future investigations might consider cross-referencing the size of the investigated effect with these data, which outline the inter-individual response estimates to cTBS.

4.5.3 Efficacy of cTBS-induced cortical inhibition: Experiment 2

The results of *Chapter 3* fail to provide support for the PPIC model of hand selection. Across three measures of hand choice, no effect of cTBS applied to the pIP-SPC relative to Sham stimulation is found. The results of *Experiment 2* could imply 1) a successful reduction in the excitability of the pIP-SPC, and failure to provide support for the PPIC model – a true null; or 2) a failure to consistently reduce the excitability of the pIP-SPC, and thus inadequate assessment of the hypotheses of the PPIC model. Here, on the basis of M1 stimulation, the results do not provide support for the suppressive after-effects of cTBS. Instead, the MEP amplitudes of participants who received active cTBS were significantly facilitated, at least when measured over M1.

Before commenting on this result, a note on the cross-validity of cTBS to alternative brain areas. As highlighted above, a comprehensive assessment of the effects of cTBS outside of M1 is not yet available. Noted effects of the cTBS protocol have been primarily extrapolated on the basis of stimulating M1 (Hu et al., 2017; Huang et al., 2005; Wischnewski & Schutter, 2015). In *Experiment 2,* it was assumed that the inhibitive effects of cTBS to M1 would hold when applied to the pIP-SPC. Several groups have also made this assumption, applying cTBS to various regions outside of the M1 (Bonni et al., 2015; Conte et al., 2012; Franca, Koch, Mochizuki, Huang, & Rothwell, 2006; Hartwigsen et al., 2013; Mochizuki, Franca, Huang, & Rothwell, 2005; Nyffeler et al., 2008, 2006; Obeso et al., 2013; Staines & Bolton, 2013; for review see Oberman et al., 2011). Results in-line with the suppressive effects have been reported with respect to the posterior parietal cortex (Kaulmann et

al., 2017; Nyffeler et al., 2008; Ross et al., 2018). As discussed previously, the after-effects of stimulation in these areas cannot be corroborated directly. The relationship between M1 excitability and MEPs presents the opportunity to qualify the after-effects of cTBS. Of course, a similar assumption now applies. On the basis of these results, which show that M1 is significantly facilitated after cTBS, it is not the claim to have increased the excitability of the pIP-SPC in *Experiment 2.* Rather, these results serve to indicate that the cortical response to cTBS within a subgroup of the *Experiment 2* sample is highly variable. It should be considered as a possibility when interpreting the data of *Experiment 2* that cTBS may not have affected the pIP-SPC as expected.

Variability in the cortical response of the pIP-SPC using cTBS would have direct consequences on the assessment of the PPIC model in *Experiment 2*. Without the successful suppression of pIP-SPC, the mechanics of neural competition are not influenced, and predictions of the PPIC model are inadequately investigated. For the sake of argument, taking the observed effects of cTBS to the M1 on the basis of the subgroup (N = 10; 7 facilitated, 3 inhibited, 1 unchanged) and applying the directionality to the full sample in *Experiment 2* (N = 20), it may not be surprising that TMS had no effect on measures of hand choice and motor performance.

In contrast, the results of *Experiment 3* could be used to suggest that group-wise facilitation should be considered as more likely. The ramifications of such a result effectively flips the predictions of the PPIC model (Figure 3.1.C). Continuous TBS applied to the pIP-SPC would *facilitate* the cells dedicated to movements with the contralateral hand, and increase the likelihood of selecting the hand contralateral to stimulation. In *Experiment 2,* cTBS of the R-pIP-SPC led to a significant reduction in right hand use around the point of subjective equality compared to Sham-cTBS, or increased use of the hand contralateral to stimulation. This result goes against the predictions of the PPIC model which assume suppression of cortical excitability following cTBS. However, under the circumstances of group facilitation, rather than inhibition, this result could be considered to be in line with the PPIC model.

On the other hand, individual-level responses to cTBS are also demonstrated to be variable. While the R-pIP-SPC stimulation led to a statistically significant

change in hand choice, other comparisons fail to reach statistical thresholds. Inter-individual variability in the response to cTBS dampens our ability to statistically detect changes in hand choice at the group level. At an individual level, the excitability of the pIP-SPC in some participants may indeed have been supressed, though their performance is treated statistically identically as those who were either facilitated by or non-responsive to stimulation in group analyses. Under these conditions, it is not altogether unexpected that other group-wise analyses yield statistically unreliable results. Subsequent exploratory analyses to investigate the performance of those truly suppressed are thwarted. The individual post-TBS response profile of participants in *Experiment 2* cannot be ascertained. Similarly, of those in the current study recalled from the previous, there are too few facilitated/inhibited for statistical analyses (N = 3).

4.5.4 Conclusion

Continuous TBS, as with other rTMS protocols, presents a certain level of risk and discomfort for participants (Oberman et al., 2011; Rossi et al., 2009). Further, the variability of after-effects presents issues for data integrity. It is important to justify, to the best of our ability, the use of cTBS as an effective method for use in cognitive neuroscience. Here, the inverse of the expected after-effects of cTBS to M1 are illustrated. At a group-level, a significant increase in the MEP compared to baseline for participants who received Active, rather than Sham, stimulation is shown. Further, the response is highly variable. The majority of participants were facilitated following cTBS, while a subgroup were suppressed and/or non-responsive. In *Experiment 2*, stimulation of the pIP-SPC did not lead to consistent alterations in hand choice behaviour. This follow-up experiment investigated the efficacy of cTBS in reducing the cortical excitability of a sample of participants recalled from *Experiment 2*. Synthesising the results of both investigations, the significant facilitation of the group MEP and the inter-individual response to cTBS could shed light on the lack of empirical support for the PPIC model demonstrated in *Experiment 2*. The data reported here also highlight how the interpretation of the results of *Experiment 2* is complex.

5. Discussion

In everyday behaviours, such as reaching for a glass of water, a constellation of information is transformed and synthesised prior to the initiation of a movement. Among the computations necessary, and amid the most elemental, is hand selection – how do you choose a hand for action? This thesis has investigated *how* hand selection is deliberated, and *where* in the brain this process takes place. The results of the empirical work contribute to our knowledge of these mechanisms, and importantly, address persisting questions in the field.

At the outset of this chapter, the findings and implications of the results of *Chapters 2*, *3*, and *4* are summarised. The data are firstly discussed with respect to hand choice and the role of the posterior parietal cortex. Secondly, the degree to which the current data speak to the hypothesis that hand selection involves competition between multiple action plans is examined. The aims, interpretations, and limitations of each study and how they synthesise with the Posterior Parietal Interhemispheric Competition (PPIC) model is considered throughout this chapter. Following the summary of findings, the persisting queries and the directions for how future work can continue to address the cognitive and neural mechanisms of human hand selection are outlined. Finally, the greater theoretical implications and applications of this line of study are briefly discussed.

5.1 Summary and implications

The cognitive and neural mechanisms of action selection present a source of consistent debate within the field of cognitive neuroscience (Gallivan et al., 2018). The selection of a hand for action and the specification of the motor parameters for movement have been theorised to unfold serially, in separate neural systems (Bernier et al., 2012; Padoa-Schioppa, 2011; Tversky & Kahneman, 1981). The empirical chapters of this thesis refute this account, and shed light on the contribution of the bilateral posterior parietal cortex, a region dedicated to the planning and online control of actions, in hand *selection*. Further, the data are

consistent with the notion that selection unfolds via a neuronal competition between concurrently specified action plans.

5.1.1 The PPIC model

In *Chapter 2* a new neurobiological model of human hand selection is proposed, which we call the Posterior Parietal Interhemispheric Completion (PPIC) model (Fitzpatrick et al., 2019). At the cognitive level, the PPIC model posits that hand selection occurs in tandem, and indeed as a function of, the preparation of multiple viable action plans which compete for selection. Further, at the neural mechanistic-level, hand selection unfolds within the frontoparietal networks that perform the sensorimotor transformations required for action planning, the bilateral posterior parietal cortex in particular. The PPIC model presents a practical contribution to the field. Here, we outline a heuristic method for investigating human hand selection. In line with this, the PPIC model is used to frame the design, hypotheses, analyses, and interpretations of all the experiments herein presented. Likewise, the PPIC model may be adopted, tested, and revised by others in the field. Throughout the empirical chapters of this thesis, a multi-method approach has been adopted to test the PPIC model. In the sections below, a summary of the findings is presented alongside the implications that the data pose.

5.1.2 Hand choice and the posterior parietal cortex

As illustrated by *Chapter 2*, the notion of a dominant cortical "hub" for action selection is inconsistent with our findings. Here, in line with the PPIC model, fMRI shows that hand selection activates a *network* of brain areas. In particular, fMRI analyses reveal extensive activation in bilateral posterior intraparietal and superior parietal cortices (pIP-SPC) for freely chosen movements. Activation is localised along the medial bank of the intraparietal sulcus, in the superior parietal lobule, and a territory more medial and posterior situated near the parieto-occipital junction. Critically, by virtue of the paradigm in use, trials included in all analyses were carefully matched for visual and motor requirements across conditions. That is, while matched for motor and visual features, the act of choosing a hand for action recruits the pIP-SPC.

The pIP-SPC regions identified correspond well to the areas of action planning outlined in the wider literature. As discussed in detail in *Chapter 1*, specific areas in the pIP-SPC specify the spatiotemporal parameters that are critical for the planning and online control of visually guided hand actions (Section 1.3). In particular, the medial bank of the intraparietal sulcus and the superior parieto-occipital cortex constitute key nodes of the parietal reaching network (see also Figure 1.3). Given the correspondence with the activation illustrated in *Experiment 1*, we take this as evidence that the neural regions that perform the sensorimotor transformations that are necessary for the planning of actions also mediate hand selection. That is, hand selection is underpinned by the same mechanisms as the preparation of motor plans for movement.

From a theoretical standpoint, the data diverge from the view outlined in the action selection literature, which suggests that hand selection is localised to the left-lateralised dorsal premotor cortex (di Pellegrino & Wise, 1993; Halsband & Passingham, 1982; Mitz et al., 1991; Rushworth et al., 2003). On the contrary, cooperation across a network of brain areas is shown to mediate hand selection. Our data contribute to the growing body of literature which poses that action selection is mediated by the same neural territories that plan and control movements (Ariani et al., 2015; Christopoulos, Bonaiuto, Kagan, et al., 2015; Christopoulos et al., 2018; Cisek, 2007; Cisek & Kalaska, 2010; Klaes et al., 2011). Importantly, the data provide the first evidence to that the pIP-SPC is involved in human hand selection.

The identified regions of pIP-SPC display a preference for the contralateral limb. In other words, within the pIP-SPC the BOLD signal is preferentially modulated by actions performed with the contralateral hand. Additional analyses reveal that the contralateral hand specificity is independent of the spatial location of targets. The hand-specificity demonstrated in our data complements the results of Valyear and Frey (2015), who show that the action plans are encoded at a hand-specific level in the posterior parietal cortex (PPC). Importantly, the data of *Experiment 1* extend this idea, and demonstrate that action selection is also outlined in hand-specific terms.

In *Experiment 2,* we applied continuous theta-burst stimulation (cTBS) to test the hypothesis that pIP-SPC is critically involved in hand choice. According to the

PPIC model, depressing excitability within the pIP-SPC using cTBS would increase the likelihood of selecting the hand ipsilateral to stimulation. Across three measures of hand choice, the majority of our results do not support this prediction. Instead, hand choice behaviour was comparable across stimulation sessions. Together with the fMRI results of *Chapter 2*, our stimulation experiment suggests that while choosing a hand for action *modulates* the pIP-SPC, the pIP-SPC does not play a *critical* role in hand choice.

Exploratory analyses in *Chapter 3* reveal an effect of stimulation. Continuous TBS to the Right-pIP-SPC is shown to decrease the proportion of right hand use compared to Sham stimulation. This effect is subtle, observable in a region of target space associated with high action competition, the point of subjective equality (PSE) (Oliveira et al., 2010; Valyear et al., 2018). The decrease in right hand use following Right-pIP-SPC relative to Sham cTBS conflicts with the hypotheses of the PPIC model. Following cTBS to Right-pIP-SPC, an increase in right hand use was expected. Though the directionality is unexpected, this result does implicate a role of the pIP-SPC in hand selection.

Ultimately, the results of *Experiment 2* do not support the PPIC model of hand selection. The data reveal that hand choice behaviour is largely insensitive to cTBS. In light of the invariable hand choice behaviour observed (Figure 3.2.A), we considered the possibility that participants adopted a fixed stimulus-response behaviour schedule according to target location. That is, the spatial locations of targets became overlearned and extinguished true choice behaviour. Additional analyses refute this possibility. In line with our previous behavioural work (Valyear et al., 2018), and others (Oliveira et al., 2010), evidence of a "cost" associated with choosing a hand in a region of highly competitive space is seen. Response times to initiate movements to the PSE are increased compared to targets in the periphery of the display. This result is taken as evidence that participants did not adopt a rule-based selection procedure. Further, that the paradigm in use was effective in assessing hand choice.

Following this qualification, the efficacy of induced cortical inhibition following cTBS was investigated in another study (*Experiment 3*). The aim of the follow-up

study was to corroborate the consistent suppression of cortical excitability across participants. *Experiment 3* demonstrates that the after-effects of cTBS can be precarious. The data show that cortical excitability was significantly facilitated following cTBS. This result represents the inverse of the expected after-effects of cTBS on cortical excitability. Continuous TBS was originally considered to suppress the excitability of neurons (Huang et al., 2005; Ortu, Ruge, Deriu, & Rothwell, 2009; Suppa et al., 2016). We fail to replicate the after-effects of cTBS outlined in these reports. Instead, in the majority of our participants facilitatory effects are induced. Further, at an individual-level our results show that the response to cTBS is highly variable. A proportion of the participants display a reduction in corticospinal excitability, while others were unchanged following cTBS. These results, group-level facilitation and inter-individual variability in after-effects, are in line with what has been reported previously (Hamada et al., 2012).

It is possible that *Experiment 3* can elucidate the results yielded in *Experiment 2*. Given the variability demonstrated in the after-effects of stimulation, cTBS may not have consistently suppressed the pIP-SPC in participants, or across sessions. Variability in the cortical response to cTBS effectively decreases our ability to statistically detect changes, if any, in hand selection as a function of cTBS. This result calls into question whether the role of the pIP-SPC in hand choice was adequately assessed in this experiment. Further, it could be considered, at least in principle, that cTBS had a facilitatory effect on the majority of our participants. The predictions of the PPIC model are effectively flipped under the circumstance of facilitation. The observation of decreased right hand use following cTBS to Right-pIP-SPC is consistent with this possibility, though the Left-pIP-SPC result is not. Altogether, the results of *Chapter 3* shed light on the lack of empirical support for the PPIC model in *Experiment 2*, though the interpretations are complex. Whether the functions of the pIP-SPC critically contribute to hand choice is yet to be determined.

5.1.3 Multi-specification and action competition

Evidence throughout the empirical chapters of this thesis support a multi-specification and action competition account. That is, hand selection involves the preparation of several viable action plans, referred to as *multi-specification*, that

compete for overt selection. Firstly, in *Experiment 1*, behavioural (response time, RT) evidence is presented which indicates that hand selection involves competition. Participants take longer to initiate their freely chosen, as compared to instructed, reaches. Again, in this study the visual and motor requirements across instruct and choice conditions are matched. The key feature dissociating these conditions is, therefore, the act of hand selection. Consistent with our prior behavioural work (Valyear et al., 2018), we consider this increase in RT to reflect competition. A neuronal competition must be resolved prior to action onset. As cells compete for overt execution, the deliberation between potential plans increases the time taken for one plan to reach threshold. The deliberation/competition is bypassed in the instructed condition.

Functional MRI data in *Chapter 2* indicates that hand selection unfolds as a competitive process within the pIP-SPC. In a separate analysis, independent from the contrasts used to identify "choice" regions, we tested for evidence of a cost associated with targets in high competition space. Our results support the PPIC model. Functional MRI response levels in regions of the pIP-SPC are increased for targets in the centre of the display, and regions surrounding the PSE, during freely chosen movements. This is in contrast with targets in the periphery, which are biased in favour of ipsilateral hand selection. This result is not observable in other "choice" regions identified – i.e. outside of the pIP-SPC (dPMC, lateral occipital temporal cortex, and inferior parietal lobule). Additional RT analyses are also consistent with a choice gradient as a function of target space. Response times in the scanner are extended for freely chosen reaches toward regions of target space presenting the highest level of uncertainty or competition, as well as the lowest bias. The results of the behavioural analyses do not meet the boundaries of statistical significance. However, when competitive space is defined as a function of a participant's PSE, or the point in space where hand choice is equally likely, this trend approaches significance.

Moreover, evidence of a choice cost associated with targets high competition (PSE) is presented in *Experiment 2*. Here, outside of the space- and time-constraints imposed by our fMRI setup, the time taken to initiate movements toward targets

surrounding the PSE is significantly prolonged, compared to targets in the periphery. That is, using a larger target display as well as an increased number of trials per target per run compared to *Experiment 1*. Taken altogether, these data corroborate previous accounts, which have also illustrated that choosing a hand for action has behavioural consequence (Oliveira et al., 2010; Valyear et al., 2018; Viswanathan et al., 2019). The results are also in line with the hypothesis that hand selection involves the resolution of competition between serval action plans.

Importantly, these neuroimaging and behavioural data extend what has been observed previously in primate neurophysiology and human behavioural studies. Multiple accounts demonstrate that concurrent action plans are represented in primate brain in response to a single stimulus (Andersen et al., 1997; Christopoulos, Bonaiuto, & Andersen, 2015; Cisek & Kalaska, 2005; Kalaska & Crammond, 1995; Klaes et al., 2011; Pastor-Bernier & Cisek, 2011b; Suriya-Arunroj & Gail, 2019). The data also correspond to human behavioural investigations, which also support the notion of simultaneously active action plans during action selection (Chapman et al., 2010; Gallivan et al., 2016; Ghez et al., 1997; Stewart et al., 2014; Van der Stigchel et al., 2006). Whether or not such a mechanism is at play in the human brain had not been assessed with neuroimaging methods previously. *Experiment 1* is the first to test the multi-specification account using fMRI. While the current data cannot capture the specificity as seen in these primate studies, we illustrate that the human brain may also develop multiple action plans in sensorimotor cortex. Of course, the explicit preparation of multiple action plans cannot be ascertained by the current dataset. That is, whether the increased level of neural activity in response to targets in the PSE are a direct result of multi-specification; this level of insight is arguably only possible through invasive means, such as cell recordings. Acknowledging this limitation, there is nonetheless a growing consensus in support of multi-specification in humans.

5.1.4 Summary

Here, using a multi-method approach, we present data that implicate a role of the pIP-SPC in hand selection. The data are also in line with the predictions of the PPIC model. Freely chosen actions are demonstrated to activate a network of brain

areas, with correspondence to nodes of the parietal reaching network. Interrogating this further, contrasting and supportive evidence for a critical role of the pIP-SPC is found. While cTBS to pIP-SPC does not result in systematic changes in hand selection, the efficacy of cTBS in consistently suppressing cortical excitability is called into question. These data advance the current understanding of the cognitive and neural mechanisms of human hand selection. Specifically, the data are consistent with the hypothesis that selection involves neural competition between concurrently specified action plans, integrated within the core sensorimotor system.

5.2 Persisting queries and directions for future investigation

The empirical works described in this thesis advance our conception of *how* and *where* human hand selection is mediated in the human brain. Of course, a number of avenues for continued investigation persist, both independent of and in light of these results. In the paragraphs below, two courses in particular are outlined in order to expand and progress this work. Firstly, in relation to the critical role of the posterior parietal cortex in hand selection. Secondly, whether hand selection is underpinned by a competition between multiple simultaneously specified action plans. The broader implications of this work are then discussed, with particular reference to potential prospective clinical translation.

5.2.1 A causal role of the posterior parietal cortex in hand selection

As evidenced by *Experiments 2* and *3*, the role of the pIP-SPC in hand choice is inconclusive. Whether or not the pIP-SPC plays a critical role in hand selection warrants further investigation. An alternative study, devised in light of the results outlined above, might incorporate a different form of TMS. Two methods in particular are possible, dissociated by an *offline* or *online* approach. In offline TMS, the after-effects of stimulation persist following the application of a protocol (e.g. cTBS). However, the data outlined in *Experiment 3* alongside the reports of others (Hamada et al., 2012; Wischnewski & Schutter, 2015) motivate the application of an alternative offline protocol. For example, low-frequency (1Hz) repetitive TMS (rTMS) applied for 10-20 minutes has been evidenced to depress the excitability of the cortex locally (Chen, Classen, et al., 1997; Grossman, Battelli, & Pascual-Leone, 2005; Knecht, Ellger, Breitenstein, Ringelstein, & Henningsen, 2003; Merabet et al., 2004; Pascual-

Leone, 1999). This protocol is arguably more established than cTBS, though in practical terms imposes additional considerations (Cárdenas-Morales et al., 2010). For instance, compared to the 40 seconds of cTBS, low-frequency rTMS is applied over the course of ~20 minutes. This requires both the participant and the TMS operator to remain still, with the coil in the same angular position on the scalp for the duration of stimulation. Further, the average stimulator intensity in conventional rTMS protocols is higher than the standard 80% of active motor threshold in use in cTBS (Cárdenas-Morales et al., 2010; Chen, Gerloff, et al., 1997; Huang et al., 2005; Pascual-Leone et al., 1994). Nonetheless, using this rTMS method might prove insightful for the current purposes. Specifically, inhibitive rTMS would follow the same procedure, in principle, as *Experiment 2.* Depressing cortical excitability would test the hypothesis that hand selection unfolds via a neural competition within the pIP-SPC.

Alternatively, online TMS could be adopted. Online TMS indiscriminately introduces noise to the system during the processing of a particular task (Silvanto & Cattaneo, 2017). Online TMS can compromise the encoding of information by reducing the signal to noise ratio within a cell population. Importantly, disruption occurs *in-time* with a pulse, or pulses, applied. An important factor to consider in online TMS experiments, then, is the timing of stimulation. This feature poses a challenge for the current work. The timeframe of "when" an action plan is consolidated and hand selection is determined is currently unknown. Following previous examples, Oliveira and colleagues (2010) elected to apply a single TMS pulse 100ms after target onset to investigate the role of the PPC in hand choice. Stimulation applied to the Left-PPC significantly increased left hand use (Oliveira et al., 2010). Adopting a similar approach, though integrating the localisation information afforded by our fMRI investigation, may further elucidate the role of bilateral pIP-SPC in hand selection.

Another possibility is available that minimises the necessity of knowing strict timing boundaries; a short burst or train of TMS pulses can be applied to infer the role of a region in a particular task(s) (Ellison & Cowey, 2006). This form of TMS has been used to assess visuomotor behaviour in the past. In particular, Vesia and

colleagues (2010) apply a burst of TMS pulses (10Hz over 300ms) to three parietal sites to assess the specificity of the PPC in reach and saccade behaviour (see also Section 1.3.5). Using online TMS, the neural competition aspect of the PPIC model is not investigated *per se*. Rather, this more liberal TMS approach would provide strong foundational evidence to implicate the pIP-SPC as necessary for selection. Additional work could then refine the timing window, to uncover the critical time point(s) underpinning selection.

Ultimately, irrespective of TMS protocol in use, the PPIC model offers a framework to test the clearly defined predictions with respect to hand choice. An inhibitive rTMS protocol (e.g. 1Hz) would be expected to reduce the excitability of pIP-SPC and manipulate the action competition in favour of selecting the hand ipsilateral to stimulation. Online TMS could be used to test whether pIP-SPC plays a causal role in hand choice, with the potential to determine the critical time points during the planning and selection processes.

5.2.2 Action competition underpinning hand selection

Throughout the empirical chapters of this thesis, reach-to-touch tasks, shown to correspond to complicated action choices (Trommershäuser, Maloney, & Landy, 2003), and free choice conditions have been employed to assess hand selection. Our data suggest that action selection is underpinned by a process of neural competition between action plans in the pIP-SPC (Section 5.1.3). However, while analyses assessing action competition consistently follow the predicted direction, not all results are statistically significant.

In *Experiment 1*, we observe a significant effect of target location in a subset of analyses. The neural response to freely selected reaches to targets surrounding the PSE is significantly increased in some, though not all, parietal regions. This effect also trends towards significance in complementary behavioural analyses. These data suggest that level of choice opportunity or action competition incited by targets surrounding the PSE can be bolstered. Relatedly, participants in *Experiment 2* display a rigidity in hand selection behaviour. That is, participants largely select the hand ipsilateral to a target. While this effect is largely unsurprising, the level of

choice-rigidity also implies that the level of competition incited by the paradigm could be reinforced.

There is a wide body of literature available outlining the factors which influence hand choice. For unimanual reaching, hand preference (Bryden, 2016; Mamolo et al., 2006; Stins et al., 2001), the spatial location of a target (Coelho, Przybyla, Yadav, & Sainburg, 2013; Gabbard & Rabb, 2000; Gonzalez, Flindall, & Stone, 2015; Kim, Buchanan, & Gabbard, 2011; Mamolo, Roy, Bryden, & Rohr, 2004; Stins et al., 2001), biomechanical state required for contact (Cos, Bélanger, & Cisek, 2011; Cos, Medleg, & Cisek, 2012; Rosenbaum et al., 1990; Sabes & Jordan, 1997; Wood, Chouinard, Major, & Goodale, 2017), effort (Schweighofer et al., 2015), task demands (Gonzalez et al., 2015; Gonzalez, Whitwell, Morrissey, Ganel, & Goodale, 2007; Gonzalez & Goodale, 2009; Liang, Wilkinson, & Sainburg, 2018; Mamolo et al., 2004), sensorimotor asymmetries (Coelho et al., 2013), reward (Rost, Hemmes, & Alvero, 2014; Stoloff, Taylor, Xu, Ridderikhoff, & Ivry, 2011), and recent action history (Valyear et al., 2018) are shown to affect effector selection. That is, manipulation of, for example, task demands can increase the use of the dominant hand, by requiring precision grip (Gonzalez et al., 2007), or increasing the cognitive-perceptual load (Liang et al., 2018). In contrast, occluding vision (Przybyla, Coelho, Akpinar, Kirazci, & Sainburg, 2013), or manipulating the reinforcement history of actions (Stoloff et al., 2011), can increase the rate of non-dominant hand selection. However, an important distinction is required when assessing the hypothesis that selection involves multiple competing action plans. It is imperative that dynamic choice options are available during deliberation (Section 1.4.2). This is acknowledged within the greater decision-making literature, which emphasises the necessity of unpredictable choice options during action selection (Cisek, Puskas, & El-Murr, 2009; Cisek & Thura, 2018, p.93; Thura, Beauregard-Racine, Fradet, & Cisek, 2012). The ultimate goal, then, is not to increase dominant/non-dominant hand use per se, but to provide the environment affording the maximal number of actions across hands.

To date, there are a limited number of behavioural investigations which have addressed whether selection involves action competition (Chapman et al., 2010;

Gallivan et al., 2016; Ghez et al., 1997; Stewart et al., 2014; Van der Stigchel et al., 2006). These studies have focussed on action selection with the same effector (usually the right hand), rather than hand selection. Nonetheless, an important feature is consistently included across these studies to support the specification of multiple action plans – the reliability of target information, or risk (Maloney, Trommershäuser, & Landy, 2007; Trommershäuser et al., 2003; Wolpert & Landy, 2012). That is, participants did not know what target was the ultimate goal for movement from the outset of a trial. A similar feature could be integrated with the reach-to-touch paradigms of this thesis to assess hand choice, and bolster the action competition incited by targets.

For example, a cuing element could be incorporated to manipulate the degree of target location certainty. At the onset of a trial, a colour and spatial cue could indicate task condition (choice, instruct) and target location (left hemispace, right hemispace), respectively. While the condition cue would be universally accurate, the spatial element would vary in reliability. Variance in the reliability of the spatial cue contributes to the level of target uncertainty and, by function, the level of multi-specification incited. Alongside additional constraints to ensure that visual and motoric features are matched, an interaction term is predicted. Behavioural (RTs) and neural measures would be increased during free choice and unreliably cued compared to the instructed unreliably cued trials. Similar to the experiments presented here, this response gradient could be further exacerbated in regions of target space presenting the highest competition (PSE) compared to the periphery.

Our data support the hypothesis that hand selection is underpinned by a neural competition between concurrently specified action plans. It would appear, however, that the salience of competition across targets, hands, and paradigms could be promoted. To this end, the manipulation of target uncertainty is suggested as a method of reinforcing and maintaining action competition within a free choice paradigm. Future investigations can perhaps include this feature to assess whether hand and action selection unfolds via a competition between multiple plans in the human brain.

5.2.3 Translation

The data presented across the empirical chapters of this thesis have clinically-relevant implications. The following paragraphs will discuss the possible applications of the current works in an applied setting. Firstly, in relation to the clinical use of cTBS. Secondly, the potential wider contributions of the PPIC model in upper limb rehabilitation interventions.

The results of *Experiment 3* indicate that cTBS presents ethical concerns, particularly when applied in a clinical setting. Continuous TBS is considered to have tremendous practical and clinical value (Di Lazzaro et al., 2006; Paulus, 2005; Suppa et al., 2016; Talelli et al., 2007, 2012; Yamada et al., 2014). The cTBS protocol has been applied globally in various patient groups, including stroke (Ackerley, Stinear, Barber, & Byblow, 2010; Di Lazzaro et al., 2013; Meehan, Dao, Linsdell, & Boyd, 2011; Talelli et al., 2007), depression (Li et al., 2014; Plewnia et al., 2014), schizophrenia (Demirtas-Tatlidede et al., 2010; Haraldsson, Ferrarelli, Kalin, & Tononi, 2004; Poulet, Brunelin, Makhlouf, D'Amato, & Saoud, 2009), and Parkinson's disease (Bologna et al., 2015; Eggers, Fink, & Nowak, 2010). Researchers have also augmented the original protocol outlined by Huang and colleagues (2005), in some cases to increase the number of TMS pulses applied to the brain (e.g. Li et al., 2014). However, the data presented by *Experiment 3*, alongside recent investigations by others (Hamada et al., 2012; Wischnewski & Schutter, 2015), indicate that cTBS has yet to undergo the rigorous investigation necessary to substantiate the after-effects in healthy controls.

Presumably, the application of cTBS in a clinical context rests upon the assumption that decreasing the excitability of neurons will have a positive therapeutic effect. Given the high inter-individual variability in the after-effects of cTBS demonstrated, it follows that the reversed after-effects of cTBS, facilitation rather than inhibition, may exacerbate the very aspect the intervention aimed to ameliorate in these patient groups. The application of, on average, 600 TMS pulses to patients with abnormal or damaged neural circuitry should be approached with due caution. Within the research domain, efforts to qualify the post-cTBS response profile of a participant have recently been adopted (Derosiere, Thura, Cisek, &

Duqué, 2019; Hamada et al., 2012). The inclusion of a similar procedure may also be prudent for the future clinical use of cTBS.

The PPIC model offers new insights into the organisation and execution of hand actions. The core features of the model outline that selection and specification occur simultaneously in an integrated fashion within bilateral pIP-SPC. Our efforts in understanding how the brain mediates basic actions has the capacity for clinical significance, particularly for individuals who have suffered a brain or bodily injury leading to the impaired use of the hand and arm. The PPIC model poses testable predictions that could contribute to evidence-based therapies for the recovery of hand and arm function.

Hemiparetic stroke is perhaps of particular pertinence. Weakness or paralysis of the contralesional hand and arm is one of the most pervasive side effects of hemiparesis (Krakauer & Carmichael, 2017, p. 20). A constellation of behavioural (Daly et al., 2019; Liepert et al., 1998; Okabe et al., 2019; Taub, Uswatte, & Pidikiti, 1999), pharmaceutical (Gekht, Burd, Selikhova, Iaish, & Beliakov, 1998; Gracies, Nance, Elovic, McGuire, & Simpson, 1997), and TMS (Hao, Wang, Zeng, & Liu, 2013; Hummel et al., 2005; Reis et al., 2008; Ward & Cohen, 2004; Webster, Celnik, & Cohen, 2006) interventions are in practise in the treatment of hemiparesis, with varying degrees of efficacy in alleviating the symptoms of impairment (Teasell et al., 2009). Here, the PPIC model offers a potential new pathway to intervention. Adopting the framework outlined in the PPIC model, TMS could be used to manipulate the mechanisms of *selection* in stroke recovery. Most stimulation interventions to date have focused on targeting primary motor and sensory cortex to ameliorate motor function after stroke (Reis et al., 2008; Ward, 2005). Explicitly targeting the "upstream" mechanisms underlying hand selection has not yet been explored.

Targeting the mechanisms of selection could reinforce the positive effects of existing upper limb therapies. For example, a behavioural intervention showing particular promise in stroke rehabilitation is Constraint Induced Movement Therapy (CIMT) (Liepert et al., 1998; Taub et al., 1999). In a randomised-controlled trial, CIMT has been reported to improve responses in the Wolf Motor Function Test, a

clinical assessment of motor function in the upper extremity (Wolf et al., 2001), and performance in common activities of daily living (Wolf et al., 2010). In CIMT, the ipsilesional, or healthier, hand is restrained for 90 percent of waking hours. Intensive behavioural training with the contralesional hand takes precedence. The beneficial effects of the forced use and skill training with the affected hand in functional recovery have also been shown by others (Daly et al., 2019; Okabe et al., 2019). A critical feature of CIMT is the promoted use of the affected hand, or the contralesional limb. By specifically targeting the mechanisms of selection with stimulation, the positive outcomes of CIMT may be further bolstered. In particular, stimulation could bias hand use in favour of selecting the affected limb. Conversely, TMS could be applied to dissuade the use of the ipsilesional, healthier, hand.

Importantly, hand impairment in injury or disease is multimodal. This research is in the infancy stage with substantial additional investigation required to substantiate, or refute, the thesis outlined by the PPIC model. Instead, the potential for translation motivates the continued investigation of the PPIC model, or indeed any evidence-based model which aims to understand how the brain mediates hand actions. The experiments outlined in this thesis have contributed a fraction toward this goal.

5.3 Conclusion

The human brain has evolved to support the intricate and indispensable functions performed by hand actions. In the face of erratic environmental demands, it follows that the computations underpinning movement are processed in a way that seamlessly supports the behaviours executed by the hand. The principal aim of this research is to understand how our brain organises and executes the processes of hand selection. Led by the framework of the Posterior Parietal Interhemispheric Competition model, important progress has been made in this pursuit. The data presented highlight a role for bilateral posterior parietal and superior parietal cortex in underpinning hand selection. Further, the results are consistent with the hypothesis that selection occurs via a neuronal competition between concurrently specified action plans. Acknowledging the limitations of the current work, prospective avenues for future research have been proposed. In particular, alternative offline and

online TMS approaches have been outlined to further assess the role of the pIP-SPC in hand choice. The manipulation of target certainty as a method of bolstering action competition when assessing hand selection behaviour is also suggested. The implications of these data have been discussed in the context of both current theoretical and potential future translational neuroscience advancements.

References

Papers included in the comparison of reaching studies are indicated as "**[*]**".

Ackerley, S. J., Stinear, C. M., Barber, P. A., & Byblow, W. D. (2010). Combining Theta Burst Stimulation With Training After Subcortical Stroke. *Stroke*, *41*(7), 1568–1572. doi: 10.1161/strokeaha.110.583278

Allen, E. A., Pasley, B. N., Duong, T., & Freeman, R. D. (2007). Transcranial magnetic stimulation elicits coupled neural and hemodynamic consequences. *Science*, *317*(5846), 1918–1921. doi: 10.1126/science.1146426

Andersen, R. A. (1995). Encoding of intention and spatial location in the posterior parietal cortex. *Cerebral Cortex*, *5*(5), 457–469.

Andersen, R. A., Andersen, K. N., Hwang, E. J., & Hauschild, M. (2014). Optic ataxia: from Balint's syndrome to the parietal reach region. *Neuron*, *81*(5), 967–983.

Andersen, R. A., & Buneo, C. A. (2002). Intentional maps in posterior parietal cortex. *Annual Review of Neuroscience*, *25*(1), 189–220.

Andersen, R. A., Snyder, L. H., Bradley, D. C., & Xing, J. (1997). Multimodal representation of space in the posterior parietal cortex and its use in planning movements. *Annual Review of Neuroscience*, *20*(1), 303–330.

Antal, A., Chaieb, L., Moliadze, V., Monte-Silva, K., Poreisz, C., Thirugnanasambandam, N., Nitsche, M., Shoukier, M., Ludwig, H., & Paulus, W. (2010). Brain-derived neurotrophic factor (BDNF) gene polymorphisms shape cortical plasticity in humans. *Brain Stimulation*, *3*(4), 230–237.

Ariani, G., Wurm, M. F., & Lingnau, A. (2015). Decoding internally and externally driven movement plans. *Journal of Neuroscience*, *35*(42), 14160–14171.

Astafiev, S. V., Stanley, C. M., Shulman, G. L., & Corbetta, M. (2004). Extrastriate body area in human occipital cortex responds to the performance of motor actions. *Nature neuroscience, 7(*5), 542.

[*] Astafiev, S. V, Shulman, G. L., Stanley, C. M., Snyder, A. Z., Van Essen, D. C., & Corbetta, M. (2003). Functional organization of human intraparietal and frontal cortex for attending, looking, and pointing. *Journal of Neuroscience*, *23*(11), 4689–4699.

Bálint, R. (1909). Seelenlahmung des" Schauens" optische ataxie, raumliche Storung der Aufmerksamkeit. *Monatsschrift für Psychiatrie und Neurologie*, *25*, 51–81.

Bakker, R. S., Selen, L. P., & Medendorp, W. P. (2018). Reference frames in the decisions of hand choice. *Journal of Neurophysiology, 119*(5), 1809–1817.

Barany, D. A., Della-Maggiore, V., Viswanathan, S., Cieslak, M., & Grafton, S. T. (2014). Feature interactions enable decoding of sensorimotor transformations for goal-directed movement. *Journal of Neuroscience*, *34*(20), 6860–6873.

Barker, A. T., Jalinous, R., & Freeston, I. L. (1985). Non-invasive magnetic stimulation of human motor cortex. *The Lancet*, *325*(8437), 1106–1107.

Bastani, A., & Jaberzadeh, S. (2012). A higher number of TMS-elicited MEP from a combined hotspot improves intra-and inter-session reliability of the upper limb muscles in healthy individuals. *PloS One, 7*(10), e47582.

Bates, D., Mächler, M., Bolker, B., & Walker, S. (2014). Fitting linear mixed-effects models using lme4. *arXiv preprint* arXiv:1406.5823.

Batista, A. P., Buneo, C. A., Snyder, L. H., & Andersen, R. A. (1999). Reach plans in eye-centered coordinates. *Science, 285*(5425), 257–260.

Battaglia-Mayer, A., Ferraina, S., Mitsuda, T., Marconi, B., Genovesio, A., Onorati, P., Lacquaniti, F., & Caminiti, R. (2000). Early coding of reaching in the parietooccipital cortex. *Journal of Neurophysiology*, *83*(4), 2374–2391.

Battaglia-Mayer, A., Ferrari-Toniolo, S., Visco-Comandini, F., Archambault, P. S., Saberi-Moghadam, S., & Caminiti, R. (2012). Impairment of online control of hand and eye movements in a monkey model of optic ataxia. *Cerebral Cortex*, *23*(11), 2644–2656.

Beck, J. M., Ma, W. J., Kiani, R., Hanks, T., Churchland, A. K., Roitman, J., Shadlen, M. N., Latham, P. E., & Pouget, A. (2008). Probabilistic population codes for Bayesian decision making. *Neuron, 60*(6), 1142–1152.

Benson, D. F., & Greenberg, J. P. (1969). Visual form agnosia: A specific defect in visual discrimination. *Archives of Neurology, 20*(1), 82–89.

Berardelli, A., Inghilleri, M., Rothwell, J. C., Romeo, S., Curra, A., Gilio, F., Modugno, N., & Manfredi, M. (1998). Facilitation of muscle evoked responses after repetitive cortical stimulation in man. *Experimental Brain Research, 122*(1), 79–84.

Bernier, P.-M., Cieslak, M., & Grafton, S. T. (2012). Effector selection precedes reach planning in the dorsal parietofrontal cortex. *Journal of Neurophysiology, 108*(1), 57–68. doi: 10.1152/jn.00011.2012

Bernier, P.-M., & Grafton, S. T. (2010). Human posterior parietal cortex flexibly determines reference frames for reaching based on sensory context. *Neuron, 68*(4), 776–788.

Beurze, S. M., Toni, I., Pisella, L., & Medendorp, W. P. (2010). Reference frames for reach planning in human parietofrontal cortex. *Journal of Neurophysiology, 104*(3), 1736–1745.

Beurze, S. M., De Lange, F. P., Toni, I., & Medendorp, W. P. (2007). Integration of target and effector information in the human brain during reach planning. *Journal of Neurophysiology, 97*(1), 188–199.

Bhattacharyya, R., Musallam, S., & Andersen, R. A. (2009). Parietal reach region encodes reach depth using retinal disparity and vergence angle signals. *Journal of Neurophysiology, 102*(2), 805–816.

Binkofski, F., & Buxbaum, L. J. (2013). Two action systems in the human brain. *Brain and Language, 127*(2), 222–229.

Bishop, D. V. M., Ross, V. A., Daniels, M. S., & Bright, P. (1996). The measurement of hand preference: A validation study comparing three groups of right-handers. *British Journal of Psychology, 87*(2), 269–285.

[*] Blangero, A., Menz, M. M., McNamara, A., & Binkofski, F. (2009). Parietal modules for reaching. *Neuropsychologia, 47*(6), 1500–1507.

Bologna, M., Di Biasio, F., Conte, A., Iezzi, E., Modugno, N., & Berardelli, A. (2015). Effects of cerebellar continuous theta burst stimulation on resting tremor in Parkinson's disease. *Parkinsonism & Related Disorders*, *21*(9), 1061–1066. doi: 10.1016/j.parkreldis.2015.06.015

Bonni, S., Koch, G., Miniussi, C., Bassi, M. S., Caltagirone, C., & Gainotti, G. (2015). Role of the anterior temporal lobes in semantic representations: paradoxical results of a cTBS study. *Neuropsychologia*, *76*, 163–169.

Brainard, D. H., & Vision, S. (1997). The psychophysics toolbox. *Spatial Vision*, *10*, 433–436.

Brasil-Neto, J. P., Araújo, V. P., & Carneiro, C. R. (1999). Postexercise facilitation of motor evoked potentials elicited by ipsilateral voluntary contraction. *Muscle & Nerve: Official Journal of the American Association of Electrodiagnostic Medicine*, *22*(12), 1710–1712.

Bremner, L. R., & Andersen, R. A. (2012). Coding of the reach vector in parietal area 5d. *Neuron*, *75*(2), 342–351.

Brett, M. (2017). The MNI brain and the Talairach atlas. Retrieved from http://imaging.mrc-cbu.cam.ac.uk/imaging/MniTalairach

Brownjohn, P. W., Reynolds, J. N. J., Matheson, N., Fox, J., & Shemmell, J. B. H. (2014). The effects of individualized theta burst stimulation on the excitability of the human motor system. *Brain Stimulation*, *7*(2), 260–268.

Bryden, P. J. (2016). The influence of MP Bryden's work on lateralization of motor skill: Is the preferred hand selected for and better at tasks requiring a high degree of skill? *Laterality: Asymmetries of Body, Brain and Cognition*, *21*(4–6), 312–328.

Bryden, P. J., Pryde, K. M., & Roy, E. A. (2000). A performance measure of the degree of hand preference. *Brain and Cognition*, *44*(3), 402–414.

Bryden, P. J., & Roy, E. A. (2006). Preferential reaching across regions of hemispace in adults and children. *Developmental Psychobiology: The Journal of the International Society for Developmental Psychobiology*, *48*(2), 121–132.

Buneo, C. A., & Andersen, R. A. (2006). The posterior parietal cortex: sensorimotor interface for the planning and online control of visually guided movements. *Neuropsychologia*, *44*(13), 2594–2606.

Buxbaum, L. J. (2001). Ideomotor apraxia: a call to action. *Neurocase, 7*(6), 445–458.

Buxbaum, L. J., Johnson-Frey, S. H., & Bartlett-Williams, M. (2005). Deficient internal models for planning hand–object interactions in apraxia. *Neuropsychologia, 43*(6), 917–929.

Caminiti, R., Ferraina, S., & Johnson, P. B. (1996). The sources of visual information to the primate frontal lobe: a novel role for the superior parietal lobule. *Cerebral Cortex, 6*(3), 319–328.

Caminiti, R., Borra, E., Visco-Comandini, F., Battaglia-Mayer, A., Averbeck, B. B., & Luppino, G. (2017). Computational architecture of the parieto-frontal network underlying cognitive-motor control in monkeys. *eneuro, 4*(1).

Capaday, C. (1997). Neurophysiological methods for studies of the motor system in freely moving human subjects. *Journal of Neuroscience Methods*, *74*(2), 201–218.

Cárdenas-Morales, L., Nowak, D. A., Kammer, T., Wolf, R. C., & Schönfeldt-Lecuona, C. (2010). Mechanisms and applications of theta-burst rTMS on the human motor cortex. *Brain Topography*, *22*(4), 294–306.

Carey, D. P., Harvey, M., & Milner, A. D. (1996). Visuomotor sensitivity for shape and orientation in a patient with visual form agnosia. *Neuropsychologia*, *34*(5), 329–337.

Cavada, C., & Goldman-Rakic, P. S. (1989). Posterior parietal cortex in rhesus monkey: II. Evidence for segregated corticocortical networks linking sensory and limbic areas with the frontal lobe. *Journal of Comparative Neurology*, *287*(4), 422–445.

[*] Cavina-Pratesi, C., Monaco, S., Fattori, P., Galletti, C., McAdam, T. D., Quinlan, D. J., Goodale, M. A., & Culham, J. C. (2010). Functional magnetic resonance imaging reveals the neural substrates of arm transport and grip formation in reach-to-grasp actions in humans. *Journal of Neuroscience*, *30*(31), 10306–10323.

Chang, S. W. C., Papadimitriou, C., & Snyder, L. H. (2009). Using a compound gain field to compute a reach plan. *Neuron*, *64*(5), 744–755.

Chang, S. W. C., & Snyder, L. H. (2010). Idiosyncratic and systematic aspects of spatial representations in the macaque parietal cortex. *Proceedings of the National Academy of Sciences*, *107*(17), 7951–7956.

Chang, S. W. C., & Snyder, L. H. (2012). The representations of reach endpoints in posterior parietal cortex depend on which hand does the reaching. *Journal of Neurophysiology*, *107*(9), 2352–2365.

Chapman, C. S., Gallivan, J. P., Wood, D. K., Milne, J. L., Culham, J. C., & Goodale, M. A. (2010). Reaching for the unknown: multiple target encoding and real-time decision-making in a rapid reach task. *Cognition*, *116*(2), 168–176.

Chavis, D. A., & Pandya, D. N. (1976). Further observations on corticofrontal connections in the rhesus monkey. *Brain Research*, *117*(3), 369–386.

Cheeran, B., Talelli, P., Mori, F., Koch, G., Suppa, A., Edwards, M., Houlden, H., Bhatia, K., Greenwood, R., & Rothwell, J. C. (2008). A common polymorphism in the brain-derived neurotrophic factor gene (BDNF) modulates human cortical plasticity and the response to rTMS. *The Journal of Physiology*, *586*(23), 5717–5725.

Chen, R., Classen, J., Gerloff, C., Celnik, P., Wassermann, E. M., Hallett, M., & Cohen, L. G. (1997). Depression of motor cortex excitability by low-frequency transcranial magnetic stimulation. *Neurology*, *48*(5), 1398–1403.

Chen, R., Gerloff, C., Classen, J., Wassermann, E. M., Hallett, M., & Cohen, L. G. (1997). Safety of different inter-train intervals for repetitive transcranial magnetic stimulation and recommendations for safe ranges of stimulation parameters. *Electroencephalography and Clinical Neurophysiology*, *105*(6), 415–421.

Chen, R., Tam, A., Bütefisch, C., Corwell, B., Ziemann, U., Rothwell, J. C., & Cohen, L. G. (1998). Intracortical inhibition and facilitation in different representations of the human motor cortex. *Journal of Neurophysiology*, *80*(6), 2870–2881.

Chen, Y., Monaco, S., Byrne, P., Yan, X., Henriques, D. Y. P., & Crawford, J. D. (2014). Allocentric versus egocentric representation of remembered reach targets in human cortex. *Journal of Neuroscience*, *34*(37), 12515–12526.

Christie, A., Fling, B., Crews, R. T., Mulwitz, L. A., & Kamen, G. (2007). Reliability of motor-evoked potentials in the ADM muscle of older adults. *Journal of Neuroscience Methods*, *164*(2), 320–324.

Christopoulos, V. N., Bonaiuto, J., & Andersen, R. A. (2015a). A biologically plausible computational theory for value integration and action selection in decisions with competing alternatives. *PLoS Computational Biology*, *11*(3), e1004104.

Christopoulos, V. N., Bonaiuto, J., Kagan, I., & Andersen, R. A. (2015b). Inactivation of parietal reach region affects reaching but not saccade choices in internally guided decisions. *Journal of Neuroscience*, *35*(33), 11719–11728.

Christopoulos, V. N., Kagan, I., & Andersen, R. A. (2018). Lateral intraparietal area (LIP) is largely effector-specific in free-choice decisions. *Scientific Reports*, *8*(1), 8611.

Chung, S. W., Hill, A. T., Rogasch, N. C., Hoy, K. E., & Fitzgerald, P. B. (2016). Use of theta-burst stimulation in changing excitability of motor cortex: a systematic review and meta-analysis. *Neuroscience & Biobehavioral Reviews*, *63*, 43–64.

Cicinelli, P., Marconi, B., Zaccagnini, M., Pasqualetti, P., Filippi, M. M., & Rossini, P. M. (2005). Imagery-induced Cortical Excitability Changes in Stroke: A Transcranial Magnetic Stimulation Study. *Cerebral Cortex, 16(*2), 247–253.

Cisek, P. (2006). Integrated neural processes for defining potential actions and deciding between them: a computational model. *Journal of Neuroscience*, *26*(38), 9761–9770.

Cisek, P. (2007). Cortical mechanisms of action selection: the affordance competition hypothesis. *Philosophical Transactions of the Royal Society B: Biological Sciences*, *362*(1485), 1585–1599.

Cisek, P. (2019). Resynthesizing behavior through phylogenetic refinement. *Attention, Perception, & Psychophysics*, 1–23.

Cisek, P., & Kalaska, J. F. (2005). Neural correlates of reaching decisions in dorsal premotor cortex: specification of multiple direction choices and final selection of action. *Neuron*, *45*(5), 801–814.

Cisek, P., & Kalaska, J. F. (2010). Neural mechanisms for interacting with a world full of action choices. *Annual Review of Neuroscience*, *33*, 269–298.

Cisek, P., & Pastor-Bernier, A. (2014). On the challenges and mechanisms of embodied decisions. *Philosophical Transactions of the Royal Society B*, *369*(1655). doi: 10.1098/rstb.2013.0479

Cisek, P., Puskas, G. A., & El-Murr, S. (2009). Decisions in changing conditions: the urgency-gating model. *Journal of Neuroscience*, *29*(37), 11560–11571.

Cisek, P., & Thura, D. (2018). Neural circuits for action seleciton. In D. Corbetta & M. Santello (Eds.), *Reach-to-Grasp Behavior: Brain, Behavior, and Modelling Across the Life Span* (pp. 91–118). Routledge.

Clavagnier, S., Prado, J., Kennedy, H., & Perenin, M.-T. (2007). How humans reach: distinct cortical systems for central and peripheral vision. *The Neuroscientist*, *13*(1), 22–27.

Coelho, C. J., Przybyla, A., Yadav, V., & Sainburg, R. L. (2013). Hemispheric differences in the control of limb dynamics: a link between arm performance asymmetries and arm selection patterns. *Journal of Neurophysiology*, *109*(3), 825–838. doi: 10.1152/jn.00885.2012

Cohen, L. G., Bandinelli, S., Findley, T. W., & Hallett, M. (1991). Motor reorganization after upper limb amputation in man: a study with focal magnetic stimulation. *Brain*, *114*(1), 615–627.

Cohen, Y. E., & Andersen, R. A. (2002). A common reference frame for movement plans in the posterior parietal cortex. *Nature Reviews Neuroscience*, *3*(7), 553.

Colby, C. L., Duhamel, J.-R., & Goldberg, M. E. (1995). Oculocentric spatial representation in parietal cortex. *Cerebral Cortex*, *5*(5), 470–481.

[*] Connolly, J. D., Goodale, M. A., Desouza, J. F., Menon, R. S., Vilis, T., & Medical Research Council Group for Action and Perception). (2000). A comparison of frontoparietal fMRI activation during anti-saccades and anti-pointing. *Journal of Neurophysiology, 84(*3), 1645-1655.

[*] Connolly, J. D., Andersen, R. A., & Goodale, M. A. (2003). FMRI evidence for a "parietal reach region" in the human brain. *Experimental Brain Research*, *153*(2), 140–145.

Conte, A., Rocchi, L., Nardella, A., Dispenza, S., Scontrini, A., Khan, N., & Berardelli, A. (2012). Theta-burst stimulation-induced plasticity over primary somatosensory cortex changes somatosensory temporal discrimination in healthy humans. *PLoS One*, *7*(3), e32979.

Corbetta, M., Kincade, M. J., Lewis, C., Snyder, A. Z., & Sapir, A. (2005). Neural basis and recovery of spatial attention deficits in spatial neglect. *Nature Neuroscience, 8(*11), 1603.

Cos, I., Bélanger, N., & Cisek, P. (2011). The influence of predicted arm biomechanics on decision making. *Journal of Neurophysiology*, *105*(6), 3022–3033.

Cos, I., Medleg, F., & Cisek, P. (2012). The modulatory influence of end-point controllability on decisions between actions. *Journal of Neurophysiology*, *108*(6), 1764–1780.

Cracco, R. Q., Cracco, J. B., Maccabee, P. J., & Amassian, V. E. (1999). Cerebral function revealed by transcranial magnetic stimulation. *Journal of Neuroscience Methods*, *86*(2), 209–219.

Crammond, D. J., & Kalaska, J. F. (1989). Neuronal activity in primate parietal cortex area 5 varies with intended movement direction during an instructed-delay period. *Experimental Brain Research*, *76*(2), 458–462.

Crammond, D. J., & Kalaska, J. F. (1994). Modulation of preparatory neuronal activity in dorsal premotor cortex due to stimulus-response compatibility. *Journal of Neurophysiology*, *71*(3), 1281–1284.

Crammond, D. J., & Kalaska, J. F. (1996). Differential relation of discharge in primary motor cortex and premotor cortex to movements versus actively maintained postures during a reaching task. *Experimental Brain Research, 108*(1), 45–61.

Culham, J. C., Cavina-Pratesi, C., & Singhal, A. (2006). The role of parietal cortex in visuomotor control: what have we learned from neuroimaging? *Neuropsychologia*, *44*(13), 2668–2684.

Culham, J. C., Danckert, S. L., De Souza, J. F. X., Gati, J. S., Menon, R. S., & Goodale, M. A. (2003). Visually guided grasping produces fMRI activation in dorsal but not ventral stream brain areas. *Experimental Brain Research*, *153*(2), 180–189.

Culham, J. C., & Kanwisher, N. G. (2001). Neuroimaging of cognitive functions in human parietal cortex. *Current Opinion in Neurobiology*, *11*(2), 157–163.

Culham, J. C., & Valyear, K. F. (2006). Human parietal cortex in action. *Current Opinion in Neurobiology*, *16*(2), 205–212.

Daly, J. J., McCabe, J. P., Holcomb, J., Monkiewicz, M., Gansen, J., & Pundik, S. (2019). Long-Dose Intensive Therapy Is Necessary for Strong, Clinically Significant, Upper Limb Functional Gains and Retained Gains in Severe/Moderate Chronic Stroke. *Neurorehabilitation and Neural Repair*, *33*(7), 523-537.

Davare, M., Zenon, A., Pourtois, G., Desmurget, M., & Olivier, E. (2012). Role of the medial part of the intraparietal sulcus in implementing movement direction. *Cerebral Cortex*, *22*(6), 1382–1394.

[*] Davare, M., Zénon, A., Desmurget, M., & Olivier, E. (2015). Dissociable contribution of the parietal and frontal cortex to coding movement direction and amplitude. *Frontiers in Human Neuroscience, 9*, 241.

Day, B. L., Dressler, D., de Noordhout, A., Marsden, C. D., Nakashima, K., Rothwell, J. C., & Thompson, P. D. (1989). Electric and magnetic stimulation of human motor cortex: surface EMG and single motor unit responses. *The Journal of Physiology*, *412*(1), 449–473.

[*] De Jong, B. M., Van der Graaf, F. H. C. E., & Paans, A. M. J. (2001). Brain activation related to the representations of external space and body scheme in visuomotor control. *NeuroImage, 14*(5), 1128–1135.

Dekleva, B. M., Kording, K. P., & Miller, L. E. (2018). Single reach plans in dorsal premotor cortex during a two-target task. *Nature Communications*, *9*(1), 3556.

Dekleva, B. M., Ramkumar, P., Wanda, P. A., Kording, K. P., & Miller, L. E. (2016). Uncertainty leads to persistent effects on reach representations in dorsal premotor cortex. *eLife*, *5*, e14316.

Demirtas-Tatlidede, A., Freitas, C., Cromer, J. R., Safar, L., Ongur, D., Stone, W. S., Seidman, L. J., Schmahmann, J. D., & Pascual-Leone, A. (2010). Safety and proof of principle study of cerebellar vermal theta burst stimulation in refractory schizophrenia. *Schizophrenia Research*, *124*(1–3), 91–100.

Derosiere, G., Thura, D., Cisek, P., & Duqué, J. (2019). M1 disruption delays motor processes but not deliberation about action choices. *Journal of Neurophysiology*, *122*(4), 1566-1577. doi: 10.1152/jn.00163.2019

[*] Desmurget, M., Epstein, C. M., Turner, R. S., Prablanc, C., Alexander, G. E., & Grafton, S. T. (1999). Role of the posterior parietal cortex in updating reaching movements to a visual target. *Nature Neuroscience*, *2*(6), 563.

Desmurget, M., & Grafton, S. (2000). Forward modeling allows feedback control for fast reaching movements. *Trends in Cognitive Science*, *4*(11), 423–431.

[*] Desmurget, M., Gréa, H., Grethe, J. S., Prablanc, C., Alexander, G. E., & Grafton, S. T. (2001). Functional anatomy of nonvisual feedback loops during reaching: a positron emission tomography study. *Journal of Neuroscience, 21*(8), 2919–2928.

DeSouza, J. F. X., Dukelow, S. P., Gati, J. S., Menon, R. S., Andersen, R. A., & Vilis, T. (2000). Eye position signal modulates a human parietal pointing region during memory-guided movements. *Journal of Neuroscience, 20*(15), 5835–5840.

Devanne, H., Lavoie, B. A., & Capaday, C. (1997). Input-output properties and gain changes in the human corticospinal pathway. *Experimental Brain Research*, *114*(2), 329–338.

Di Lazzaro, V., Dileone, M., Pilato, F., Profice, P., Ranieri, F., Musumeci, G., Angelucci, F., Sabatelli, M., & Tonali, P. A. (2006). Repetitive transcranial magnetic stimulation for ALS: a preliminary controlled study. *Neuroscience Letters, 408*(2), 135–140.

Di Lazzaro, V., Oliviero, A., Mazzone, P., Insola, A., Pilato, F., Saturno, E., Accurso, A., Tonali, P., & Rothwell, J. (2001). Comparison of descending volleys evoked by monophasic and biphasic magnetic stimulation of the motor cortex in conscious humans. *Experimental Brain Research*, *141*(1), 121–127.

Di Lazzaro, V., Oliviero, A., Profice, P., Ferrara, L., Saturno, E., Pilato, F., & Tonali, P. (1999). The diagnostic value of motor evoked potentials. *Clinical Neurophysiology*, *110*(7), 1297–1307.

Di Lazzaro, V., Pilato, F., Saturno, E., Oliviero, A., Dileone, M., Mazzone, P., Insola, P., Tonali, P. A., Ranieri, F., Huang, Y. Z., & Rothwell, J. (2005). Theta-burst repetitive transcranial magnetic stimulation suppresses specific excitatory circuits in the human motor cortex. *The Journal of Physiology*, *565*(3), 945–950.

Di Lazzaro, V., Rothwell, J. C., Talelli, P., Capone, F., Ranieri, F., Wallace, A. C., Musumeci, G., & Dileone, M. (2013). Inhibitory theta burst stimulation of affected hemisphere in chronic stroke: A proof of principle, sham-controlled study. *Neuroscience Letters*, *553*, 148–152. doi: 10.1016/j.neulet.2013.08.013

di Pellegrino, G., & Wise, S. P. (1993). Visuospatial versus visuomotor activity in the premotor and prefrontal cortex of a primate. *Journal of Neuroscience*, *13*(3), 1227–1243.

Diedrichsen, J., Hashambhoy, Y., Rane, T., & Shadmehr, R. (2005). Neural correlates of reach errors. *Journal of Neuroscience*, *25*(43), 9919–9931.

Do, M., Kirkovski, M., Davies, C. B., Bekkali, S., Byrne, L. K., & Enticott, P. G. (2018). Intra-and Inter-Regional Priming of Ipsilateral Human Primary Motor Cortex With Continuous Theta Burst Stimulation Does Not Induce Consistent Neuroplastic Effects. *Frontiers in Human Neuroscience*, *12*, 123.

Doeltgen, S. H., Ridding, M. C., O'Beirne, G. A., Dalrymple-Alford, J., & Huckabee, M.-L. (2009). Test--retest reliability of motor evoked potentials (MEPs) at the submental muscle group during volitional swallowing. *Journal of Neuroscience Methods*, *178*(1), 134–137.

Dounskaia, N., & Goble, J. A. (2011). The role of vision, speed, and attention in overcoming directional biases during arm movements. *Experimental Brain Research, 209*(2), 299–309.

Downing, P. E., Jiang, Y., Shuman, M., & Kanwisher, N. (2001). A cortical area selective for visual processing of the human body. *Science, 293(*5539), 2470–2473.

Duecker, F., & Sack, A. T. (2013). Pre-stimulus sham TMS facilitates target detection. *PLoS One*, *8*(3), e57765.

Eggers, C., Fink, G. R., & Nowak, D. A. (2010). Theta burst stimulation over the primary motor cortex does not induce cortical plasticity in Parkinson's disease. *Journal of Neurology, 257*(10), 1669–1674. doi: 10.1007/s00415-010-5597-1

Ellaway, P. H., Davey, N. J., Maskill, D. W., Rawlinson, S. R., Lewis, H. S., & Anissimova, N. P. (1998). Variability in the amplitude of skeletal muscle responses to magnetic stimulation of the motor cortex in man. *Electroencephalography and Clinical Neurophysiology/Electromyography and Motor Control, 109*(2), 104–113.

Ellison, A., & Cowey, A. (2006). TMS can reveal contrasting functions of the dorsal and ventral visual processing streams. *Experimental Brain Research, 175*(4), 618–625. doi: 10.1007/s00221-006-0582-8

Eskandar, E. N., & Assad, J. A. (1999). Dissociation of visual, motor and predictive signals in parietal cortex during visual guidance. *Nature Neuroscience, 2*(1), 88.

Eskandar, E. N., & Assad, J. A. (2002). Distinct nature of directional signals among parietal cortical areas during visual guidance. *Journal of Neurophysiology, 88*(4), 1777–1790.

Fabbri, S., Caramazza, A., & Lingnau, A. (2010). Tuning curves for movement direction in the human visuomotor system. *Journal of Neuroscience, 30*(40), 13488–13498.

Fattori, P., Breveglieri, R., Marzocchi, N., Filippini, D., Bosco, A., & Galletti, C. (2009). Hand orientation during reach-to-grasp movements modulates neuronal activity in the medial posterior parietal area V6A. *Journal of Neuroscience, 29*(6), 1928–1936.

Fattori, P., Breveglieri, R., Raos, V., Bosco, A., & Galletti, C. (2012). Vision for action in the macaque medial posterior parietal cortex. *Journal of Neuroscience, 32*(9), 3221–3234.

Fattori, P., Gamberini, M., Kutz, D. F., & Galletti, C. (2001). 'Arm-reaching' neurons in the parietal area V6A of the macaque monkey. *European Journal of Neuroscience, 13*(12), 2309–2313.

Faul, F., Erdfelder, E., Lang, A.-G., & Buchner, A. (2007). G* Power 3: A flexible statistical power analysis program for the social, behavioral, and biomedical sciences. *Behavior Research Methods*, *39*(2), 175–191.

[*] Fernandez-Ruiz, J., Goltz, H. C., DeSouza, J. F. X., Vilis, T., & Crawford, J. D. (2007). Human parietal "reach region" primarily encodes intrinsic visual direction, not extrinsic movement direction, in a visual--motor dissociation task. *Cerebral Cortex*, *17*(10), 2283–2292.

Ferraina, S., & Bianchi, L. (1994). Posterior parietal cortex: functional properties of neurons in area 5 during an instructed-delay reaching task within different parts of space. *Experimental Brain Research*, *99*(1), 175–178.

Ferraina, S., Brunamonti, E., Giusti, M. A., Costa, S., Genovesio, A., & Caminiti, R. (2009). Reaching in depth: hand position dominates over binocular eye position in the rostral superior parietal lobule. *Journal of Neuroscience*, *29*(37), 11461–11470.

[*] Filimon, F., Nelson, J. D., Hagler, D. J., & Sereno, M. I. (2007). Human cortical representations for reaching: mirror neurons for execution, observation, and imagery. *NeuroImage, 37*(4), 1315–1328.

Fitzgerald, P. B., Fountain, S., & Daskalakis, Z. J. (2006). A comprehensive review of the effects of rTMS on motor cortical excitability and inhibition. *Clinical Neurophysiology*, *117*(12), 2584–2596.

Fitzpatrick, A. M., Dundon, N. M., & Valyear, K. F. (2019). The neural basis of hand choice: An fMRI investigation of the Posterior Parietal Interhemispheric Competition model. *NeuroImage*, *185*, 208–221. doi: 10.1016/j.neuroimage.2018.10.039

Franca, M., Koch, G., Mochizuki, H., Huang, Y.-Z., & Rothwell, J. C. (2006). Effects of theta burst stimulation protocols on phosphene threshold. *Clinical Neurophysiology, 117*(8), 1808–1813.

Freedman, D. J., & Assad, J. A. (2011). A proposed common neural mechanism for categorization and perceptual decisions. *Nature Neuroscience*, *14*(2), 143.

Gabbard, C., & Rabb, C. (2000). What determines choice of limb for unimanual reaching movements? *The Journal of General Psychology*, *127*(2), 178–184.

Gail, A., & Andersen, R. A. (2006). Neural Dynamics in Monkey Parietal Reach Region Reflect Context-Specific Sensorimotor Transformations. *The Journal of Neuroscience*, *26*(37), 9376 LP – 9384. doi: 10.1523/jneurosci.1570-06.2006

Gail, A., Klaes, C., & Westendorff, S. (2009). Implementation of spatial transformation rules for goal-directed reaching via gain modulation in monkey parietal and premotor cortex. *The Journal of Neuroscience : The Official Journal of the Society for Neuroscience*, *29*(30), 9490–9499. doi: 10.1523/jneurosci.1095-09.2009

Gallese, V., Fadiga, L., Fogassi, L., Luppino, G., & Murata, A. (1997). A parietalfrontal circuit for hand grasping movements in the monkey: evidence from reversible inactivation experiments. In P. Thier & H. O. Karnath (Eds.), *Parietal Lobe Contributions to Orientation in 3D Space* (pp. 255–270). Heidelberg: Springer.

Galletti, C., Battaglini, P. P., & Fattori, P. (1991). Functional properties of neurons in the anterior bank of the parieto-occipital sulcus of the macaque monkey. *European Journal of Neuroscience*, *3*(5), 452–461.

Galletti, C., & Fattori, P. (2018). The dorsal visual stream revisited: Stable circuits or dynamic pathways? *Cortex*, *98*, 203–217.

Galletti, C., Fattori, P., Battaglini, P. P., Shipp, S., & Zeki, S. (1996). Functional demarcation of a border between areas V6 and V6A in the superior parietal gyrus of the macaque monkey. *European Journal of Neuroscience*, *8*(1), 30–52.

Galletti, C., Fattori, P., Kutz, D. F., & Battaglini, P. P. (1997). Arm movement-related neurons in the visual area V6A of the macaque superior parietal lobule. *European Journal of Neuroscience*, *9*(2), 410–413.

Gallivan, J. P., Cavina-Pratesi, C., & Culham, J. C. (2009). Is that within reach? fMRI reveals that the human superior parieto-occipital cortex encodes objects reachable by the hand. *Journal of Neuroscience, 29*(14), 4381–4391.

Gallivan, J. P., Chapman, C. S., Wolpert, D. M., & Flanagan, J. R. (2018). Decision-making in sensorimotor control. *Nature Reviews Neuroscience, 19*(9), 519–534.

Gallivan, J. P., & Culham, J. C. (2015). Neural coding within human brain areas involved in actions. *Current Opinion in Neurobiology, 33*, 141–149.

Gallivan, J. P., Logan, L., Wolpert, D. M., & Flanagan, J. R. (2016). Parallel specification of competing sensorimotor control policies for alternative action options. *Nature Neuroscience, 19*(2), 320.

Gallivan, J. P., McLean, D. A., Valyear, K. F., & Culham, J. C. (2013). Decoding the neural mechanisms of human tool use. *eLife, 2*, e00425.

[*] Gallivan, J. P., McLean, D. A., Smith, F. W., & Culham, J. C. (2011). Decoding effector-dependent and effector-independent movement intentions from human parieto-frontal brain activity. *Journal of Neuroscience, 31*(47), 17149–17168.

Gallivan, J. P., Stewart, B. M., Baugh, L. A., Wolpert, D. M., & Flanagan, J. R. (2017). Rapid automatic motor encoding of competing reach options. *Cell Reports, 18*(7), 1619–1626.

Gallivan, J. P., McLean, D. A., Valyear, K. F., Pettypiece, C. E., & Culham, J. C. (2011). Decoding action intentions from preparatory brain activity in human parieto-frontal networks. *Journal of Neuroscience, 31*(26), 9599–9610.

Gamberini, M., Passarelli, L., Fattori, P., & Galletti, C. (2019). Structural connectivity and functional properties of the macaque superior parietal lobule. *Brain Structure and Function*, 1-19.

Gandolfo, M., & Downing, P. E. (2019). Causal evidence for expression of perceptual expectations in category-selective extrastriate regions. *Current Biology, 29*(15), 2496–2500.

Gekht, A. B., Burd, G. S., Selikhova, M. V, Iaish, F., & Beliakov, V. V. (1998). Disorders of muscle tonus and their treatment with sirdalud in patients in the early recovery period of ischemic stroke. *Zhurnal Nevrologii i Psikhiatrii Imeni S.S. Korsakova*, *98*(10), 22–29.

Gentner, R., Wankerl, K., Reinsberger, C., Zeller, D., & Classen, J. (2007). Depression of human corticospinal excitability induced by magnetic theta-burst stimulation: evidence of rapid polarity-reversing metaplasticity. *Cerebral Cortex*, *18*(9), 2046–2053.

Ghez, C., Favilla, M., Ghilardi, M. F., Gordon, J., Bermejo, R., & Pullman, S. (1997). Discrete and continuous planning of hand movements and isometric force trajectories. *Experimental Brain Research*, *115*(2), 217–233.

Ghosh, S., Brinkman, C., & Porter, R. (1987). A quantitative study of the distribution of neurons projecting to the precentral motor cortex in the monkey (M. fascicularis). *Journal of Comparative Neurology*, *259*(3), 424–444.

Gibson, J. J. (1979). *The ecological approach to visual perception*. Boston: Houghton Mifflin.

[*] Glover, S., Miall, R. C., & Rushworth, M. F. S. (2005). Parietal rTMS disrupts the initiation but not the execution of on-line adjustments to a perturbation of object size. *Journal of Cognitive Neuroscience*, *17*(1), 124–136.

Godschalk, M., Lemon, R. N., Kuypers, H. G., & Ronday, H. K. (1984). Cortical afferents and efferents of monkey postarcuate area: an anatomical and electrophysiological study. *Experimental Brain Research*, *56*(3), 410–424.

Gold, J. I., & Shadlen, M. N. (2007). The neural basis of decision making. *Annual Review of Neuroscience*, *30*, 535–574. doi: 10.1146/annurev.neuro.29.051605.113038

Goldenberg, G. (2009). Apraxia and the parietal lobes. *Neuropsychologia, 47*(6), 1449–1459.

Goldsworthy, M. R., Hordacre, B., & Ridding, M. C. (2016). Minimum number of trials required for within-and between-session reliability of TMS measures of corticospinal excitability. *Neuroscience*, *320*, 205–209.

Goldsworthy, M. R., Vallence, A.-M., Hodyl, N. A., Semmler, J. G., Pitcher, J. B., & Ridding, M. C. (2016). Probing changes in corticospinal excitability following theta burst stimulation of the human primary motor cortex. *Clinical Neurophysiology*, *127*(1), 740–747.

Gonzalez, C. L. R., Flindall, J. W., & Stone, K. D. (2015). Hand preference across the lifespan: effects of end-goal, task nature, and object location. *Frontiers in Psychology*, *5*, 1579.

Gonzalez, C. L. R., & Goodale, M. A. (2009). Hand preference for precision grasping predicts language lateralization. *Neuropsychologia*, *47*(14), 3182–3189.

Gonzalez, C. L. R., Whitwell, R. L., Morrissey, B., Ganel, T., & Goodale, M. A. (2007). Left handedness does not extend to visually guided precision grasping. *Experimental Brain Research*, *182*(2), 275–279. doi: 10.1007/s00221-007-1090-1

Goodale, M. A., Meenan, J. P., Bülthoff, H. H., Nicolle, D. A., Murphy, K. J., & Racicot, C. I. (1994). Separate neural pathways for the visual analysis of object shape in perception and prehension. *Current Biology*, *4*(7), 604–610.

Goodale, M. A., & Milner, A. D. (1992). Separate visual pathways for perception and action. *Trends in Neurosciences*, *15*(1), 20–25.

Goodale, M. A., Milner, A. D., Jakobson, L. S., & Carey, D. P. (1991). A neurological dissociation between perceiving objects and grasping them. *Nature*, *349*(6305), 154.

Gordon, J., Ghilardi, M. F., Cooper, S. E., & Ghez, C. (1994). Accuracy of planar reaching movements. II. Systematic extent errors resulting from inertial anisotropy. *Experimental Brain Research, 99*(1), 112–130.

Gracies, J.-M., Nance, P., Elovic, E., McGuire, J., & Simpson, D. M. (1997). Traditional pharmacological treatments for spasticity part II: general and regional treatments. *Muscle & Nerve: Official Journal of the American Association of Electrodiagnostic Medicine, 20*(S6), 92–120.

Grefkes, C., & Fink, G. R. (2005). The functional organization of the intraparietal sulcus in humans and monkeys. *Journal of Anatomy, 207*(1), 3–17.

Grefkes, C., Ritzl, A., Zilles, K., & Fink, G. R. (2004). Human medial intraparietal cortex subserves visuomotor coordinate transformation. *NeuroImage, 23*(4), 1494–1506.

Grill-Spector, K., & Malach, R. (2004). The human visual cortex. *Annual Review of Neuroscience, 27,* 649–677.

Gross, C. G., Rocha-Miranda, C. E. de, & Bender, D. B. (1972). Visual properties of neurons in inferotemporal cortex of the macaque. *Journal of Neurophysiology, 35*(1), 96–111.

Grossman, E. D., Battelli, L., & Pascual-Leone, A. (2005). Repetitive TMS over posterior STS disrupts perception of biological motion. *Vision Research, 45*(22), 2847–2853.

Grünbaum, A. S. F., & Sherrington, C. S. (1902). Observations on the physiology of the cerebral cortex of some of the higher apes.(Preliminary communication.). *Proceedings of the Royal Society of London, 69*(451–458), 206–209.

Habagishi, C., Kasuga, S., Otaka, Y., Liu, M., & Ushiba, J. (2014). Different strategy of hand choice after learning of constant and incremental dynamical perturbation in arm reaching. *Frontiers in Human Neuroscience, 8,* 92.

Hadjidimitrakis, K., Bertozzi, F., Breveglieri, R., Bosco, A., Galletti, C., & Fattori, P. (2013). Common neural substrate for processing depth and direction signals for reaching in the monkey medial posterior parietal cortex. *Cerebral Cortex, 24*(6), 1645–1657.

Halsband, U., & Passingham, R. (1982). The role of premotor and parietal cortex in the direction of action. *Brain Research, 240*(2), 368–72.

Halsband, U., & Passingham, R. E. (1985). Premotor cortex and the conditions for movement in monkeys (Macaca fascicularis). *Behavioural Brain Research*, *18*(3), 269–277.

Hamada, M., Murase, N., Hasan, A., Balaratnam, M., & Rothwell, J. C. (2012). The role of interneuron networks in driving human motor cortical plasticity. *Cerebral Cortex*, *23*(7), 1593–1605.

Hamel-Thibault, A., Thénault, F., Whittingstall, K., & Bernier, P.-M. (2016). Delta-band oscillations in motor regions predict hand selection for reaching. *Cerebral Cortex*, *28*(2), 574–584.

Hanks, T. D., Ditterich, J., & Shadlen, M. N. (2006). Microstimulation of macaque area LIP affects decision-making in a motion discrimination task. *Nature Neuroscience, 9*(5), 682.

Hanks, T. D., Kopec, C. D., Brunton, B. W., Duan, C. A., Erlich, J. C., & Brody, C. D. (2015). Distinct relationships of parietal and prefrontal cortices to evidence accumulation. *Nature, 520*(7546), 220.

Hao, Z., Wang, D., Zeng, Y., & Liu, M. (2013). Repetitive transcranial magnetic stimulation for improving function after stroke. *Cochrane Database of Systematic Reviews*, (5).

Haraldsson, H. M., Ferrarelli, F., Kalin, N. H., & Tononi, G. (2004). Transcranial magnetic stimulation in the investigation and treatment of schizophrenia: a review. *Schizophrenia Research, 71*(1), 1–16.

Hartwigsen, G., Saur, D., Price, C. J., Ulmer, S., Baumgaertner, A., & Siebner, H. R. (2013). Perturbation of the left inferior frontal gyrus triggers adaptive plasticity in the right homologous area during speech production. *Proceedings of the National Academy of Sciences, 110*(41), 16402–16407.

Hecaen, H., & De Ajuriaguerra, J. (1954). *Balint's syndrome (psychic paralysis of visual fixation) and its minor forms. Brain, 77,* 373–400.

Helbig, C. R., & Gabbard, C. (2004). What determines limb selection for reaching? *Research Quarterly for Exercise and Sport*, *75*(1), 47–59.

Hess, C. W., Mills, K. R., & Murray, N. M. (1987). Responses in small hand muscles from magnetic stimulation of the human brain. *The Journal of Physiology*, *388*(1), 397–419.

Hinder, M. R., Goss, E. L., Fujiyama, H., Canty, A. J., Garry, M. I., Rodger, J., & Summers, J. J. (2014). Inter-and intra-individual variability following intermittent theta burst stimulation: implications for rehabilitation and recovery. *Brain Stimulation*, *7*(3), 365–371.

[*] Hinkley, L. B. N., Krubitzer, L. A., Padberg, J., & Disbrow, E. A. (2009). Visual-manual exploration and posterior parietal cortex in humans. *Journal of Neurophysiology*, *102*(6), 3433–3446.

Hoshi, E., & Tanji, J. (2004). Functional specialization in dorsal and ventral premotor areas. In *Progress in Brain Research* (Vol. 143, pp. 507–511). Elsevier.

Hsu, Y.-F., Liao, K.-K., Lee, P.-L., Tsai, Y.-A., Yeh, C.-L., Lai, K.-L., Huang, Y.-Z., Lin, Y.-Y., & Lee, I.-H. (2011). Intermittent theta burst stimulation over primary motor cortex enhances movement-related beta synchronisation. *Clinical Neurophysiology*, *122*(11), 2260–2267.

Hu, R., Zhu, Y., Tang, X., Du, X., Zhang, H., Liu, Q., Wu, J., Fan, S., Hao, Y., & Wu, Y. (2017). Continuous theta burst stimulation inhibits the bilateral hemispheres. *Neuroscience Letters*, *657*, 134–139.

Huang, Y.-Z., Chen, R.-S., Rothwell, J. C., & Wen, H.-Y. (2007). The after-effect of human theta burst stimulation is NMDA receptor dependent. *Clinical Neurophysiology*, *118*(5), 1028–1032.

Huang, Y.-Z., Edwards, M. J., Rounis, E., Bhatia, K. P., & Rothwell, J. C. (2005). Theta burst stimulation of the human motor cortex. *Neuron*, *45*(2), 201–206.

Huang, Y.-Z., Rothwell, J. C., Edwards, M. J., & Chen, R.-S. (2007). Effect of physiological activity on an NMDA-dependent form of cortical plasticity in human. *Cerebral Cortex*, *18*(3), 563–570.

Hummel, F., Celnik, P., Giraux, P., Floel, A., Wu, W.-H., Gerloff, C., & Cohen, L. G. (2005). Effects of non-invasive cortical stimulation on skilled motor function in chronic stroke. *Brain*, *128*(3), 490–499.

Hwang, E. J., Hauschild, M., Wilke, M., & Andersen, R. A. (2012). Inactivation of the parietal reach region causes optic ataxia, impairing reaches but not saccades. *Neuron*, *76*(5), 1021–1029.

Hwang, E. J., Hauschild, M., Wilke, M., & Andersen, R. A. (2014). Spatial and temporal eye--hand coordination relies on the Parietal Reach Region. *Journal of Neuroscience*, *34*(38), 12884–12892.

Hyvärinen, J. (1982). Posterior parietal lobe of the primate brain. *Physiological Reviews*, *62*(3), 1060–1129.

Hyvärinen, J., & Poranen, A. (1974). Function of the parietal associative area 7 as revealed from cellular discharges in alert monkeys. *Brain*, *97*(4), 673–692.

Iezzi, E., Conte, A., Suppa, A., Agostino, R., Dinapoli, L., Scontrini, A., & Berardelli, A. (2008). Phasic voluntary movements reverse the aftereffects of subsequent theta-burst stimulation in humans. *Journal of Neurophysiology*, *100*(4), 2070–2076.

[*] Inoue, K., Kawashima, R., Satoh, K., Kinomura, S., Goto, R., Koyama, M., Sugiura, M., Ito, M., & Fukuda, H. (1998). PET study of pointing with visual feedback of moving hands. *Journal of Neurophysiology, 79*(1), 117–125.

Iverson, J. M., & Thelen, E. (1999). Hand, mouth and brain. The dynamic emergence of speech and gesture. *Journal of Consciousness Studies, 6*(11-12), 19-40.

Jacobs, S., Danielmeier, C., & Frey, S. H. (2010). Human anterior intraparietal and ventral premotor cortices support representations of grasping with the hand or a novel tool. *Journal of Cognitive Neuroscience, 22*(11), 2594–2608.

Jakobson, L. S., Archibald, Y. M., Carey, D. P., & Goodale, M. A. (1991). A kinematic analysis of reaching and grasping movements in a patient recovering from optic ataxia. *Neuropsychologia*, *29*(8), 803–809.

Jannati, A., Block, G., Oberman, L. M., Rotenberg, A., & Pascual-Leone, A. (2017). Interindividual variability in response to continuous theta-burst stimulation in healthy adults. *Clinical Neurophysiology*, *128*(11), 2268–2278.

Jeannerod, M., Arbib, M., Rizzolatti, G., & Sakata, H. (1995). Grasping objects: the cortical mechanisms of visuomotor transformation. *Trends in Neurosciences*, *18*, 314–320.

Johansen-Berg, H., Rushworth, M. F. S., Bogdanovic, M. D., Kischka, U., Wimalaratna, S., & Matthews, P. M. (2002). The role of ipsilateral premotor cortex in hand movement after stroke. *Proceedings of the National Academy of Sciences*, *99*(22), 14518–14523. doi: 10.1073/pnas.222536799

Johanson, D., Edey, M., & Edey, M. A. (1990). *Lucy: The beginnings of humankind*. Simon and Schuster.

Johnson, P. B., Ferraina, S., Bianchi, L., & Caminiti, R. (1996). Cortical networks for visual reaching: physiological and anatomical organization of frontal and parietal lobe arm regions. *Cerebral Cortex*, *6*(2), 102–119.

Johnson, P. B., Ferraina, S., & Caminiti, R. (1993). Cortical networks for visual reaching. *Experimental Brain Research*, *97*(2), 361–365.

Kalaska, J. F. (1996). Parietal cortex area 5 and visuomotor behavior. *Canadian Journal of Physiology and Pharmacology*, *74*(4), 483–498.

Kalaska, J. F., & Crammond, D. J. (1995). Deciding not to GO: neuronal correlates of response selection in a GO/NOGO task in primate premotor and parietal cortex. *Cerebral Cortex*, *5*(5), 410–428.

Kalaska, J. F., Scott, S. H., Cisek, P., & Sergio, L. E. (1997). Cortical control of reaching movements. *Current Opinion in Neurobiology*, *7*(6), 849–859.

Kamen, G. (2004). Reliability of motor-evoked potentials during resting and active contraction conditions. *Medicine and Science in Sports and Exercise*, *36*(9), 1574–1579.

Kammer, T., Beck, S., Thielscher, A., Laubis-Herrmann, U., & Topka, H. (2001). Motor thresholds in humans: a transcranial magnetic stimulation study comparing different pulse waveforms, current directions and stimulator types. *Clinical Neurophysiology, 112*(2), 250–258.

Karnath, H.-O., & Perenin, M.-T. (2005). Cortical control of visually guided reaching: evidence from patients with optic ataxia. *Cerebral Cortex, 15*(10), 1561–1569.

Kaulmann, D., Hermsdörfer, J., & Johannsen, L. (2017). Disruption of right posterior parietal cortex by continuous Theta Burst Stimulation alters the control of body balance in quiet stance. *European Journal of Neuroscience, 45*(5), 671–678. doi: 10.1111/ejn.13522

Kay, R. F., Williams, B. A., Ross, C. F., Takai, M., & Shigehara, N. (2004). Anthropoid origins: a phylogenetic analysis. In *Anthropoid Origins* (pp. 91–135). Springer.

[*] Kertzman, C., Schwarz, U., Zeffiro, T. A., & Hallett, M. (1997). The role of posterior parietal cortex in visually guided reaching movements in humans. *Experimental Brain Research, 114*(1), 170–183.

Khan, A. Z., Pisella, L., Vighetto, A., Cotton, F., Luaute, J., Boisson, D., Salemme, R., Crawford, J. D., & Rossetti, Y. (2005). Optic ataxia errors depend on remapped, not viewed, target location. *Nature Neuroscience, 8*(4), 418.

Kiers, L., Cros, D., Chiappa, K. H., & Fang, J. (1993). Variability of motor potentials evoked by transcranial magnetic stimulation. *Electroencephalography and Clinical Neurophysiology/Evoked Potentials Section, 89*(6), 415–423.

Kim, W., Buchanan, J., & Gabbard, C. (2011). Constraints on arm selection processes when reaching: degrees of freedom and joint amplitudes interact to influence limb selection. *Journal of Motor Behavior, 43*(5), 403–411. doi: 10.1080/00222895.2011.619222

Kimura, D. (1963). Right temporal-lobe damage: Perception of unfamiliar stimuli after damage. *Archives of Neurology, 8*(3), 264–271.

Klaes, C., Westendorff, S., Chakrabarti, S., & Gail, A. (2011). Choosing goals, not rules: deciding among rule-based action plans. *Neuron*, *70*(3), 536–548.

Kleiner, M., Brainard, D., & Pelli, D. (2007). *What's new in Psychtoolbox-3?*

Knecht, S., Ellger, T., Breitenstein, C., Ringelstein, E. B., & Henningsen, H. (2003). Changing cortical excitability with low-frequency transcranial magnetic stimulation can induce sustained disruption of tactile perception. *Biological Psychiatry*, *53*(2), 175–179.

Koch, G., Franca, M., Del Olmo, M. F., Cheeran, B., Milton, R., Sauco, M. A., & Rothwell, J. C. (2006). Time course of functional connectivity between dorsal premotor and contralateral motor cortex during movement selection. *Journal of Neuroscience*, *26*(28), 7452–7459.

[*] Konen, C. S., Mruczek, R. E., Montoya, J. L., & Kastner, S. (2013). Functional organization of human posterior parietal cortex: grasping-and reaching-related activations relative to topographically organized cortex. J*ournal of Neurophysiology, 109*(12), 2897–2908.

Krakauer, J. W., & Carmichael, S. T. (2017). *Broken movement: the neurobiology of motor recovery after stroke*. MIT Press.

Kuang, S., Morel, P., & Gail, A. (2015). Planning movements in visual and physical space in monkey posterior parietal cortex. *Cerebral Cortex*, *26*(2), 731–747.

Kurata, K. (1991). Corticocortical inputs to the dorsal and ventral aspects of the premotor cortex of macaque monkeys. *Neuroscience Research*, *12*(1), 263–280.

Kuznetsova, A., Brockhoff, P. B., & Christensen, R. H. B. (2017). lmerTest package: tests in linear mixed effects models. J*ournal of Statistical Software, 82*(13).

Lacquaniti, F., Guigon, E., Bianchi, L., Ferraina, S., & Caminiti, R. (1995). Representing spatial information for limb movement: role of area 5 in the monkey. *Cerebral Cortex*, *5*(5), 391–409.

Lakhani, B., Bolton, D. A. E., Miyasike-daSilva, V., Vette, A. H., & McIlroy, W. E. (2014). Speed of processing in the primary motor cortex: a continuous theta burst stimulation study. *Behavioural Brain Research*, *261*, 177–184.

[*] Le, A., Vesia, M., Yan, X., Crawford, J. D., & Niemeier, M. (2016). Parietal area BA7 integrates motor programs for reaching, grasping, and bimanual coordination. *Journal of Neurophysiology, 117*(2), 624–636.

Lee, M., Kim, S. E., Kim, W. S., Lee, J., Yoo, H. K., Park, K.-D., Choi, K.-G., Jeong, S.-Y., Kim, B. G., & Lee, H. W. (2013). Interaction of motor training and intermittent theta burst stimulation in modulating motor cortical plasticity: influence of BDNF Val66Met polymorphism. *PLoS One, 8*(2), e57690.

Lenth, R. V. (2016). Least-squares means: the R package lsmeans. *Journal of Statistical Software, 69*: 1–33.

Li, C.-T., Chen, M.-H., Juan, C.-H., Huang, H.-H., Chen, L.-F., Hsieh, J.-C., Tu, P.-C., Bai, Y.-M., Tsai, S.-J., Lee, Y.-C., & Su, T.-P. (2014). Efficacy of prefrontal theta-burst stimulation in refractory depression: a randomized sham-controlled study. *Brain*, *137*(7), 2088–2098. doi: 10.1093/brain/awu109

Liang, J., Wilkinson, K., & Sainburg, R. L. (2018). Is Hand Selection Modulated by Cognitive–perceptual Load? *Neuroscience*, *369*, 363–373. doi: 10.1016/j.neuroscience.2017.11.005

Liepert, J., Miltner, W. H. R., Bauder, H., Sommer, M., Dettmers, C., Taub, E., & Weiller, C. (1998). Motor cortex plasticity during constraint-induced movement therapy in stroke patients. *Neuroscience Letters*, *250*(1), 5–8.

Lisanby, S. H., Gutman, D., Luber, B., Schroeder, C., & Sackeim, H. A. (2001). Sham TMS: intracerebral measurement of the induced electrical field and the induction of motor-evoked potentials. *Biological Psychiatry*, *49*(5), 460–463.

Logothetis, N. K. (2003). The underpinnings of the BOLD functional magnetic resonance imaging signal. *Journal of Neuroscience*, *23*(10), 3963–3971.

Logothetis, N. K., Pauls, J., Augath, M., Trinath, T., & Oeltermann, A. (2001). Neurophysiological investigation of the basis of the fMRI signal. *Nature*, *412*(6843), 150.

Logothetis, N. K., & Wandell, B. A. (2004). Interpreting the BOLD signal. *Annual Review of Physiology*, *66*, 735–769.

Luke, S. G. (2017). Evaluating significance in linear mixed-effects models in R. *Behavior Research Methods, 49*(4), 1494–1502.

Lundborg, G. (2013). *The hand and the brain: From Lucy's thumb to the thought-controlled robotic hand.* doi: 10.1007/978-1-4471-5334-4_1

Maeda, F., Keenan, J. P., Tormos, J. M., Topka, H., & Pascual-Leone, A. (2000). Modulation of corticospinal excitability by repetitive transcranial magnetic stimulation. *Clinical Neurophysiology*, *111*(5), 800–805.

Maloney, L. T., Trommershäuser, J., & Landy, M. S. (2007). Questions without words: A comparison between decision making under risk and movement planning under risk. *Integrated Models of Cognitive Systems*, *29*, 7–313.

Mamolo, C. M., Roy, E. A., Bryden, P. J., & Rohr, L. E. (2004). The effects of skill demands and object position on the distribution of preferred hand reaches. *Brain and Cognition*, *55*(2), 349–351. doi: 10.1016/j.bandc.2004.02.041

Mamolo, C. M., Roy, E. A., Rohr, L. E., & Bryden, P. J. (2006). Reaching patterns across working space: The effects of handedness, task demands, and comfort levels. *Laterality: Asymmetries of Body, Brain and Cognition*, *11*(5), 465–492. doi: 10.1080/13576500600775692

Marigold, D. S., Lajoie, K., & Heed, T. (2019). No effect of triple-pulse TMS medial to intraparietal sulcus on online correction for target perturbations during goal-directed hand and foot reaches. *PloS One, 14*(10), e0223986. doi: 10.1371/journal.pone.0223986.

Martin, J. A., Karnath, H.-O., & Himmelbach, M. (2015). Revisiting the cortical system for peripheral reaching at the parieto-occipital junction. *Cortex*, *64*, 363–379.

McKee, S. P., Klein, S. A., & Teller, D. Y. (1985). Statistical properties of forced-choice psychometric functions: Implications of probit analysis. *Perception & Psychophysics*, *37*(4), 286–298.

Medendorp, W. P., Goltz, H. C., Crawford, J. D., & Vilis, T. (2005). Integration of target and effector information in human posterior parietal cortex for the planning of action. *Journal of Neurophysiology, 93*(2), 954–962.

[*] Medendorp, W. P., Goltz, H. C., Vilis, T., & Crawford, J. D. (2003). Gaze-centered updating of visual space in human parietal cortex. *Journal of Neuroscience*, *23*(15), 6209–6214.

Meehan, S. K., Dao, E., Linsdell, M. A., & Boyd, L. A. (2011). Continuous theta burst stimulation over the contralesional sensory and motor cortex enhances motor learning post-stroke. *Neuroscience Letters*, *500*(1), 26–30. doi: 10.1016/j.neulet.2011.05.237

Merabet, L., Thut, G., Murray, B., Andrews, J., Hsiao, S., & Pascual-Leone, A. (2004). Feeling by sight or seeing by touch? *Neuron, 42*(1), 173–179.

Mills, K. R., Boniface, S. J., & Schubert, M. (1992). Magnetic brain stimulation with a double coil: the importance of coil orientation. *Electroencephalography and Clinical Neurophysiology/Evoked Potentials Section, 85*(1), 17–21.

Milner, A. D., & Goodale, M. A. (1995). *The visual brain in action.* (Vol. 27). OUP Oxford.

Milner, A. D., & Goodale, M. A. (2008). Two visual systems re-viewed. *Neuropsychologia, 46*(3), 774–785.

Miniussi, C., Harris, J. A., & Ruzzoli, M. (2013). Modelling non-invasive brain stimulation in cognitive neuroscience. *Neuroscience & Biobehavioral Reviews*, *37*(8), 1702–1712.

Mishkin, M., & Ungerleider, L. G. (1982). Contribution of striate inputs to the visuospatial functions of parieto-preoccipital cortex in monkeys. *Behavioural Brain Research, 6*(1), 57–77.

Mitz, A. R., Godschalk, M., & Wise, S. P. (1991). Learning-dependent neuronal activity in the premotor cortex: activity during the acquisition of conditional motor associations. *Journal of Neuroscience*, *11*(6), 1855–1872.

Mochizuki, H., Franca, M., Huang, Y.-Z., & Rothwell, J. C. (2005). The role of dorsal premotor area in reaction task: comparing the "virtual lesion" effect of paired pulse or theta burst transcranial magnetic stimulation. *Experimental Brain Research*, *167*(3), 414–421.

Monaco, S., Sedda, A., Cavina-Pratesi, C., & Culham, J. C. (2015). Neural correlates of object size and object location during grasping actions. *European Journal of Neuroscience, 41*(4), 454–465.

Mountcastle, V. B., Lynch, J. C., Georgopoulos, A., Sakata, H., & Acuna, C. (1975). Posterior parietal association cortex of the monkey: command functions for operations within extrapersonal space. *Journal of Neurophysiology*, *38*(4), 871–908.

Muakkassa, K. F., & Strick, P. L. (1979). Frontal lobe inputs to primate motor cortex: evidence for four somatotopically organized 'premotor' areas. *Brain Research*, *177*(1), 176–182.

Muellbacher, W., Ziemann, U., Boroojerdi, B., & Hallett, M. (2000). Effects of low-frequency transcranial magnetic stimulation on motor excitability and basic motor behavior. *Clinical Neurophysiology*, *111*(6), 1002–1007.

Mullette-Gillman, O. A., Cohen, Y. E., & Groh, J. M. (2005). Eye-centered, head-centered, and complex coding of visual and auditory targets in the intraparietal sulcus. *Journal of Neurophysiology, 94*(4), 2331–2352.

Mullette-Gillman, O. A., Cohen, Y. E., & Groh, J. M. (2008). Motor-related signals in the intraparietal cortex encode locations in a hybrid, rather than eye-centered reference frame. *Cerebral Cortex*, *19*(8), 1761–1775.

Murase, N., Duqué, J., Mazzocchio, R., & Cohen, L. G. (2004). Influence of interhemispheric interactions on motor function in chronic stroke. *Annals of Neurology, 55*(3), 400–409. https://doi.org/10.1002/ana.10848

Napier, J. R. (1956). The prehensile movements of the human hand. The Journal of bone and joint surgery. *British volume, 38*(4), 902-913.

Nyffeler, T., Cazzoli, D., Wurtz, P., Lüthi, M., Von Wartburg, R., Chaves, S., Déruaz, A., Hess, C. W., & Müri, R. M. (2008). Neglect-like visual exploration behaviour after theta burst transcranial magnetic stimulation of the right posterior parietal cortex. *European Journal of Neuroscience*, *27*(7), 1809–1813.

Nyffeler, T., Wurtz, P., Luscher, H. R., Hess, C. W., Senn, W., Pflugshaupt, T., vonWartburg, R., Lüthi, M., & Müri, R. M. (2006). Repetitive TMS over the human oculomotor cortex: comparison of 1-Hz and theta burst stimulation. *Neuroscience Letters*, *409*(1), 57–60. doi: 10.1016/j.neulet.2006.09.011

Oberman, L., Edwards, D., Eldaief, M., & Pascual-Leone, A. (2011). Safety of theta burst transcranial magnetic stimulation: a systematic review of the literature. *Journal of Clinical Neurophysiology*, *28*(1), 67–74. doi: 10.1097/wnp.0b013e318205135f

Obeso, I., Cho, S. S., Antonelli, F., Houle, S., Jahanshahi, M., Ko, J. H., & Strafella, A. P. (2013). Stimulation of the pre-SMA influences cerebral blood flow in frontal areas involved with inhibitory control of action. *Brain Stimulation*, *6*(5), 769–776.

Okabe, N., Himi, N., Nakamura-Maruyama, E., Hayashi, N., Sakamoto, I., Hasegawa, T., & Miyamoto, O. (2019). Very Early Initiation Reduces Benefits of Poststroke Rehabilitation Despite Increased Corticospinal Projections. *Neurorehabilitation and Neural Repair*, 37(7), 53–552.

Oliveira, F. T. P., Diedrichsen, J., Verstynen, T., Duqué, J., & Ivry, R. B. (2010). Transcranial magnetic stimulation of posterior parietal cortex affects decisions of hand choice. *Proceedings of the National Academy of Sciences*, *107*(41), 17751–17756.

Opitz, A., Legon, W., Mueller, J., Barbour, A., Paulus, W., & Tyler, W. J. (2015). Is sham cTBS real cTBS? The effect on EEG dynamics. *Frontiers in Human Neuroscience*, *8*, 1043.

Orlov, T., Makin, T. R., & Zohary, E. (2010). Topographic representation of the human body in the occipitotemporal cortex. *Neuron, 68*(3), 586–600.

Ortu, E., Ruge, D., Deriu, F., & Rothwell, J. C. (2009). Theta Burst Stimulation over the human primary motor cortex modulates neural processes involved in movement preparation. *Clinical Neurophysiology, 120*(6), 1195–1203. doi: 10.1016/j.clinph.2009.04.001

Padoa-Schioppa, C. (2011). Neurobiology of economic choice: a good-based model. *Annual Review of Neuroscience, 34*, 333–359. doi.: 10.1146/annurev-neuro-061010-113648

Padoa-Schioppa, C., & Assad, J. A. (2006). Neurons in the orbitofrontal cortex encode economic value. *Nature, 441*(7090), 223–226. doi: 10.1038/nature04676

Palmer, E., & Ashby, P. (1992). Corticospinal projections to upper limb motoneurones in humans. *The Journal of Physiology, 448*(1), 397–412.

Parzen, E. (1962). On estimation of a probability density function and mode. *The Annals of Mathematical Statistics, 33*(3), 1065–1076.

Pascual-Leone, A. (1999). Transcranial magnetic stimulation: studying the brain--behaviour relationship by induction of 'virtual lesions'. *Philosophical Transactions of the Royal Society of London. Series B: Biological Sciences, 354*(1387), 1229–1238.

Pascual-Leone, A., Tormos, J. M., Keenan, J., Tarazona, F., Cañete, C., & Catalá, M. D. (1998). Study and modulation of human cortical excitability with transcranial magnetic stimulation. *Journal of Clinical Neurophysiology, 15*(4), 333–343.

Pascual-Leone, A., Valls-Solé, J., Wassermann, E. M., & Hallett, M. (1994). Responses to rapid-rate transcranial magnetic stimulation of the human motor cortex. *Brain, 117*(4), 847–858.

Pascual-Leone, A., Walsh, V., & Rothwell, J. (2000). Transcranial magnetic stimulation in cognitive neuroscience--virtual lesion, chronometry, and functional connectivity. *Current Opinion in Neurobiology*, *10*(2), 232–237. doi: 10.1016/S0959-4388(00)00081-7

Passingham, R. E. (1989). Premotor cortex and the retrieval of movement. *Brain, Behavior and Evolution*, *33*(2–3), 189–192.

Pastor-Bernier, A., & Cisek, P. (2011a). Neural correlates of biased competition in premotor cortex. *Journal of Neuroscience*, *31*(19), 7083–7088.

Pastor-Bernier, A., & Cisek, P. (2011b). Making Choices between Rules or between Actions. *Neuron*, *70*(3), 382–384. doi: 10.1016/j.neuron.2011.04.017

Pastor-Bernier, A., Tremblay, E., & Cisek, P. (2012). Dorsal premotor cortex is involved in switching motor plans. *Frontiers in Neuroengineering*, *5*, 5.

Paulus, W. (2005). Toward establishing a therapeutic window for rTMS by theta burst stimulation. *Neuron*, *45*(2), 181–183.

Peele, T. L. (1942). Cytoarchitecture of individual parietal areas in the monkey (Macaca mulatta) and the distribution of the efferent fibers. *Journal of Comparative Neurology*, *77*(3), 693–737.

Peele, T. L. (1944). Acute and chronic parietal lobe ablations in monkeys. *Journal of Neurophysiology*, *7*(5), 269–286.

Pelli, D. G., & Vision, S. (1997). The VideoToolbox software for visual psychophysics: Transforming numbers into movies. *Spatial Vision*, *10*, 437–442.

[*] Pellijeff, A., Bonilha, L., Morgan, P. S., McKenzie, K., & Jackson, S. R. (2006). Parietal updating of limb posture: an event-related fMRI study. *Neuropsychologia, 44*(13), 2685–2690.

Perenin, M.-T., & Vighetto, A. (1988). Optic ataxia: A specific disruption in visuomotor mechanisms: I. Different aspects of the deficit in reaching for objects. *Brain*, *111*(3), 643–674.

Pesaran, B., Nelson, M. J., & Andersen, R. A. (2006). Dorsal premotor neurons encode the relative position of the hand, eye, and goal during reach planning. *Neuron*, *51*(1), 125–134.

Pesaran, B., Nelson, M. J., & Andersen, R. A. (2008). Free choice activates a decision circuit between frontal and parietal cortex. *Nature*, *453*(7193), 406.

Petrides, M., & Pandya, D. N. (1984). Projections to the frontal cortex from the posterior parietal region in the rhesus monkey. *Journal of Comparative Neurology*, *228*(1), 105–116.

Piserchia, V., Breveglieri, R., Hadjidimitrakis, K., Bertozzi, F., Galletti, C., & Fattori, P. (2017). Mixed body/hand reference frame for reaching in 3D space in macaque parietal area PEc. *Cerebral Cortex*, *27*(3), 1976–1990.

Pitzalis, S., Sereno, M. I., Committeri, G., Fattori, P., Galati, G., Tosoni, A., & Galletti, C. (2013). The human homologue of macaque area V6A. *NeuroImage*, *82*, 517–530.

Pitzalis, S., Sereno, M. I., Committeri, G., Fattori, P., Galati, G., Patria, F., & Galletti, C. (2009). Human V6: the medial motion area. *Cerebral Cortex, 20*(2), 411–424.

Player, M. J., Taylor, J. L., Alonzo, A., & Loo, C. K. (2012). Paired associative stimulation increases motor cortex excitability more effectively than theta-burst stimulation. *Clinical Neurophysiology*, *123*(11), 2220–2226.

Plewnia, C., Pasqualetti, P., Große, S., Schlipf, S., Wasserka, B., Zwissler, B., & Fallgatter, A. (2014). Treatment of major depression with bilateral theta burst stimulation: A randomized controlled pilot trial. *Journal of Affective Disorders*, *156*, 219–223. doi 10.1016/j.jad.2013.12.025

Pohl, W. (1973). Dissociation of spatial discrimination deficits following frontal and parietal lesions in monkeys. *Journal of Comparative and Physiological Psychology*, *82*(2), 227.

Poulet, E., Brunelin, J., Makhlouf, W. Ben, D'Amato, T., & Saoud, M. (2009). A case report of cTBS for the treatment of auditory hallucinations in a patient with schizophrenia. *Brain Stimulation: Basic, Translational, and Clinical Research in Neuromodulation*, *2*(2), 118–119.

[*] Prado, J., Clavagnier, S., Otzenberger, H., Scheiber, C., Kennedy, H., & Perenin, M.-T. (2005). Two cortical systems for reaching in central and peripheral vision. *Neuron*, *48*(5), 849–858.

Przybyla, A., Coelho, C. J., Akpinar, S., Kirazci, S., & Sainburg, R. L. (2013). Sensorimotor performance asymmetries predict hand selection. *Neuroscience*, *228*, 349–360.

R Core Team. (2018). R: A language and environment for statistical computing. R Foundation for Statistical Computing, Vienna, Austria. URL http://www. R-project. org.

Rafal, R. (2003). Balint's syndrome: A disorder of visual cognition. *Neurological Foundations of Cognitive Neuroscience*, 27–40.

Ramkumar, P., Dekleva, B., Cooler, S., Miller, L., & Kording, K. (2016). Premotor and motor cortices encode reward. *PloS One*, *11*(8), e0160851.

Ratcliff, G., & Davies-Jones, G. A. (1972). Defective visual localization in focal brain wounds. *Brain: A Journal of Neurology*, *95*, 49–60.

[*] Reichenbach, A., Bresciani, J. P., Peer, A., Bülthoff, H. H., & Thielscher, A. (2010). Contributions of the PPC to online control of visually guided reaching movements assessed with fMRI-guided TMS. *Cerebral Cortex, 21*(7), 1602–1612.

Reis, J., Robertson, E. M., Krakauer, J. W., Rothwell, J., Marshall, L., Gerloff, C., Wassermann, E. M., Pascual-Leone, A., Hummel, F., Celnik, P. A., Classen, J., Floel, A., Ziemann, U., Paulus, W., Siebner, H. R., Born, J., & Cohen, L. G. (2008). Consensus: Can transcranial direct current stimulation and transcranial magnetic stimulation enhance motor learning and memory formation? *Brain Stimulation*, *1*(4), 363–369. doi: 10.1016/j.brs.2008.08.001

Rizzolatti, G., Fogassi, L., & Gallese, V. (1997). Parietal cortex: from sight to action. *Current Opinion in Neurobiology*, *7*(4), 562–567.

Rizzolatti, G., & Luppino, G. (2001). The cortical motor system. *Neuron*, *31*(6), 889–901. doi: 10.1016/S0896-6273(01)00423-8

Rizzolatti, G., Luppino, G., & Matelli, M. (1998). The organization of the cortical motor system: new concepts. *Electroencephalography and Clinical Neurophysiology*, *106*(4), 283–296.

Rizzolatti, G., & Matelli, M. (2003). Two different streams form the dorsal visual system: anatomy and functions. *Experimental Brain Research*, *153*(2), 146–157.

Robinson, D. L., Goldberg, M. E., & Stanton, G. B. (1978). Parietal association cortex in the primate: sensory mechanisms and behavioral modulations. *Journal of Neurophysiology*, *41*(4), 910–932.

Rocchi, L., Ibáñez, J., Benussi, A., Hannah, R., Rawji, V., Casula, E., & Rothwell, J. (2018). Variability and predictors of response to continuous theta burst stimulation: a TMS-EEG study. *Frontiers in Neuroscience*, *12*, 400. doi:10.3389/fnins.2018.00400

Rondot, P., & Dumas, J. L. (1977). Visuomotor ataxia. *Brain: A Journal of Neurology*, *100*(2), 355–376.

Rorden, C., & Karnath, H.-O. (2004). Using human brain lesions to infer function: a relic from a past era in the fMRI age? *Nature Reviews Neuroscience*, *5*(10), 812.

Rosenbaum, D. A., Marchak, F., Barnes, H. J., Vaughan, J., Slotta, J., & Jorgensen, M. J. (1990). Constraints for action selection: Overhand versus underhand grips. In M. Jeannerod (Ed.), *Attention and performance XIII: Motor representation and control.* (pp. 321–342). Hillsdale, NJ: Lawrence Erlbaum Associates.

Ross, J. M., Iversen, J. R., & Balasubramaniam, R. (2018). The Role of Posterior Parietal Cortex in Beat-based Timing Perception: A Continuous Theta Burst Stimulation Study. *Journal of Cognitive Neuroscience*, *30*(5), 634–643. doi: 10.1162/jocn_a_01237

Rossi, S., Hallett, M., Rossini, P. M., Pascual-Leone, A., & Safety of TMS Consensus Group. (2009). Safety, ethical considerations, and application guidelines for the use of transcranial magnetic stimulation in clinical practice and research. *Clinical Neurophysiology*, *120*(12), 2008–2039.

Rossini, P. M., Barker, A. T., Berardelli, A., Caramia, M. D., Caruso, G., Cracco, R. Q., Dimitrijević, M. R., Hallett, M., Katayama, Y., Lücking, C. H., & De Noordhout., A. M. (1994). Non-invasive electrical and magnetic stimulation of the brain, spinal cord and roots: basic principles and procedures for routine clinical application. Report of an IFCN committee. *Electroencephalography and Clinical Neurophysiology*, *91*(2), 79–92.

Rossini, P. M., Burke, D., Chen, R., Cohen, L. G., Daskalakis, Z., Di Iorio, R., Di Lazzaro, V., Ferreri, F., Fitzgerald, P. B., George, M. S., & Hallett, M. (2015). Non-invasive electrical and magnetic stimulation of the brain, spinal cord, roots and peripheral nerves: basic principles and procedures for routine clinical and research application. An updated report from an IFCN Committee. *Clinical Neurophysiology*, *126*(6), 1071–1107.

Rossini, P. M., & Rossi, S. (1998). Clinical applications of motor evoked potentials. *Electroencephalography and Clinical Neurophysiology*, *106*(3), 180–194.

Rost, K. A., Hemmes, N. S., & Alvero, A. M. (2014). Effects of the relative values of alternatives on preference for free-choice in humans. *Journal of the Experimental Analysis of Behavior*, *102*(2), 241–251.

Rothwell, J. C., Thompson, P. D., Day, B. L., Dick, J. P. R., Kachi, T., Cowan, J. M. A., & Marsden, C. D. (1987). Motor cortex stimulation in intact man: 1. General characteristics of EMG responses in different muscles. *Brain*, *110*(5), 1173–1190.

Rushworth, M. F. S., Ellison, A., & Walsh, V. (2001). Complementary localization and lateralization of orienting and motor attention. *Nature Neuroscience*, *4*(6), 656–661. doi: 10.1038/88492

Rushworth, M. F. S., Johansen-Berg, H., Göbel, S. M., & Devlin, J. T. (2003). The left parietal and premotor cortices: Motor attention and selection. *NeuroImage, 20,* S89–S100. doi: 10.1016/j.neuroimage.2003.09.011

Sabes, P. N., & Jordan, M. I. (1997). Obstacle avoidance and a perturbation sensitivity model for motor planning. *Journal of Neuroscience, 17*(18), 7119–7128.

Santandrea, E., Breveglieri, R., Bosco, A., Galletti, C., & Fattori, P. (2018). Preparatory activity for purposeful arm movements in the dorsomedial parietal area V6A: Beyond the online guidance of movement. *Scientific Reports, 8*(1), 6926.

Savaki, H. E., Kennedy, C., Sokoloff, L., & Mishkin, M. (1993). Visually guided reaching with the forelimb contralateral to a" blind" hemisphere: a metabolic mapping study in monkeys. *Journal of Neuroscience, 13*(7), 2772–2789.

Schaffelhofer, S., & Scherberger, H. (2016). Object vision to hand action in macaque parietal, premotor, and motor cortices. *eLife, 5,* e15278. doi: 10.7554/eLife.15278

Scherberger, H., & Andersen, R. A. (2007). Target selection signals for arm reaching in the posterior parietal cortex. *Journal of Neuroscience, 27*(8), 2001–2012. doi: 10.1523/jneurosci.4274-06.2007

Scherberger, H., Jarvis, M. R., & Andersen, R. A. (2005). Cortical local field potential encodes movement intentions in the posterior parietal cortex. *Neuron, 46*(2), 347–354.

Schluter, N. D., Krams, M., Rushworth, M. F. S., & Passingham, R. E. (2001). Cerebral dominance for action in the human brain: The selection of actions. *Neuropsychologia.* doi: 10.1016/S0028-3932(00)00105-6

Schluter, N. D., Rushworth, M. F. S., Passingham, R. E., & Mills, K. R. (1998). Temporary interference in human lateral premotor cortex suggests dominance for the selection of movements. A study using transcranial magnetic stimulation. *Brain: a journal of neurology, 121*(5), 785–799.

Schwarz, R. J., & Taylor, C. L. (1955). The anatomy and mechanics of the human hand. *Artificial limbs, 2*(2), 22-35.

Schweighofer, N., Xiao, Y., Kim, S., Yoshioka, T., Gordon, J., & Osu, R. (2015). Effort, success, and nonuse determine arm choice. *Journal of Neurophysiology, 114*(1), 551–559.

Scott, S. H., Sergio, L. E., & Kalaska, J. F. (1997). Reaching movements with similar hand paths but different arm orientations. II. Activity of individual cells in dorsal premotor cortex and parietal area 5. *Journal of Neurophysiology, 78*(5), 2413–2426.

Shadlen, M. N., & Newsome, W. T. (2001). Neural basis of a perceptual decision in the parietal cortex (area LIP) of the rhesus monkey. *Journal of Neurophysiology, 86*(4), 1916–1936.

Shen, L., & Alexander, G. E. (1997a). Neural correlates of a spatial sensory-to-motor transformation in primary motor cortex. *Journal of Neurophysiology, 77*(3), 1171–1194.

Shen, L., & Alexander, G. E. (1997b). Preferential representation of instructed target location versus limb trajectory in dorsal premotor area. *Journal of Neurophysiology, 77*(3), 1195–1212.

Siebner, H. R., Hartwigsen, G., Kassuba, T., & Rothwell, J. C. (2009). How does transcranial magnetic stimulation modify neuronal activity in the brain? Implications for studies of cognition. *Cortex; a Journal Devoted to the Study of the Nervous System and Behavior, 45*(9), 1035–1042. doi: 10.1016/j.cortex.2009.02.007

Silvanto, J., & Cattaneo, Z. (2017). Common framework for "virtual lesion" and state-dependent TMS: the facilitatory/suppressive range model of online TMS effects on behavior. *Brain and Cognition, 119*, 32–38.

Smyrnis, N., Theleritis, C., Evdokimidis, I., Müri, R. M., & Karandreas, N. (2003). Single-pulse transcranial magnetic stimulation of parietal and prefrontal areas in a memory delay arm pointing task. *Journal of Neurophysiology*, *89*(6), 3344–3350.

Snyder, L. H., Batista, A. P., & Andersen, R. A. (1997). Coding of intention in the posterior parietal cortex. *Nature*, *386*(6621), 167.

Snyder, L. H., Batista, A. P., & Andersen, R. A. (2000). Intention-related activity in the posterior parietal cortex: a review. *Vision Research*, *40*(10–12), 1433–1441.

Sommer, M., Alfaro, A., Rummel, M., Speck, S., Lang, N., Tings, T., & Paulus, W. (2006). Half sine, monophasic and biphasic transcranial magnetic stimulation of the human motor cortex. *Clinical Neurophysiology*, *117*(4), 838–844.

Staines, W. R., & Bolton, D. A. E. (2013). Transcranial magnetic stimulation techniques to study the somatosensory system: research applications. In *Handbook of clinical neurology* (Vol. 116, pp. 671–679). Elsevier.

Stedman, A., Davey, N. J., & Ellaway, P. H. (1998). Facilitation of human first dorsal interosseous muscle responses to transcranial magnetic stimulation during voluntary contraction of the contralateral homonymous muscle. *Muscle & Nerve: Official Journal of the American Association of Electrodiagnostic Medicine*, *21*(8), 1033–1039.

Steenhuis, R. E., & Bryden, M. P. (1989). Different dimensions of hand preference that relate to skilled and unskilled activities. *Cortex*, *25*(2), 289–304.

Stewart, B. M., Gallivan, J. P., Baugh, L. A., & Flanagan, J. R. (2014). Motor, not visual, encoding of potential reach targets. *Current Biology*, *24*(19), R953–R954.

Stins, J. F., Kadar, E. E., & Costall, A. (2001). A kinematic analysis of hand selection in a reaching task. *Laterality: Asymmetries of Body, Brain and Cognition*, *6*(4), 347–367.

Stoloff, R. H., Taylor, J. A., Xu, J., Ridderikhoff, A., & Ivry, R. B. (2011). Effect of reinforcement history on hand choice in an unconstrained reaching task. *Frontiers in Neuroscience*, *5*, 41. doi: 10.3389/fnins.2011.00041

Strick, P. L., & Kim, C. C. (1978). Input to primate motor cortex from posterior parietal cortex (area 5). I. Demonstration by retrograde transport. *Brain Research*, *157*(2), 325–330.

[*] Striemer, C. L., Chouinard, P. A., & Goodale, M. A. (2011). Programs for action in superior parietal cortex: a triple-pulse TMS investigation. *Neuropsychologia*, *49*(9), 2391–2399.

Suppa, A., Huang, Y.-Z., Funke, K., Ridding, M. C., Cheeran, B., Di Lazzaro, V., Ziemann, U., & Rothwell, J. C. (2016). Ten Years of Theta Burst Stimulation in Humans: Established Knowledge, Unknowns and Prospects. *Brain Stimulation*, *9*(3), 323–335. doi: 10.1016/j.brs.2016.01.006

Suriya-Arunroj, L., & Gail, A. (2019). Complementary encoding of priors in monkey frontoparietal network supports a dual process of decision-making. *eLife*, *8*, e47581.

Taira, M., Mine, S., Georgopoulos, A. P., Murata, A., & Sakata, H. (1990). Parietal cortex neurons of the monkey related to the visual guidance of hand movement. *Experimental Brain Research*, *83*(1), 29–36.

Taira, M., Tsutsui, K. I., Jiang, M., Yara, K., & Sakata, H. (2000). Parietal neurons represent surface orientation from the gradient of binocular disparity. *Journal of Neurophysiology*, *83*(5), 3140–3146.

Talairach, J., & Tournoux, P. (1988). *Co-planar stereotaxic atlas of the human brain-3-dimensional proportional system*. New York: Thieme Medical Publishers.

Talelli, P., Greenwood, R. J., & Rothwell, J. C. (2007). Exploring Theta Burst Stimulation as an intervention to improve motor recovery in chronic stroke. *Clinical Neurophysiology*, *118*(2), 333–342. doi: 10.1016/j.clinph.2006.10.014

Talelli, P., Wallace, A., Dileone, M., Hoad, D., Cheeran, B., Oliver, R., VandenBos, M., Hammerback, U., Barratt, K., Gillini, C., & Musumeci, G. (2012). Theta burst stimulation in the rehabilitation of the upper limb: a semirandomized, placebo-controlled trial in chronic stroke patients. *Neurorehabilitation and Neural Repair*, *26*(8), 976–987.

Taub, E., Uswatte, G., & Pidikiti, R. (1999). Constraint-induced movement therapy: a new family of techniques with broad application to physical rehabilitation-a clinical review. *Journal of Rehabilitation Research and Development*, *36*(3), 237–251.

Teasell, R., Foley, N., Salter, K., Bhogal, S., Jutai, J., & Speechley, M. (2009). Evidence-based review of stroke rehabilitation: executive summary. *Topics in Stroke Rehabilitation*, *16*(6), 463–488.

Teo, J. T., Swayne, O. B., & Rothwell, J. C. (2007). Further evidence for NMDA-dependence of the after-effects of human theta burst stimulation. *Clinical Neurophysiology: Official Journal of the International Federation of Clinical Neurophysiology*, *118*(7), 1649–1651.

Thoenissen, D., Zilles, K., & Toni, I. (2002). Differential Involvement of Parietal and Precentral Regions in Movement Preparation and Motor Intention. *Journal of Neuroscience*, *22*(20), 9024–9034. doi: 10.1523/jneurosci.22-20-09024.2002

Thura, D., Beauregard-Racine, J., Fradet, C.-W., & Cisek, P. (2012). Decision making by urgency gating: theory and experimental support. *Journal of Neurophysiology*, *108*(11), 2912–2930.

Thura, D., & Cisek, P. (2014). Deliberation and commitment in the premotor and primary motor cortex during dynamic decision making. *Neuron*, *81*(6), 1401–1416. doi: 10.1016/j.neuron.2014.01.031

Thura, D., & Cisek, P. (2016). Modulation of premotor and primary motor cortical activity during volitional adjustments of speed-accuracy trade-offs. *Journal of Neuroscience*, *36*(3), 938–956.

Tinazzi, M., & Zanette, G. (1998). Modulation of ipsilateral motor cortex in man during unimanual finger movements of different complexities. *Neuroscience Letters*, *244*(3), 121–124.

Toni, I., Thoenissen, D., & Zilles, K. (2001). Movement preparation and motor intention. *NeuroImage*, *14*(1), S110-S117.

Tosoni, A., Galati, G., Romani, G. L., & Corbetta, M. (2008). Sensory-motor mechanisms in human parietal cortex underlie arbitrary visual decisions. *Nature Neuroscience*, *11*(12), 1446–1453. doi: 10.1038/nn.2221

Traversa, R., Cicinelli, P., Bassi, A., Rossini, P. M., & Bernardi, G. (1997). Mapping of motor cortical reorganization after stroke: a brain stimulation study with focal magnetic pulses. *Stroke*, *28*(1), 110–117.

Trommershäuser, J., Maloney, L. T., & Landy, M. S. (2003). Statistical decision theory and the selection of rapid, goal-directed movements. *Journal of the Optical Society of America*, *20*(7), 1419–1433.

Trompetto, C., Assini, A., Buccolieri, A., Marchese, R., & Abbruzzese, G. (2000). Motor recovery following stroke: a transcranial magnetic stimulation study. *Clinical Neurophysiology*, *111*(10), 1860–1867.

Tversky, A., & Kahneman, D. (1981). The Framing of Decisions and the Psychology of Choice. *Science*, *211*(4481), 453–458.

Umilta, M. A., Brochier, T., Spinks, R. L., & Lemon, R. N. (2007). Simultaneous recording of macaque premotor and primary motor cortex neuronal populations reveals different functional contributions to visuomotor grasp. *Journal of Neurophysiology, 98*(1), 488–501.

Ungerleider, L. G., Mishkin, M. (1982) Two cortical visual systems. In *Analysis of visual behavior.* (Ingle, D. J., Goodale, M. A., & Mansfield, R. J. W., ed), 549–586. Cambridge, MA: MIT Press.

Urgesi, C., Berlucchi, G., & Aglioti, S. M. (2004). Magnetic stimulation of extrastriate body area impairs visual processing of nonfacial body parts. *Current Biology, 14(*23), 2130–2134.

Valyear, K. F., Fitzpatrick, A. M., & Dundon, N. M. (2018). Now and then: Hand choice is influenced by recent action history. *Psychonomic Bulletin & Review*, *26*(1), 305–314. doi: 10.3758/s13423-018-1510-1

Valyear, K. F., & Frey, S. H. (2015). Human posterior parietal cortex mediates hand-specific planning. *NeuroImage, 114*, 226–238.

Van der Stigchel, S., Meeter, M., & Theeuwes, J. (2006). Eye movement trajectories and what they tell us. *Neuroscience & Biobehavioral Reviews, 30*(5), 666–679.

Van Der Werf, J., Jensen, O., Fries, P., & Medendorp, W. P. (2010). Neuronal synchronization in human posterior parietal cortex during reach planning. *Journal of Neuroscience, 30*(4), 1402–1412.

Van Donkelaar, P., & Adams, J. (2005). Gaze-dependent deviation in pointing induced by transcranial magnetic stimulation over the human posterior parietal cortex. *Journal of Motor Behavior, 37*(2), 157–163.

Vernet, M., Bashir, S., Yoo, W.-K., Oberman, L., Mizrahi, I., Ifert-Miller, F., Beck, C. J., & Pascual-Leone, A. (2014). Reproducibility of the effects of theta burst stimulation on motor cortical plasticity in healthy participants. *Clinical Neurophysiology, 125*(2), 320–326.

Vesia, M., & Crawford, J. D. (2012). Specialization of reach function in human posterior parietal cortex. *Experimental Brain Research, 221*(1), 1–18.

Vesia, M., Vander, H., Yan, X., & Sergio, L. E. (2005). The time course for kinetic versus kinematic planning of goal-directed human motor behavior. *Experimental Brain Research, 160*(3), 290–301.

[*] Vesia, M., Prime, S. L., Yan, X., Sergio, L. E., & Crawford, J. D. (2010). Specificity of human parietal saccade and reach regions during transcranial magnetic stimulation. *Journal of Neuroscience, 30*(39), 13053–13065.

Viswanathan, S., Wang, B. A., Abdollahi, R. O., Daun, S., Grefkes, C., & Fink, G. R. (2019). Freely chosen and instructed actions are terminated by different neural mechanisms revealed by kinematics-informed EEG. *NeuroImage, 188*, 26–42.

Walsh, V., & Cowey, A. (2000). Transcranial magnetic stimulation and cognitive neuroscience. *Nature Reviews Neuroscience, 1*(1), 73.

Ward, N S. (2005). Mechanisms underlying recovery of motor function after stroke. *Postgraduate Medical Journal, 81*(958), 510–514.

Ward, N S, & Cohen, L. G. (2004). Mechanisms underlying recovery of motor function after stroke. *Archives of Neurology*, *61*(12), 1844–1848. doi: 10.1001/archneur.61.12.1844

Ward, Nick S, Newton, J. M., Swayne, O. B. C., Lee, L., Thompson, A. J., Greenwood, R. J., Rothwell, J. C., & Frackowiak, R. S. J. (2006). Motor system activation after subcortical stroke depends on corticospinal system integrity. *Brain*, *129*(3), 809–819.

Warrington, E. K. (1982). Neuropsychological studies of object recognition. *Philosophical Transactions of the Royal Society of London. B, Biological Sciences*, *298*(1089), 15–33.

Warrington, E. K., & James, M. (1967). Disorders of visual perception in patients with localised cerebral lesions. *Neuropsychologia*, *5*(3), 253–266.

Wassermann, E. M. (1998). Risk and safety of repetitive transcranial magnetic stimulation: report and suggested guidelines from the International Workshop on the Safety of Repetitive Transcranial Magnetic Stimulation, June 5-7, 1996. *Electroencephalography and Clinical Neurophysiology/Evoked Potentials Section*, *108*(1), 1–16.

Wassermann, E. M. (2002). Variation in the response to transcranial magnetic brain stimulation in the general population. *Clinical Neurophysiology*, *113*(7), 1165–1171.

Webster, B. R., Celnik, P. A., & Cohen, L. G. (2006). Noninvasive brain stimulation in stroke rehabilitation. *NeuroRx, 3*(4), 474–481.

Weinrich, M., Wise, S. P., & Mauritz, K.-H. (1984). A neurophysiological study of the premotor cortex in the rhesus monkey. *Brain*, *107*(2), 385–414.

White, T. D., Asfaw, B., Beyene, Y., Haile-Selassie, Y., Lovejoy, C. O., Suwa, G., & WoldeGabriel, G. (2009). Ardipithecus ramidus and the paleobiology of early hominids. *Science, 326*(5949), 64–86.

Wilson, F. R. (1998). *The Hand*. New York: Vintage Books.

Wischnewski, M., & Schutter, D. J. L. G. (2015). Efficacy and Time Course of Theta Burst Stimulation in Healthy Humans. *Brain Stimulation*, *8*(4), 685–692. doi: 10.1016/j.brs.2015.03.004

Wise, S. P., Boussaoud, D., Johnson, P. B., & Caminiti, R. (1997). Premotor and parietal cortex: corticocortical connectivity and combinatorial computations. *Annual Review of Neuroscience*, *20*(1), 25–42.

Wise, S. P., di Pellegrino, G., & Boussaoud, D. (1996). The premotor cortex and nonstandard sensorimotor mapping. *Canadian Journal of Physiology and Pharmacology*, *74*(4), 469–482.

Wise, S. P., Weinrich, M., & Mauritz, K.-H. (1983). Motor aspects of cue-related neuronal activity in premotor cortex of the rhesus monkey. *Brain Research*, *260*(2), 301–305.

Wolf, S. L., Catlin, P. A., Ellis, M., Archer, A. L., Morgan, B., & Piacentino, A. (2001). Assessing Wolf motor function test as outcome measure for research in patients after stroke. *Stroke, 32*(7), 1635–1639.

Wolf, S. L., Thompson, P. A., Winstein, C. J., Miller, J. P., Blanton, S. R., Nichols-Larsen, D. S., Morris, D. M., Uswatte, G., Taub, E., Light, K. E., & Sawaki, L. (2010). The EXCITE stroke trial: comparing early and delayed constraint-induced movement therapy. *Stroke, 41*(10), 2309–2315. doi; 10.1161/strokeaha.110.588723

Wolpert, D. M., & Landy, M. S. (2012). Motor control is decision-making. *Current Opinion in Neurobiology*, *22*(6), 996–1003.

Wood, D. K., Chouinard, P. A., Major, A. J., & Goodale, M. A. (2017). Sensitivity to biomechanical limitations during postural decision-making depends on the integrity of posterior superior parietal cortex. *Cortex, 97*, 202–220.

Yamada, N., Kakuda, W., Kondo, T., Shimizu, M., Sageshima, M., Mitani, S., & Abo, M. (2014). Continuous theta-burst stimulation combined with occupational therapy for upper limb hemiparesis after stroke: a preliminary study. *Acta Neurologica Belgica, 114*(4), 279–284.

Yttri, E. A., Wang, C., Liu, Y., & Snyder, L. H. (2014). The parietal reach region is limb specific and not involved in eye-hand coordination. *Journal of Neurophysiology*, *111*(3), 520–532. doi: 10.1152/jn.00058.2013

Ziemann, U., Ilić, T. V, Alle, H., & Meintzschel, F. (2004). Cortico-motoneuronal excitation of three hand muscles determined by a novel penta-stimulation technique. *Brain*, *127*(8), 1887–1898.

Appendix A

Chapter 2: Supplemental Materials

S1.1. In-scanner videos

Supplementary videos 1 and 2 demonstrate in-scanner reaching performance to Target 15 during the Choice (Video1.mp4) and Instruct (Video2.mp4) conditions, respectively. Participants make minimal-amplitude movements, involving mainly the wrist and fingers, with some forearm movement. Critically, video data provide no evidence for systematic differences in the types of actions made during Choice relative to Instruct conditions. Primary task constraints were to make smooth movements without moving the head.

Supplementary videos 3 and 4 demonstrate two types of error trials. In Video3.mp4, the participant incorrectly uses their right hand to point to Target 12 during an Instruct-LHand trial, where instead, they should have performed the task using their left hand. In Video4.mp4, the right hand is used during an Instruct-LHand trial, followed by an online – 'mid-flight' – correction, where the participant then completes the task with their left hand. Error trials such as these were removed from both RT and fMRI analyses.

Videos 5 and 6 provide examples of reaching during the Instruct condition to Targets 1 (far left hemispace) and 16 (far right hemispace), respectively, using the contralateral hand (i.e. reaching to contralateral hemispace). For Targets 1-4 (left-Lateral quadrant) and 13-16 (right-Lateral quadrant), these kinds of actions were rarely performed during the Choice condition, where instead, participants showed a strong bias for the use of the ipsilateral hand (Figure 3B of the main manuscript).

S1.2. Error coding

Video data were scored for errors by three independent Raters. Supplementary Table 1 provides a summary of these data, both as raw numbers of trials, and as a percentage of total trials (shown in brackets).

Supplementary Table S1.1. Errors.

Error Type	Total (%)	Condition: Choice/Instruct (%)	LH	RH	Number Ps affected	Max incidence
Incorrect hand used	22 (0.39)	0 / 22 (0.58)	8 (0.21)	14 (0.37)	7 (30.43)	12 (33.33)
Initiation error	15 (0.26)	3 (0.16) / 12 (0.32)	12 (0.21)	7 (0.12)	9 (39.13)	4 (11.10)
No response made	5 (0.09)	2 (0.11) / 3 (0.08)	1 (0.03)	2 (0.05)	5 (21.74)	1 (2.70)
Video failure	5 (0.09)	2 (0.11) / 3 (0.08)	2 (0.05)	1 (0.03)	2 (8.70)	3 (8.30)

Few errors were made (< 1% of data). Additionally, it is worth being clear that only those errors that involved Choice or matched-Instruct condition trials (see Methods 2.7.1) influenced our primary fMRI and RT analyses. Errors involving these trials were less common (13/47 error trials). The majority of errors were made during unmatched-Instruct condition trials.

S1.3. Response times: Repeated-measures ANOVAs

Motivated by feedback from a reviewer, response time (RT) data are analysed in the main manuscript using linear mixed-effects models. Here, we provide results using conventional repeated measures analysis of variance (RM-ANOVA).

(S1.3.1) Response times: Task and Hand

Task (Choice, Instruct) by Hand (LH, RH) RM-ANOVA reveal a significant main effect of Task ($F(1, 18) = 123.34$, $p < 0.001$), with no significant main effect of Hand ($F(1, 18) = 0.10$, $p = 0.76$), and a significant Task by Hand interaction ($F(1, 18) = 9.24$, $p < 0.05$). Post-hoc pairwise comparisons reveal faster RTs for Instruct versus Choice conditions for both the left ($t = 9.92$, $p < 0.001$) and right hand ($t = 8.42$, $p < 0.001$), and this difference was significantly greater for the left hand.

(S1.3.2) Response times: Task by Target Location (Central, Lateral)

We define Target Location according to Central (targets 5-12) versus Lateral (targets 1-4 and 13-16) positions in the display. Contrary to our predictions, the result of the RM-ANOVA Task (Choice, Instruct) by Target Location (Central, Lateral) interaction is non-significant ($F(1, 18) = 0.17$, $p = 0.68$).

(S1.3.3) Response times: Task by Target Location (PSE, ExLat)

Target Location is defined per individual as those nearest to the PSE, versus those in extreme lateral positions, -/+7.6 mm (ExLat; targets 1, 4, 13, 16). RM-ANOVA reveal a non-significant Task by Lateral Target Location interaction in the predicted direction: (Choice-PSE > Instruct-PSE) > (Choice-ExLat > Instruct-ExLat) ($F(1, 18) = 2.00$, $p = 0.09$, one-tailed t-test).

Consistent with analysis (S3-1), the results of both analyses (S3-2) and (S3-3) reveal a significant main effect of Task ($p < 0.001$). No other significant main effects or interaction terms are identified.

S4. Task > rest inclusion mask.

Supplementary Figure S1 shows the results of the contrast used to define the inclusion mask (see Methods 2.3.7.3).
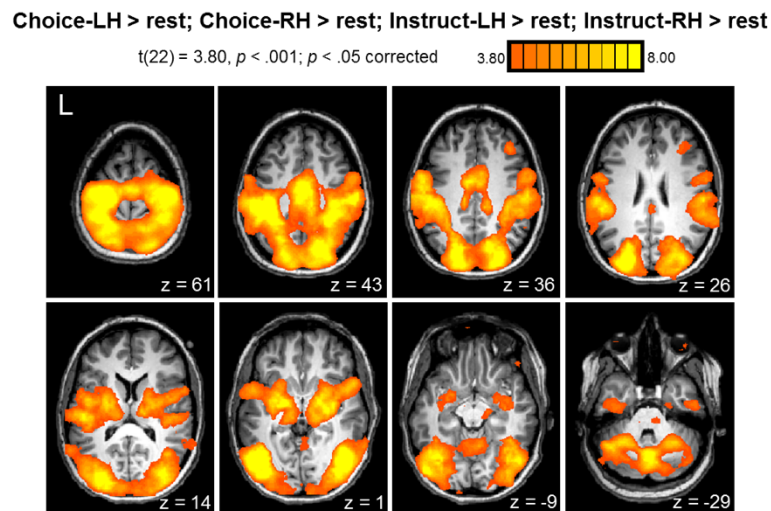
Supplementary Figure S1.1. Group-level inclusion mask of task-positive active voxels. The contrast identifies voxels that are significantly activated by any of the following contrasts: (1) Choice-LHand > rest; (2) Choice-RHand > rest; (3) Instruct-LHand > rest; (4) Instruct-RHand > rest.

The purpose of this method is to increase the sensitivity of subsequent statistical tests by reducing the number of voxels considered for correction for multiple comparisons to those that show task-related fMRI activity increases. The results reveal widespread bilateral activation including primary motor and sensorimotor cortices, supplementary motor area, basal ganglia, lateral occipital-temporal cortex, and the cerebellum.

S1.5. Hand choice per target quadrant

To test for differences in hand choice expressed as a function of quadrants of the target display (see Figure 2.3B) – left-Lateral (targets 1-4), left-central (targets 5-8), right-central (targets 9-12), right-Lateral (targets 13-16) –, hand-choice data were expressed as proportions of right-hand use, and arcsine transformed, calculated as the arcsine square root of the proportions. The arcsine transformation stretches the upper and lower ends of the data. This makes the distributions more symmetrical and reduces problems with violations of the assumption of normality. The transformed proportions were then tested using a one-way RM-ANOVA, with Target Quadrant as the fixed-effects factor.

Results reveal a significant main effect of Target Quadrant ($F(2.46, 54.2) = 211$, $p < 0.0001$). Post-hoc t-tests reveal significant differences between all possible pair-wise comparisons (all $p < 0.01$, corrected for multiple comparisons). These data indicate that participants varied significantly in their hand choice behaviour as a function of Target Quadrant, and that hand choice differed significantly between all four quadrants.

S1.6. Head motion data

Keeping the head still while performing manual actions in the MRI scanner can be
challenging. Supplementary Figure S2 demonstrates that our participants were able
to perform the task while keeping their head very still (see also, pre-scan behavioural
training; Methods 2.3.4).
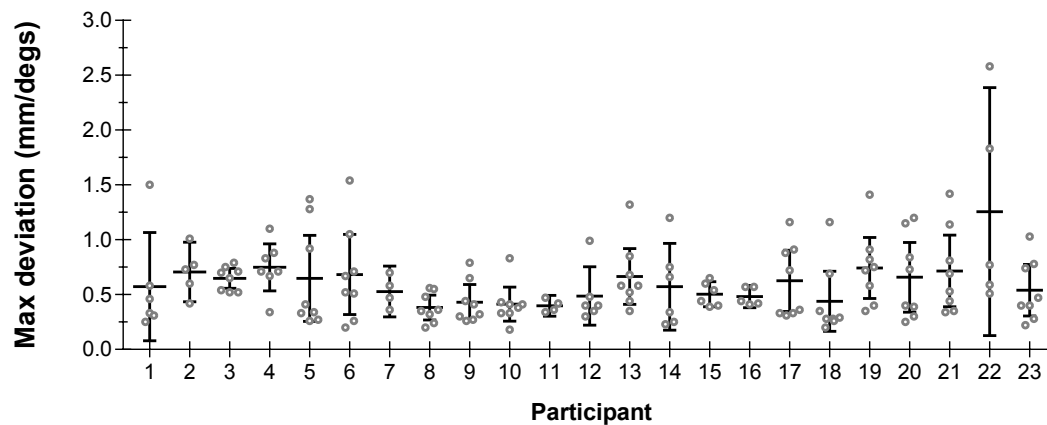
Supplementary Figure S1.2. Head motion. Scatter plot illustrating the maximum
deviation in any translation/rotation dimension per run per participant (N = 23). Solid
lines indicate the mean maximum deviation per run, and 95% confidence intervals.
Data per run are shown as unfilled circles.

Brain Voyager QX (Brain Innovation, Maastricht, The Netherlands) 3D motion
detection identified a maximum within-run deviation of only 2.58 mm/° across all
participants across all translation/rotation dimensions – i.e. the maximum detected
head motion independent of directionality. Critically, this was the largest detected
movement across all subjects, and less than the size of a single functional voxel. In
the complete sample of 23 participants, group mean = 0.60 +/- 0.35, range = 0.175°
– 2.58mm.

Appendix B

AsPredicted pre-registration

Changing hand selection with brain stimulation. (#15261)

Created: 10/18/2018 10:54 AM (PT)
Shared: 08/21/2019 08:18 AM (PT)

1) Have any data been collected for this study already?
No, no data have been collected for this study yet.

2) What's the main question being asked or hypothesis being tested in this study?
We predict that high-frequency repetitive transcranial magnetic stimulation applied separately to the left and right hemisphere posterior parietal cortex (PPC) will subsequently reduce the likelihood of selecting to use the hand ipsilateral to the site of stimulation during a unimanual reaching task, used previously by our group (Valyear et al., 2018).
Specifically, we will apply 40s of continuous theta burst stimulation following the original protocol developed by Huang et al. (2005).

Targeted areas of the left and right hemisphere PPC will be localized on the basis anatomical landmarks – specifically, the medial bank of the posterior intraparietal sulcus – within individuals, and prior (group-level) fMRI results from our group (Fitzpatrick et al., in press).

A Sham-cTBS condition will be included, for comparison with left and right hemisphere PPC stimulation, respectively. Sham-cTBS will involve turning the stimulator on for 40s of cTBS, but with the coil held away from the scalp so that no brain stimulation occurs.

Participants complete each stimulation condition in separate sessions, spaced one-week apart.

References:
Huang, Y. Z., Edwards, M. J., Rounis, E., Bhatia, K. P., & Rothwell, J. C. (2005). Theta burst stimulation of the human motor cortex. Neuron, 45(2), 201-206.
Valyear KF, Fitzpatrick AM, Dundon NM (2018). Now and then: Hand choice is influenced by recent action history. Psychonomic Bulletin and Review. DOI: 10.3758/s13423-018-1510-1
Fitzpatrick AM, Dundon N, and Valyear KF (in press). The neural basis of hand choice: An fMRI investigation of the Posterior Parietal Interhemispheric Competition model. NeuroImage. https://doi.org/10.1016/j.neuroimage.2018.10.039

3) Describe the key dependent variable(s) specifying how they will be measured.
Our primary dependent measure will be participant's hand choice behaviour, measured using our previously developed methods (Valyear et al., 2018).

Specifically, hand choice is quantified as the point in space where the use of either hand is equally probable – the Point of Subjective Equality (PSE). PSE values are estimated by fitting a general linear model to each participant's hand choice data. The model contains target positions and a constant term, and uses a logit link function to estimate the binomial distribution of hand choice responses (1 = right | 0 = left). Model coefficients are evaluated at 1,000 linearly spaced points between the outermost values of the target array (i.e. ± 65 degrees), and the value closest to a 0.50 probability estimate is defined as the PSE. The model will be fitted separately per individual, per session.

We will also quantify and evaluate hand choice as arcsine transformed proportions, as we have done previously (Valyear et al., 2018).

References:
Valyear KF, Fitzpatrick AM, Dundon NM (2018). Now and then: Hand choice is influenced by recent action history. Psychonomic Bulletin and Review. DOI: 10.3758/s13423-018-1510-1

4) How many and which conditions will participants be assigned to?
Three within-subject conditions. Each participant will complete a behavioural reaching task following 1) cTBS stimulation to Left-PPC, 2) cTBS stimulation to Right-PPC, and 3) Sham stimulation.

5) Specify exactly which analyses you will conduct to examine the main question/hypothesis.
Main analyses:

We will use two independent repeated measures analyses of variance (ANOVA) to investigate whether PSE values and arcsine transformed proportions differ across stimulation conditions: (1) Left-PPC, (2) Right-PPC, (3) Sham-TMS.
Significant main effects of condition will be investigated using follow-up pairwise t-tests, Bonferroni corrected for multiple comparisons.

Verify authenticity: http://aspredicted.org/blind.php?x=rx4dk9

Wharton
UNIVERSITY OF PENNSYLVANIA CREDIBILITY LAB

As additional complementary analyses, we will perform simple pairwise t-tests on the difference scores between (1) Left-PPC – Sham-TMS versus (2) Right-PPC – Sham-TMS on the basis of PSE values and (overall) arcsine transformed proportions.

6) Describe exactly how outliers will be defined and handled, and your precise rule(s) for excluding observations.
Outliers will be defined as ± 2.5 standard deviations from the group mean, per statistical test.

7) How many observations will be collected or what will determine sample size? No need to justify decision, but be precise about exactly how the number will be determined.
We will collect 20 complete datasets. If a participant does not complete all three experimental conditions (testing sessions), their data will be replaced. We anticipate a potential drop-out rate of 20%.

A power analysis using G*Power (Faul et al., 2007) indicated that a total sample size of 20 people would be needed to detect an effect size of d=0.76, with 95% power using a paired-samples t-test with alpha at .05.

The effect size (d=0.76) was calculated on the basis of results from Oliveira et al. (2010). In this study, (N=10) stimulation to left posterior parietal cortex resulted in a mean shift in PSE of 2.68° ± 3.5° SD, compared to a no-TMS condition.

References:
Faul, F., Erdfelder, E., Lang, A.-G., & Buchner, A. (2007). G*Power 3: A flexible statistical power analysis program for the social, behavioral, and biomedical sciences. Behavior Research Methods, 39, 175-191.
Oliveira, F. T., Diedrichsen, J., Verstynen, T., Duque, J., & Ivry, R. B. (2010). Transcranial magnetic stimulation of posterior parietal cortex affects decisions of hand choice. Proceedings of the National Academy of Sciences, 107(41), 17751-17756.

8) Anything else you would like to pre-register? (e.g., secondary analyses, variables collected for exploratory purposes, unusual analyses planned?)
Exploratory analyses:

We predict the effects of stimulation to be maximal around the target locations nearest to the PSE, as compared to the targets in the extreme lateral sides of space. Specifically, we expect to see the greatest change in proportion of hand use for targets bounding the PSE.

We will collect end-point touch accuracy measures during the task, and test for potential stimulation-induced changes across conditions. We do not expect significant conditional alterations to participants' accuracy – i.e. reaches to targets should not be more/less accurate following active/sham stimulation.

Unlike online TMS protocols, cTBS is hypothesized to suppress excitability, with effects reported to persist for up to 60mins post stimulation (Huang et al., 2005). We don't expect this manipulation to have detectable effects on measures of motor performance, including reach end-point accuracy. PPC should compensate for reductions in excitability, and motor performance – the kinematics of reach behaviour – should be unaffected. It is important to test this hypothesis, however.

References:
Huang, Y. Z., Edwards, M. J., Rounis, E., Bhatia, K. P., & Rothwell, J. C. (2005). Theta burst stimulation of the human motor cortex. Neuron, 45(2), 201-206.

Appendix C

Chapter 3: Supplementary materials

Table S3.1. Hand choice

(S3.1.1) Full dataset (N = 26)

One-way ANOVA:

PSE per stimulation condition: $F_{(2, 50)} = 1.73$, $p = 0.19$
PSE per stimulation condition with No-cTBS: $F_{(3, 75)} = 1.58$, $p = 0.20$

Proportion RHU per stimulation condition: $F_{(2, 50)} = 1.05$, $p = 0.36$
Proportion RHU per stimulation condition with No-cTBS: $F_{(3, 75)} = 0.98$, $p = 0.41$

Proportion RHU at Sham-PSE per stimulation condition: $F_{(2, 50)} = 1.23$, $p = 0.30$
Proportion RHU at No-cTBS-PSE per stimulation condition with No-cTBS: $F_{(3, 75)} = 3.35$, $p = 0.02$

(S3.1.2) Left-handers removed (N = 23)

One-way ANOVA:

PSE per stimulation condition: $F_{(2, 44)} = 1.44$, $p = 0.25$
PSE per stimulation condition with No-cTBS: $F_{(3, 66)} = 1.32$, $p = 0.28$

Proportion RHU per stimulation condition: $F_{(2, 44)} = 0.97$, $p = 0.39$
Proportion RHU per stimulation condition with No-cTBS: $F_{(3, 66)} = 0.91$, $p = 0.44$

Proportion RHU at Sham-PSE per stimulation condition: $F_{(2, 44)} = 1.41$, $p = 0.26$
Proportion RHU at No-cTBS-PSE per stimulation condition with No-cTBS: $F_{(3, 66)} = 3.38$, $p = 0.02$

(S3.1.3) Right-handers with strategy removed (N = 24)

One-way ANOVA:

PSE per stimulation condition: $F_{(2, 46)} = 1.57$, $p = 0.22$
PSE per stimulation condition with No-cTBS: $F_{(3, 69)} = 1.40$, $p = 0.25$

Proportion RHU per stimulation condition: $F_{(2, 46)} = 0.99$, $p = 0.38$
Proportion RHU per stimulation condition with No-cTBS: $F_{(3, 69)} = 0.94$, $p = 0.43$

Proportion RHU at Sham-PSE per stimulation condition: $F_{(2, 46)} = 0.99$, $p = 0.38$
Proportion RHU at No-cTBS-PSE per stimulation condition with No-cTBS: $F_{(3, 69)} = 3.07$, $p = 0.03$

(S3.1.4) TMS-averse removed (N = 25)

One-way ANOVA:

PSE per stimulation condition: $F_{(2, 48)} = 1.63$, $p = 0.21$
PSE per stimulation condition with No-cTBS: $F_{(3, 72)} = 1.50$, $p = 0.22$

Proportion RHU per stimulation condition: $F_{(2, 48)} = 0.99$, $p = 0.38$
Proportion RHU per stimulation condition with No-cTBS: $F_{(3, 72)} = 0.92$, $p = 0.43$

Proportion RHU at Sham-PSE per stimulation condition: $F_{(2, 48)} = 1.18$, $p = 0.32$
Proportion RHU at No-cTBS-PSE per stimulation condition with No-cTBS: $F_{(3, 72)} = 3.20$, $p = 0.03$

(S3.1.5) Right-handers, no strategy (N = 20)

One-way ANOVA:

PSE per stimulation condition: $F_{(2, 38)} = 1.19$, $p = 0.31$
PSE per stimulation condition with No-cTBS: $F_{(3, 57)} = 1.07$, $p = 0.37$

Proportion RHU per stimulation condition: $F_{(2, 38)} = 0.84$, $p = 0.44$
Proportion RHU per stimulation condition with No-cTBS: $F_{(3, 57)} = 0.80$, $p = 0.50$

Proportion RHU at Sham-PSE per stimulation condition: $F_{(2, 38)} = 1.09$, $p = 0.35$

Proportion RHU at No-cTBS-PSE per stimulation condition with No-cTBS: F (3, 57) = 2.96, p = 0.04

(S3.1.6) Right-handers, no strategy, outlier removed (N = 19)

One-way ANOVA:

PSE per stimulation condition: F (2, 36) = 0.56, p = 0.58
PSE per stimulation condition with No-cTBS: F (3, 54) = 0.48, p = 0.70

Proportion RHU per stimulation condition: F (2, 36) = 0.71, p = 0.50
Proportion RHU per stimulation condition with No-cTBS: F (3, 54) = 0.60, p = 0.62

Proportion RHU at Sham-PSE per stimulation condition: F (2, 36) = 1.26, p = 0.30
Proportion RHU at No-cTBS-PSE per stimulation condition with No-cTBS: F (3, 54) = 2.51, p = 0.07

197

Table S3.2. Response times

(S3.2.1) Full dataset (N = 26)

Two-way ANOVA: **Hand x Stimulation condition**
Main effect of Hand: F (1, 25) = 1.83, p = 0.19
Main effect of Stimulation condition: F (2, 50) = 0.19, p = 0.83
Interaction term: F (2, 50) = 0.38, p = 0.69

Choice costs
Space x Stimulation condition: Sham-PSE
Main effect of Space: F (1, 25) = 18.33, p = 0.0002
Main effect of Stimulation condition: F (2, 50) = 0.11, p = 0.89
Interaction term: F (2, 50) = 1.40, p = 0.26

Space x Stimulation condition: No-cTBS-PSE
Main effect of Space: F (1, 25) = 16.51, p = 0.0004
Main effect of Stimulation condition: F (2, 50) = 0.18, p = 0.84
Interaction term: F (2, 50) = 1.42, p = 0.25

(S3.2.2) Left-handers removed (N = 23)

Two-way ANOVA: **Hand x Stimulation condition**
Main effect of Hand: F (1, 22) = 0.82, p = 0.38
Main effect of Stimulation condition: F (2, 44) = 0.86, p = 0.43
Interaction term: F (2, 44) = 0.10, p = 0.90

Choice costs
Space x Stimulation condition: Sham-PSE
Main effect of Space: F (1, 22) = 15.10, p = 0.0008
Main effect of Stimulation condition: F (2, 44) = 0.66, p = 0.52
Interaction term: F (2, 44) = 1.82, p = 0.17

Space x Stimulation condition: No-cTBS-PSE
Main effect of Space: F (1, 22) = 14.95, p = 0.0008
Main effect of Stimulation condition: F (2, 44) = 0.33, p = 0.72
Interaction term: F (2, 44) = 0.69, p = 0.51

(S3.2.3) Right-handers with strategy removed (N = 24)

Two-way ANOVA: **Hand x Stimulation condition**
Main effect of Hand: F (1, 23) = 2.50, p = 0.13
Main effect of Stimulation condition: F (2, 46) = 0.21, p = 0.81
Interaction term: F (2, 46) = 0.18, p = 0.84

Choice costs
Space x Stimulation condition: Sham-PSE
Main effect of Space: F (1, 23) = 15.68, p = 0.0006
Main effect of Stimulation condition: F (2, 46) = 0.15, p = 0.86
Interaction term: F (2, 46) = 0.87, p = 0.43

Space x Stimulation condition: No-cTBS-PSE
Main effect of Space: F (1, 23) = 13.96, p = 0.001
Main effect of Stimulation condition: F (2, 46) = 0.19, p = 0.83
Interaction term: F (2, 46) = 0.90, p = 0.41

(S3.2.4) TMS-averse removed (N = 25)

Two-way ANOVA: **Hand x Stimulation condition**
Main effect of Hand: F (1, 24) = 1.48, p = 0.24
Main effect of Stimulation condition: F (2, 48) = 0.13, p = 0.88
Interaction term: F (2, 48) = 0.36, p = 0.70

Choice costs
Space x Stimulation condition: Sham-PSE
Main effect of Space: F (1, 24) = 16.71, p = 0.0004
Main effect of Stimulation condition: F (2, 48) = 0.06, p = 0.94
Interaction term: F (2, 48) = 1.51, p = 0.23

Space x Stimulation condition: No-cTBS-PSE
Main effect of Space: F (1, 24) = 14.99, p = 0.0007
Main effect of Stimulation condition: F (2, 48) = 0.11, p = 0.90
Interaction term: F (2, 48) = 1.62, p = 0.21

(S3.2.5) Right-handers, no strategy (N = 20)

Two-way ANOVA: **Hand x Stimulation condition**
Main effect of Hand: F (1, 19) = 1.05, p = 0.32
Main effect of Stimulation condition: F (2, 38) = 0.85, p = 0.43
Interaction term: F (2, 38) = 0.07, p = 0.93

Choice costs
Space x Stimulation condition: Sham-PSE
Main effect of Space: F (1, 19) = 11.02, p = 0.004
Main effect of Stimulation condition: F (2, 38) = 0.64, p = 0.53
Interaction term: F (2, 50) = 1.24, p = 0.30

Space x Stimulation condition: No-cTBS-PSE
Main effect of Space: F (1, 19) = 12.90, p = 0.002
Main effect of Stimulation condition: F (2, 38) = 0.71, p = 0.50
Interaction term: F (2, 50) = 0.82, p = 0.45

(S3.2.6) Right-handers, no strategy, outlier removed (N = 19)

Two-way ANOVA: **Hand x Stimulation condition**
Main effect of Hand: F (1, 18) = 0.73, p = 0.40
Main effect of Stimulation condition: F (2, 36) = 0.90, p = 0.42
Interaction term: F (2, 36) = 0.41, p = 0.66

Choice costs
Space x Stimulation condition: Sham-PSE
Main effect of Space: F (1, 18) = 9.05, p = 0.008
Main effect of Stimulation condition: F (2, 36) = 0.72, p = 0.49
Interaction term: F (2, 36) = 0.67, p = 0.52

Space x Stimulation condition: No-cTBS-PSE
Main effect of Space: F (1, 18) = 10.75, p = 0.004
Main effect of Stimulation condition: F (2, 36) = 0.79, p = 0.46
Interaction term: F (2, 36) = 0.26, p = 0.77

Table S3.3.1. Post-stimulation questionnaire data. Full dataset (N = 26)

A.

Type of Session	Reported as Real	Reported as Sham	Reported "I don't know"	Percent correct identification
				Total sample | Respondents
Real cTBS	28	5	19	53.85% | 84.85%
Sham cTBS	13	2	11	7.69% | 13.33%

B.

Type of Sensation	Reported after Real	Reported after Sham
Itching	6	1
Pain	6	1
Burning	-	1
Warmth/heat	7	4
Pinching	6	1
Metallic/iron taste	2	-
Fatigue	8	4
Dazed	1	-
Tapping	4	1
Twitching	1	-

Table S3.3.2. Post-stimulation questionnaire data. TMS-averse removed (N = 25)

A.

Type of Session	Reported as Real	Reported as Sham	Reported "I don't know"	Percent correct identification
				Total sample I Respondents
Real cTBS	26	5	19	52.00% I 81.25%
Sham cTBS	12	2	11	8.00% I 14.29%

B.

Type of Sensation	Reported after Real	Reported after Sham
Itching	5	1
Pain	4	-
Burning	-	-
Warmth/heat	5	3
Pinching	5	-
Metallic/iron taste	-	-
Fatigue	6	3
Dazed	1	-
Tapping	4	1
Twitching	1	-

Table S3.3.3. Post-stimulation questionnaire data. Right-handers, no strategy (N = 20)

A.

Type of Session	Reported as Real	Reported as Sham	Reported "I don't know"	Percent correct identification
				Total sample I Respondents
Real cTBS	19	4	17	47.50% I 82.61%
Sham cTBS	10	0	10	0%

B.

Type of Sensation	Reported after Real	Reported after Sham
Itching	5	1
Pain	1	-
Burning	-	-
Warmth/heat	3	2
Pinching	4	-
Metallic/iron taste	-	-
Fatigue	4	1
Dazed	1	-
Tapping	4	1
Twitching	5	1

Appendix D

Chapter 4: Supplementary materials

Table S4.1. Post-stimulation questionnaire data. Full dataset (N = 21)

A.

Type of Session	Reported as Real	Reported as Sham	Reported "I don't know"	Percent correct identification
Real cTBS	7	-	4	33.33%
Sham cTBS	4	3	3	30.00%

B.

Type of Sensation	Reported after Real	Reported after Sham
Itching	1	2
Pain	-	-
Burning	-	-
Warmth/heat	-	2
Pinching	-	-
Metallic/iron taste	-	-
Fatigue	-	4
Dazed	-	-
Tapping	-	-
Twitching	-	-